NUSC Technical Document 6029

NUSC Technology Monographs, No. 1

HANDBOOK for the ANALYSIS of PIEZOELECTRIC TRANSDUCERS

(Using Electrical Equivalent Circuits)

Part I: The Untuned Transducer

Harry B. Miller
Special Projects Department

14 Sept 1978

NUSC-TD-6029-PT-1

NUSC
NAVAL UNDERWATER SYSTEMS CENTER
Newport, Rhode Island • New London, Connecticut

PREFACE

This work was conducted as part of NUSC's program of Independent Research and Exploratory Development (Project No. A70227). The Principal Investigator was Harry B. Miller (Code 316).

The author would like to thank James M. Powers for his careful review of the entire handbook. Thanks are extended also to Mark B. Moffett, William R. Hazard, and Theodore J. Meyers for their helpful advice on selected chapters.

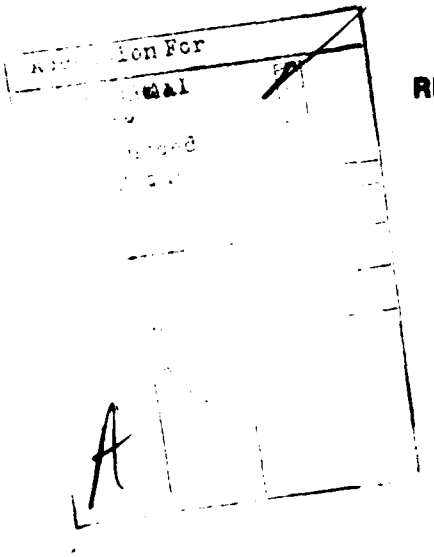

REVIEWED AND APPROVED: 14 September 1978

W. A. Von Winkle

W. A. VON WINKLE
Associate Technical Director
for Technology

The author of this document is located at the
New London Laboratory, Naval Underwater Systems Center
New London, Connecticut 06320.

CONTENTS

Chapter I. Introductory Chapter

Chapter I. Introductory Chapter

A. Aims and Guiding Principles of this Handbook.

1. This handbook is based on approaches which have been useful to the author. These approaches do not always conform to a "standard treatment" of the subject. For example, the literature contains many analyses based on the impedance circle diagram and the admittance circle diagram, which comprise offset "circles" in the complex plane. Here Y or Z is given as A + jB.

2. The author has for the most part used an alternative approach, by extracting the two components of [A + jB] from the complex plane and plotting them separately in the real plane, versus frequency. Eventually the interrelationship is shown between the plots in the real plane and the plots in the complex plane.

The handbook thus presents the reader with a choice of ways of analyzing transducers.

3. A situation constantly imagined was: If you are handed, e.g., an old impedance-vs-frequency curve, unearthed in a file, what is the maximum amount of information you can extract from it? One aim of this handbook is to help the reader maximize the obtainable information. (A well-documented circle diagram contains everything you need; but too often the frequencies desired by the next inquirer are not called out. Hence the diagram loses its value.)

4. This first volume is limited to an analysis of the untuned piezoelectric transducer, with no dielectric losses, using either the Mason- or the Van Dyke-circuit approximations. The analysis includes a discussion of the various <u>forms</u> of the performance data as commonly presented by a computer simulation or by a measurement station. This means, e.g., when discussing

the input impedance: the graphical appearance of Z-mag vs. frequency, Z-angle vs. frequency; X and B and R and G vs. frequency; X vs. R, B vs. G; etc.

Profuse illustrations are given of many equivalent sub-circuits and their responses. Inverse relationships and not-quite-inverse relationships are discussed.

5. All curves have been normalized around the frequency 1.0, and in most cases log frequency rather than linear frequency has been used. This not only confers left-right symmetry on the plot, but allows the reader to make direct use of these curves for his own design projects. For, the curves are now universal; and in addition the frequency markings are quite accurate.

Occasionally a curve is plotted both ways, log frequency and linear frequency, to help the reader visualize the quite different <u>appearances</u> of the plotted function.

6. For the most part, the illustrations are on the left page. They contain a minimum of explanatory statements, since these are given fully on the right page. The illustrations are repeated as the left page is turned, with the added feature that they move up the page, as in a Chinese scroll, to keep them synchronized with the text.

This arrangement was chosen so that the handbook can provide the asked-for information in an easily retrievable form.

7. Whenever deemed helpful, a geometrical interpretation of the numerator or denominator of an equation is separately plotted; or even a portion of the numerator or denominator may be plotted.

8. Two repeating sets of illustrations are used throughout.

a) An equivalent circuit has been chosen using simple numerical values, viz: C_o = 1.5 nF, C_m = 0.5 nF, L_m = 0.5 henry, and R_m = 3200 ohms. These give a resonance frequency $f_r \approx$ 10,000 Hz and an antiresonance frequency $f_a \approx$ 11,500 Hz. When normalized these become 1.0 and 1.15 frequency units. The coupling coefficient $\underline{k}$ is thus seen to be 50%; and the $Q_m \approx 10$ at either f_r or f_a. The choice of these above values allows the reader to verify a point by mental calculation, without resorting to a slide rule or calculator.

b) A computer-simulation of a realistic sonar transducer has been chosen, having three different radiation loadings which are purely resistive. These frequencies have all been shifted so that $f_r = 1.0$. Since the $\underline{k}$ is 50%, f_a again = 1.15. All relative magnitudes, on a dB scale, have been preserved in the frequency translation; but the absolute magnitudes are now not correct at the normalized frequency. However, since both susceptance and reactance components (for example) were operated on by the same transformation, the originally computed numbers will retain much useful correlation between e.g. susceptance and reactance.

B. A Figure-of-Merit for Transducers

A figure-of-merit is usally an arbitrary formula which has proven useful in a given discipline. People who design piezoelectric filters choose k^2Q_m for their figure-of-merit. They would like a coupling coefficient $\underline{k} > 60\%$ and a mechanical Q (i.e. Q_m) > 100; and the higher each component the better, since a high Q_m means low friction losses.

But designers of transducers for radiating or receiving sound energy have a different criterion. They still would like a high $\underline{k}$; but not too high a Q_m. In fact if the Q_m became lowered due to an increased radiation loss R_{load} (while maintaining the friction losses at a steady value), this could be a highly desirable situation. It is known as matching the transducer impedance to the load impedance. Hence a Q_m in the range of 2 to 5 is usually very desirable.

We will leave out Q_m entirely from our figure-of-merit formula, preferring to choose the optimum value of Q_m on a case-by-case consideration. Then our figure-of-merit reduces merely to k^2 or, more simply, to $\underline{k}$ the coupling coefficient. (Note that we always use it in the form k^2 or k^4, never as $\underline{k}$.)

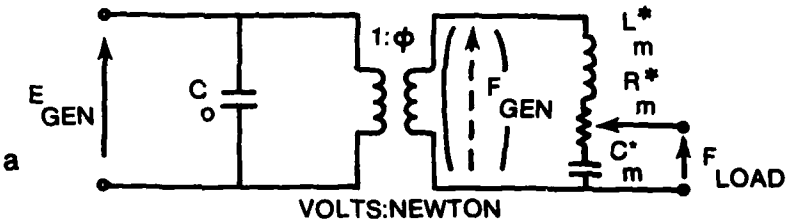

FIG: I.1a

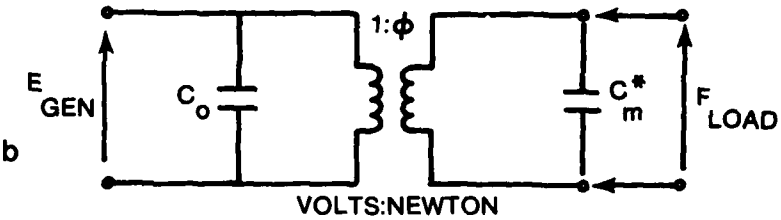

FIG: I.1b

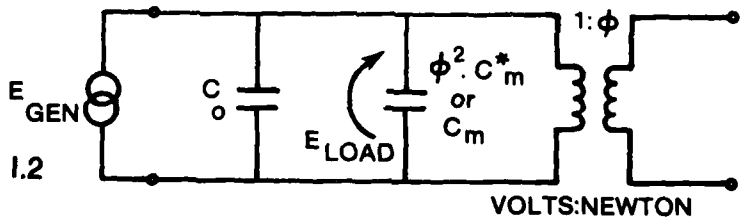

FIG: I.2

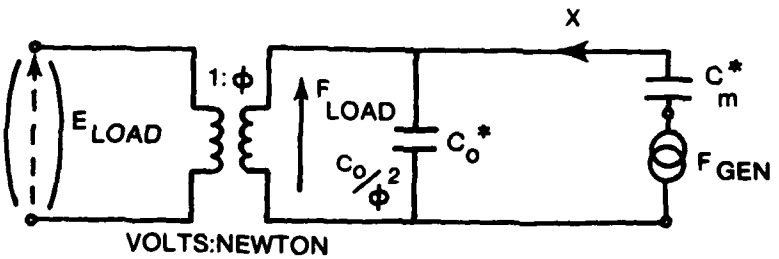

FIG: I.3a

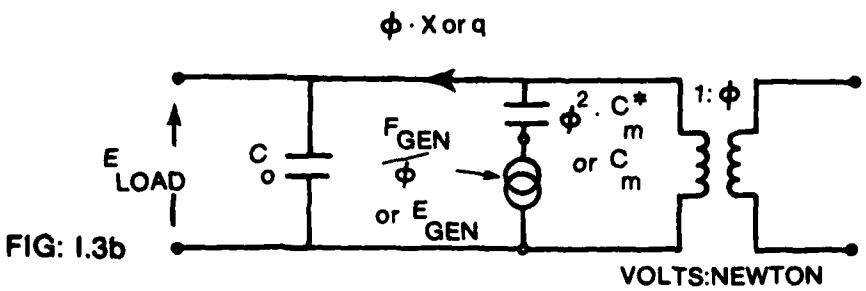

FIG: I.3b

B. (cont.)

A Figure-of-Merit for Transducers (Coupling Coefficient)

The coupling coefficient k can be obtained from measurements on the untuned transducer, which give us k^2. Basically k^2 starts with the total reactive energy stored on the two sides of the transducer, mechanical and electrical. Then $1/k^2$ is the ratio of this total reactive energy to the partial reactive energy transferred and stored on the other side; or k^2 is the ratio of the transferred stored energy to the total stored energy. On the electrical side, the reactive energy is stored in the capacitor (for a piezoelectric transducer). On the mechanical side, all the reactive energy is stored in the spring if we measure at dc (or extrapolate down to dc); the value of the mass is thus irrelevant.

Figure I.1a shows the equivalent circuit we will work with. This is the Mason-circuit or modified Van Dyke-circuit. It is valid in the neighborhood of the fundamental resonance and at dc; but invalid elsewhere. The mechanical branch uses the analog of force with voltage, and velocity with current. It then can be shown that springs in parallel must be represented by "mechanical condensers" in series. Also, a force generator which produces the same displacement "X" across two springs in parallel, is here represented by the force generator F which produces constant displacement "X" through two "mechanical condensers" in series. "Mechanical inductances" L_m^* and "mechanical resistances" R_m^* combine in series precisely as do true masses M and true viscosities R. The perfect electromechanical turns-ratio (or perfect transformer) $1:\phi$ has the dimensions (volt: Newton) in the MKS system.

Figure I.1b shows the low-frequency approximate equivalent circuit, which is exact at dc.

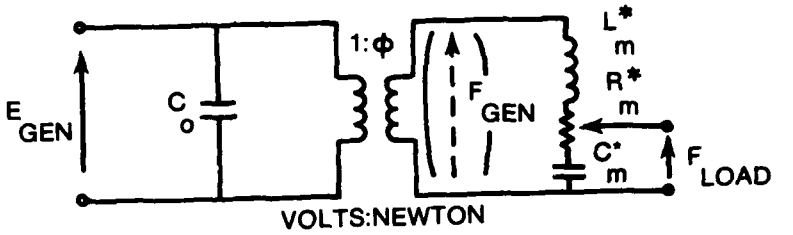

FIG: I.1a

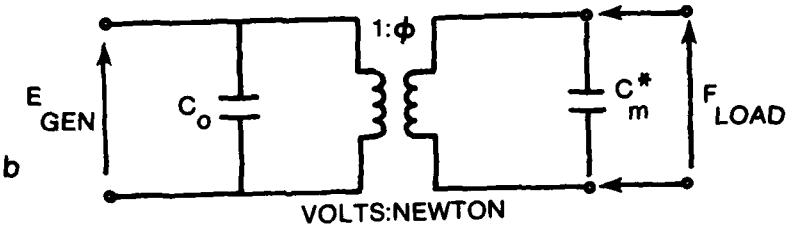

FIG: I.1b

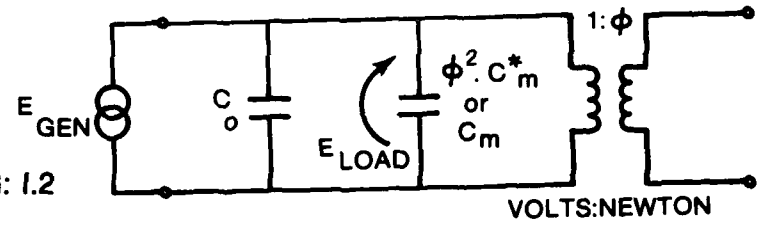

FIG: I.2

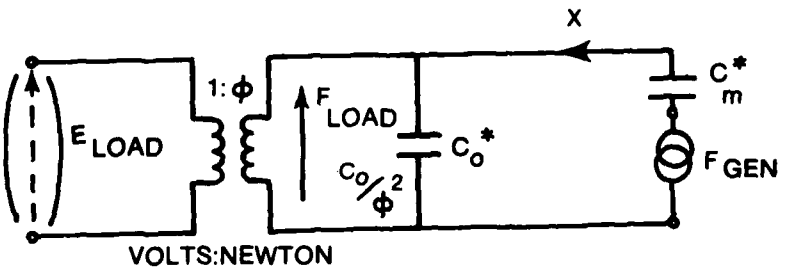

FIG: I.3a

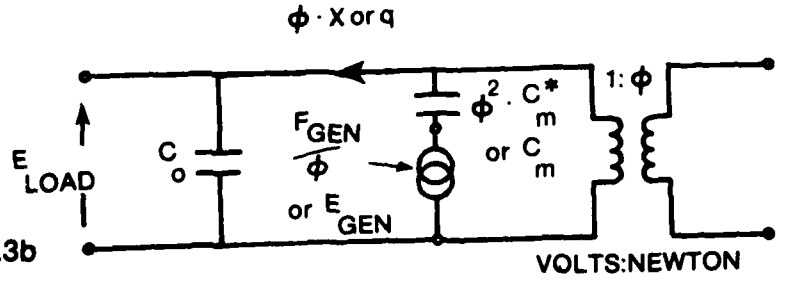

FIG: I.3b

Then at dc, $k^2 = \dfrac{\text{Energy transferred to mechanical condenser}}{\text{Energy in mechanical condenser + Energy in electrical capacitor}}$

Two approaches are now possible, in calculating these energies.

1. It is sometimes convenient to send the mechanical condenser C_m^* through the perfect transformer 1:ϕ, and work with Figure I.2. The mechanical condenser C_m^* has now become the "motional capacitor" C_m. The circuit of Fig I.2 suggests that we should apply a voltage E to the electric terminals and measure the energy transferred to the motional element C_m (which is in parallel).

$$\text{Then } k^2 = \frac{1/2\ C_m E_G^2}{1/2\ C_m E_G^2 + 1/2\ C_o E_G^2} = \frac{C_m}{C_m + C_o} \qquad (I.1)$$

From this it follows that:

$$\underbrace{\qquad\qquad}_{\text{Fig 2c}} \qquad \underbrace{\qquad\qquad}_{\text{Fig 2e}} \quad \text{(see Chapter 2)}$$

$$1-k^2 = 3:4 = \frac{C_o}{C_m + C_o} = \frac{C_{clamped}}{C_{free}} = \frac{X_{free}}{X_{clamped}} = \frac{X_o'(free)}{X_{clamped}'} \qquad (I.2)$$

$$\text{And } \frac{1}{1-k^2} = 4:3 = \frac{C_m + C_o}{C_o} = \frac{C_{free}}{C_{clamped}} = \frac{X_{clamped}}{X_{free}} = \frac{X_{clamped}'}{X_o'(free)} \qquad (I.3)$$

$$\text{And } \frac{k^2}{1-k^2} = 1:3 = \frac{C_m}{C_o} = \frac{C_{mot}}{C_{clamped}} = \frac{X_{clamped}}{X_{mot}} = \frac{\left(X_{mot}'\right)}{X_{o(free)}'} \qquad (I.4)$$

$$\text{And } \frac{1-k^2}{k^2} = 3:1 = \frac{C_o}{C_m} = \frac{C_{clamped}}{C_{mot}} = \frac{X_{mot}}{X_{clamped}} = \frac{X_o'(free)}{X_{mot}'} \qquad (I.5)$$

2. It is sometimes more convenient to send the capacitor C_o through the perfect transformer 1:ϕ, and work with Figure 1.3a. The capacitor C_o has now become the "mechanical condenser" C_o^*. The circuit of Fig I.3a suggests that we should apply a force F in series with the "mechanical

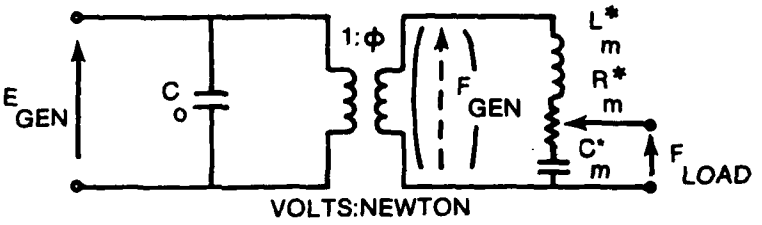

FIG: I.1a

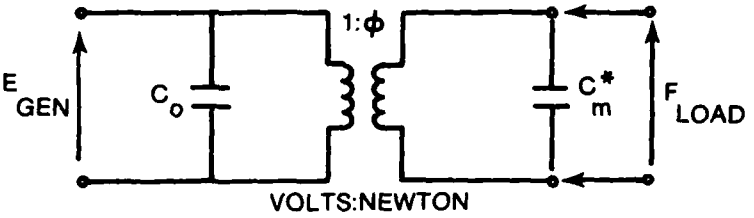

FIG: I.1b

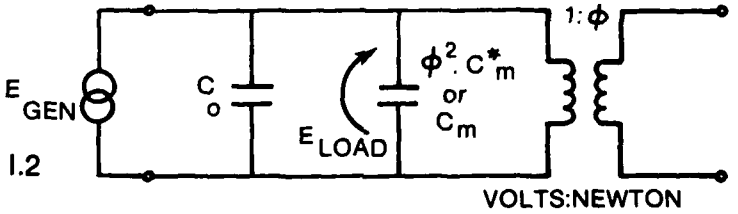

FIG: I.2

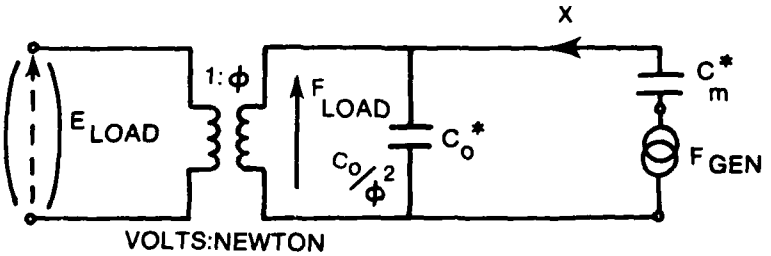

FIG: I.3a

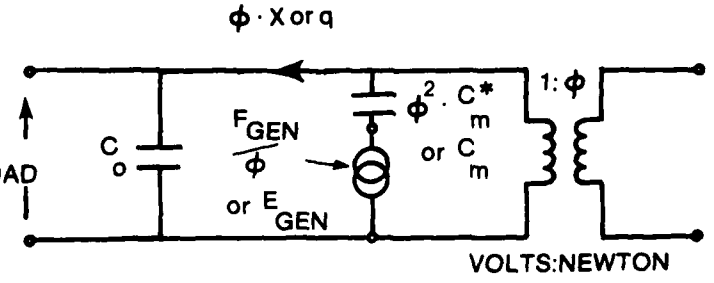

FIG: I.3b

condenser" C_m^*, and measure the energy transferred to the "electrical" element C_o^* (which is in series). Since the force generator F must have zero internal impedance, the mechanical boundary is still "free", as is required in these measurements.

$$\text{Then } k^2 = \frac{\frac{1}{2}\frac{X^2}{C_o^*}}{\frac{1}{2}\frac{X^2}{C_o^*} + \frac{1}{2}\frac{X^2}{C_m^*}} = \frac{\frac{1}{C_o^*}}{\frac{1}{C_o^*} + \frac{1}{C_m^*}} = \frac{C_m^*}{C_m^* + C_o^*} = \frac{C_m^* \cdot \phi^2}{C_m^* \cdot \phi^2 + C_o^* \cdot \phi^2} = \frac{C_m}{C_m + C_o}. \tag{I.6}$$

Equally true, we could have sent the whole mechanical branch through the transformer 1:ϕ, so that we could work with the circuit of Figure I.3b. Note that displacement "X" then becomes charge "q".

$$\text{Then } k^2 = \frac{\frac{1}{2}\frac{q^2}{C_o}}{\frac{1}{2}\frac{q^2}{C_o} + \frac{1}{2}\frac{q^2}{C_m}} = \frac{\frac{1}{C_o}}{\frac{1}{C_o} + \frac{1}{C_m}} = \frac{C_m}{C_m + C_o}. \tag{I.7}$$

Thus the value of k^2 is invariant, whether we inject electrical energy and measure the transferred mechanical energy; or whether we inject mechanical energy and measure the transferred electrical energy.

In closing, it should be mentioned that this dc value of k^2, called the static coupling coefficient, is not always duplicated at resonance. For many designs the resonance coupling coefficient has a lower value than the static value, sometimes dropping to as low as 75% static $\underline{k}$. The static value is still worth finding, however, as an upper-limit to the possibilities of a newly-built model.

Chapter 1. Some Information Obtainable from the Input Immittance Magnitude (Untuned).

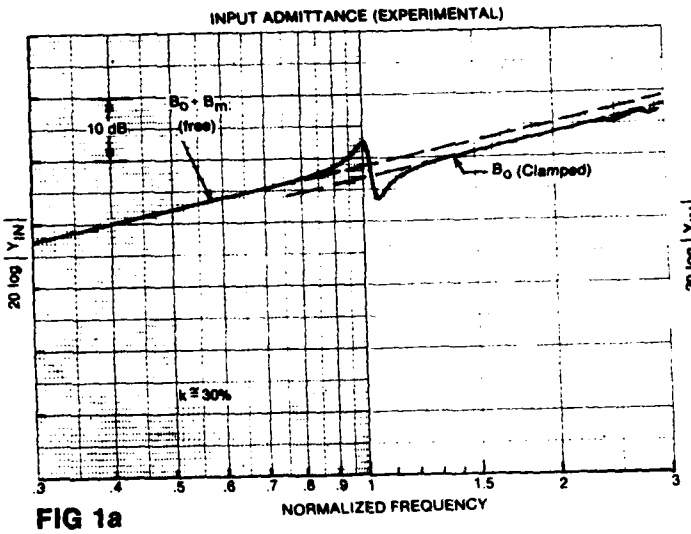

FIG 1a

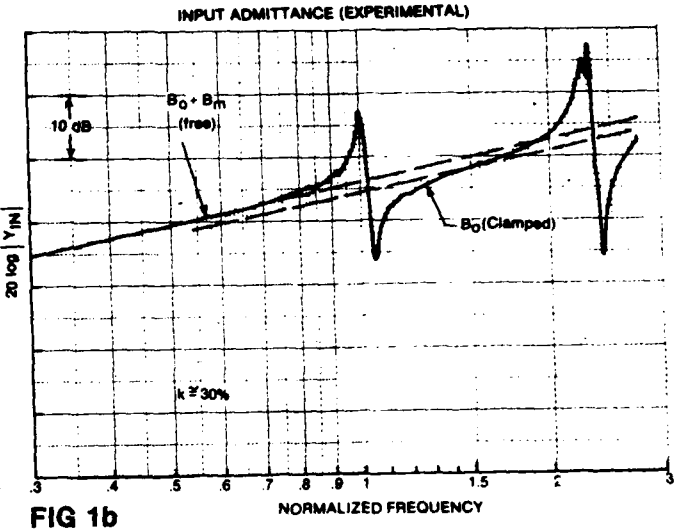

FIG 1b

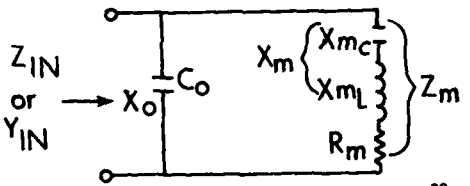

FIG 1c

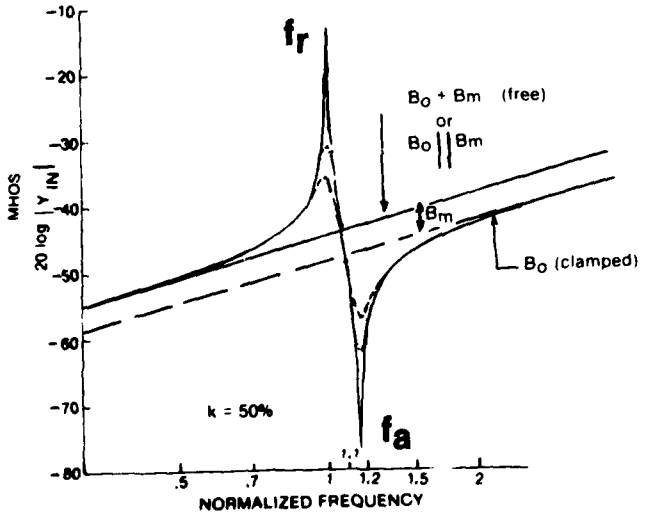

FIG 1d

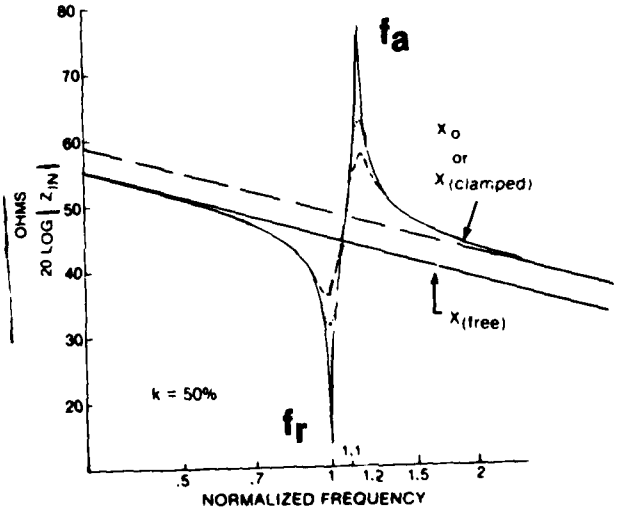

FIG 1e

Chapter 1. Some Information Obtainable from the Input Immittance Magnitude (Untuned).

1. Input Admittance and Input Impedance Magnitude shown as 20 log $|Y|$ or 20 log $|Z|$ vs. log frequency.
2. Asymptotes B_0 and $(B_0 + B_m)$ for "clamped" and "free" portions of the frequency band.
3. Two aspects of coupling coefficient $\underline{k}$.

Preliminary Note: In this Handbook the operator || (parallel), when used with impedance elements, will mean for example: $Z_1 || Z_2 = \frac{Z_1 \cdot Z_2}{Z_1 + Z_2}$. With admittance elements it means: $Y_1 || Y_2 = Y_1 + Y_2$. Likewise the operator $\$$ (series), when used with admittance elements, will mean for example: $Y_1 \$ Y_2 = \frac{Y_1 \cdot Y_2}{Y_1 + Y_2}$. With impedance elements it means: $Z_1 \$ Z_2 = Z_1 + Z_2$.

In this chapter we will try to illustrate the usefulness of the logarithmic scale in plotting magnitude of immittance. Not only does the log scale make the max. and min. values of Y or Z more or less symmetrical about their mean value (which is not the case with a linear scale); but in addition the two asymptotic baselines are now displayed as parallel straight lines (rather than converging or diverging hyperbolas). This facilitates finding the separation between the "free" and "clamped" asymptotes. This mechanical terminology is analogous to electric circuit terminology as follows. As will be shown in Fig. 1c, mechanical "free" (where the motional resistance $R_m = 0$) corresponds to a 4-terminal electric circuit whose output terminals are short-circuit. And mechanical "clamped" (where the motional resistance $R_m = \infty$) corresponds to a 4-terminal electric circuit whose output terminals are open-circuit. Note that the "free" immittance occurs only below the resonance, f_r; and the "clamped" immittance occurs only above the anti-resonance, f_a.

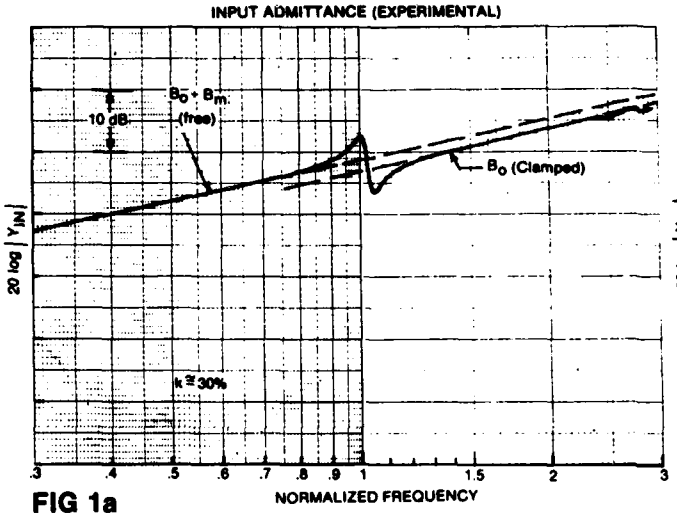

FIG 1a

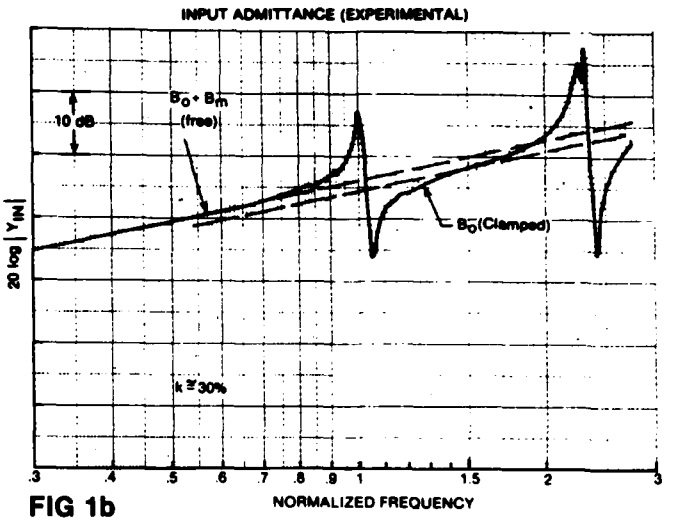

FIG 1b

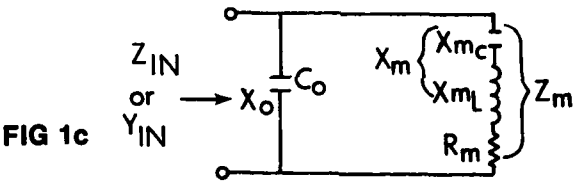

FIG 1c

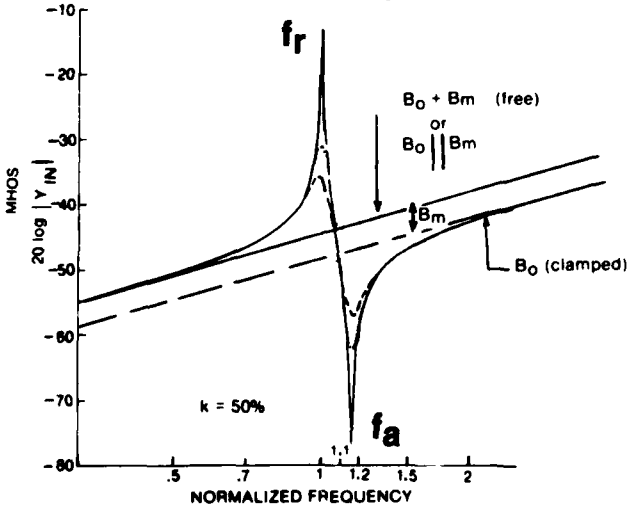

FIG 1d

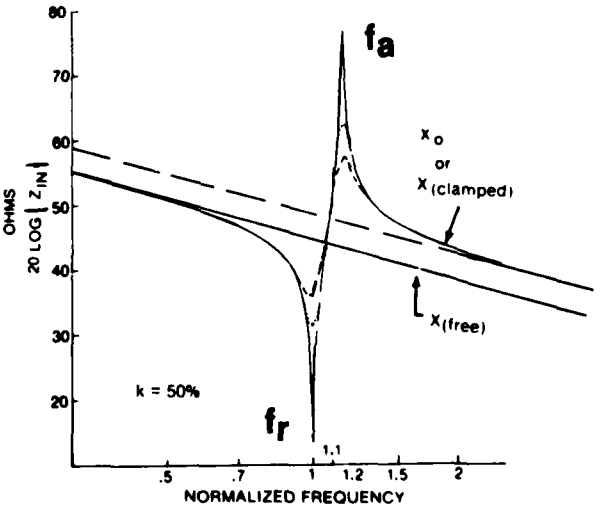

FIG 1e

The separation between the "free" baseline and the "clamped" baseline determines the static coupling coefficient. This static $\underline{k}$ is usually higher than the dynamic $\underline{k}$ which prevails at resonance.

1. Figures 1a and 1b show experimental measurements of the magnitude of the input admittance of two different barium titanate transducers, air-loaded, plotted on semilog paper. We plot 20 log |admittance| as the ordinate.

Looking briefly at "the Basic Circuit" shown in Figure 1c, which is a simplified equivalent circuit (the Van Dyke-circuit) for the transducers measured in Figures 1a and 1b: we see that since $Z_{in} = jX_o \| Z_m$ and $Y_{in} = \frac{1}{Z_{in}}$, then $|Y_{in}|_{free} \simeq |\frac{1}{jX_o} + \frac{1}{jX_{m_c}}|$ at low frequencies; and

$|Y_{in}|$ clamped $\simeq |\frac{1}{jX_o}|$ at high frequencies. Or identically,

$|Y_{in}| \simeq |jB_o + jB_m|$ at low frequencies; and $|Y_{in}| \simeq |jB_o|$ at high frequencies.

Z_m and X_{m_c} and B_m are "mechanical" components which have been transformed to the electric side. They are then called <u>motional</u> components.

2. In Figures 1d and 1e the two baseline susceptances or reactances are seen to plot as two parallel straight-line asymptotes: B or $X\big]_{clamped}$; and B or $X\big]_{free}$.

3. The coupling coefficient $\underline{k}$ can be determined from each graph in two independent ways.

(a) Static $\underline{k}$.

When the Q_m is low, the asymptote B_o can be guessed at and drawn (Fig 1a). Then it can be shown that $1-k^2 = \frac{B_o}{B_o + B_m}$; or 20 log $(1-k^2) = \Delta_{dB}$ of $\left[B_o^{dB} \text{minus } (B_o + B_m)^{dB}\right]$. Thus the larger the spacing B_m between the asymptotes, the higher the $\underline{k}$ static.

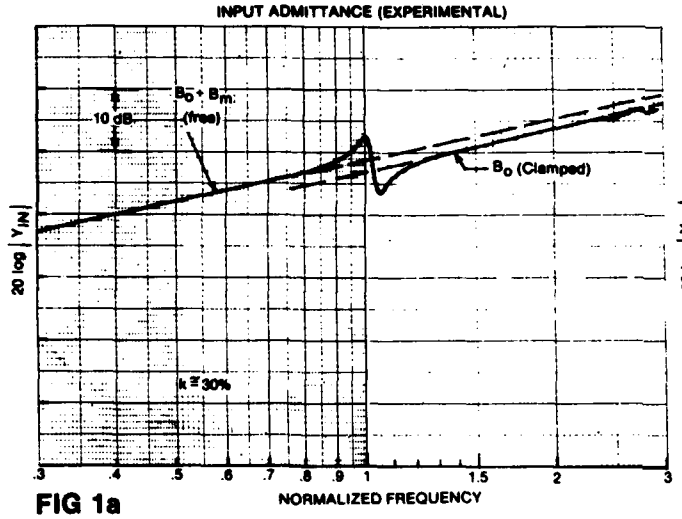

FIG 1a

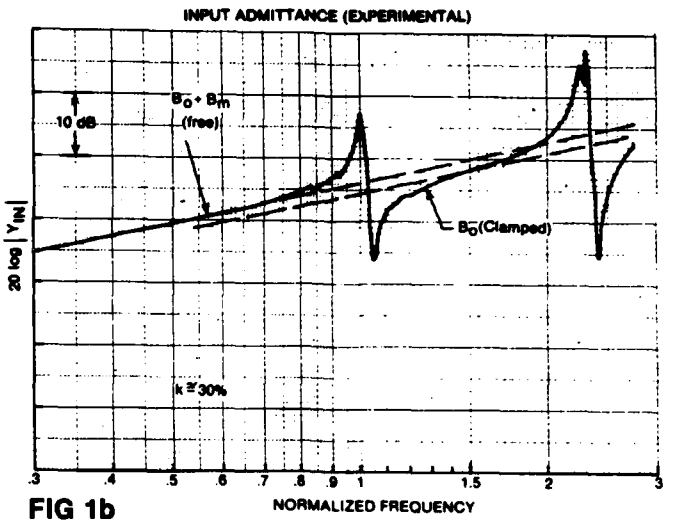

FIG 1b

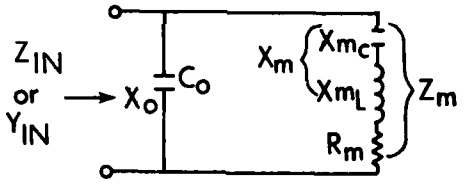

FIG 1c

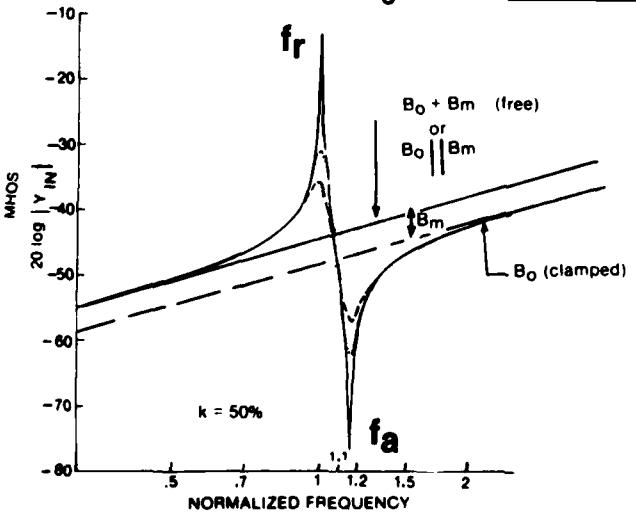

FIG 1d

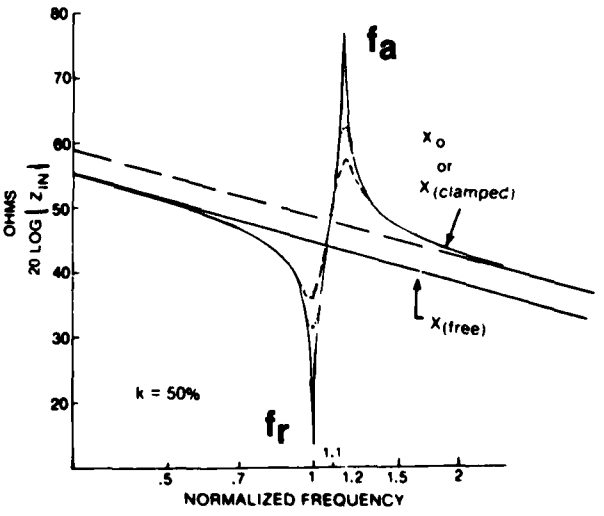

FIG 1e

In practice, for an assembled PZT ceramic transducer in the 33 mode using a stack of rings, static k_{33} is usually not greater than about 0.55. A PZT transducer using the 31 mode in a stack of rings, will usually have static k_{31} not greater than about 0.30.

The meaning of k_{31} and k_{33} is the following. A long tube of piezoelectric ceramic, electroded on its outer and inner faces and polarized (or "poled") radially, is said to be working in the 3-1 mode when it vibrates either longitudinally or radially. If this tube is now sliced up into rings and reassembled as a stack of rings, it is still working in the 3-1 mode. We say we have a stack comprised of 3-1 rings.

But if, after slicing the tube into rings, we take these rings and depolarize them and remove the electroding; and then electrode each ring on its top and bottom flat surface, and then pole each ring longitudinally (i.e. parallel to the axis): We say that each ring is now working in the 3-3 mode. And if we reassemble these 3-3 rings (or any 3-3 rings) into a stack, we say we have a 3-3 stack.

If barium titanate is the ceramic, then using a stack of rings, static k_{33} is usually not greater than 0.35; and static k_{31} is usually not greater than 0.14.

If a single long tube of barium titanate is used, however, static k_{31} might $\simeq$ 0.19 (since now there are no multiple cement joints, which act to decouple the mechanical domain from the electrical domain, thereby reducing k).

Figure 1a shows the input admittance of an underwater transducer measured in air, on the bench. The "motor" was a stack of PZT rings operating in the 3-3 mode. But the rings were known to be partially depolarized. The coupling coefficient was therefore not calculable in advance (i.e. via theory).

In the figure, $\Delta dB \simeq -1.5$ dB. So $(1-k^2) \simeq 0.84$. And $k_{static} \simeq 0.40$. If we had read $\Delta dB \simeq -1.4$ dB, then $k_{static} \simeq 0.385$. The dynamic value of k

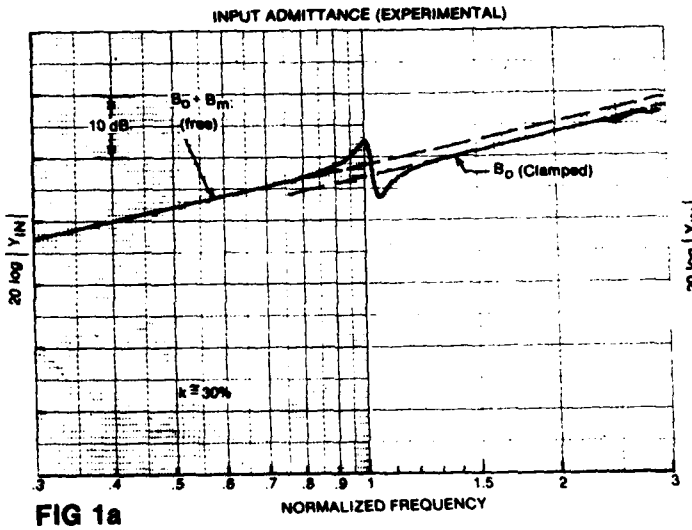

FIG 1a

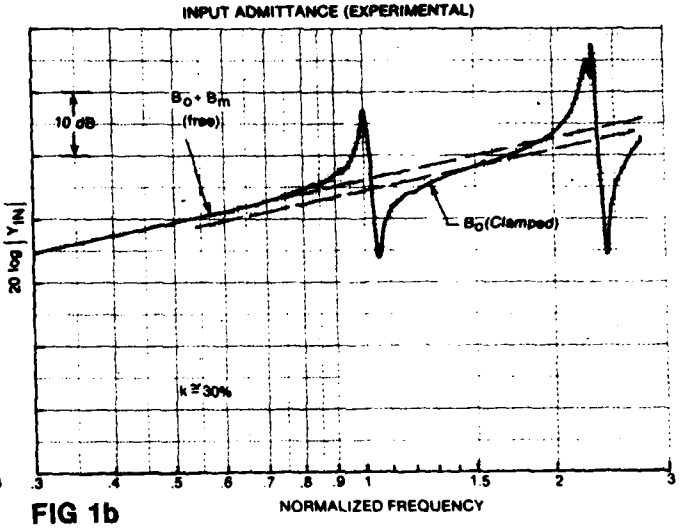

FIG 1b

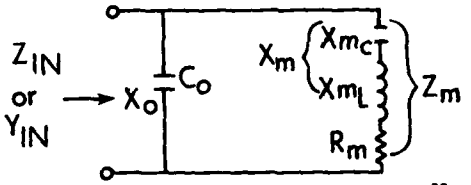

FIG 1c

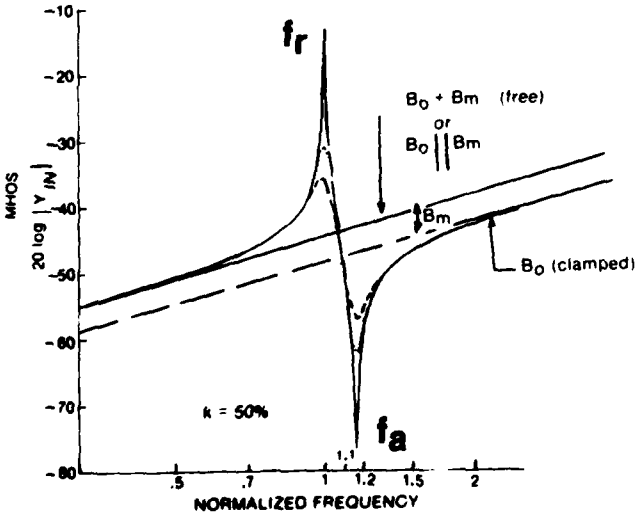

FIG 1d

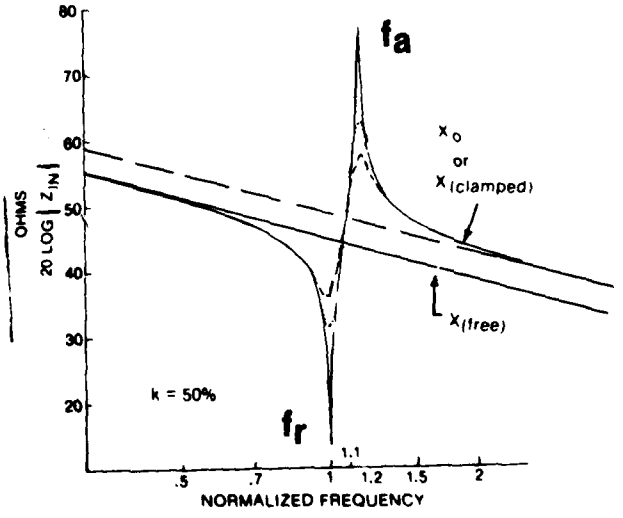

FIG 1e

runs lower, say 75% of these values, when the head and tail are relatively light weight. If they are heavy, the dynamic value can be > 90% of k_{static}.

(b) Dynamic $\underline{k}$.

Since we are primarily concerned with the behavior of an assembled transducer around resonance, we can try going directly to the frequency-variation method, using f_a, f_r, and $\Delta f = (f_a - f_r)$. These terms are usually derived at the electric terminals. However, if we look into the mechanical instead of electrical terminals, f_a (the "anti-resonance") is merely the mechanical resonance when the electric terminals are open-circuit; f_r is the mechanical resonance when the electric terminals are short-circuit; and Δf is the difference between the two. These three values can be determined fairly accurately when the Q_m is high (>10); but Δf, the most important quantity, becomes blurry when the Q_m, or mechanical Q, is low. Q_m is defined here as f_r divided by the -3dB bandwidth in Hz, as measured on a constant-voltage untuned Transmitting Response curve. The basic relationship for dynamic $\underline{k}$ is

$$k^2 = \frac{f_a^2 - f_r^2}{f_a^2}$$

This can be converted to other useful forms.

$$\text{Thus } k^2 = \frac{(f_a + f_r)\,\Delta f}{f_a^2} = \left(2 - \frac{\Delta f}{f_a}\right) \cdot \frac{\Delta f}{f_a}.$$

$$\text{Then } k^2 = \frac{2\Delta f}{f_a} - \left(\frac{\Delta f}{f_a}\right)^2. \quad \text{And if the second}$$

term is very small (as when $\underline{k} \approx 0.30$ or less), $k^2 \approx \frac{2\Delta f}{f_a}$.

In Figure 1a, Δf happened to equal 0.049 frequency units and $\frac{\Delta f}{f_a} = 0.047$.

Then $k^2 = 0.094 - .0022 = .0918$. So $\underline{k} \leq 0.305$. This is about 78% of the k static value.

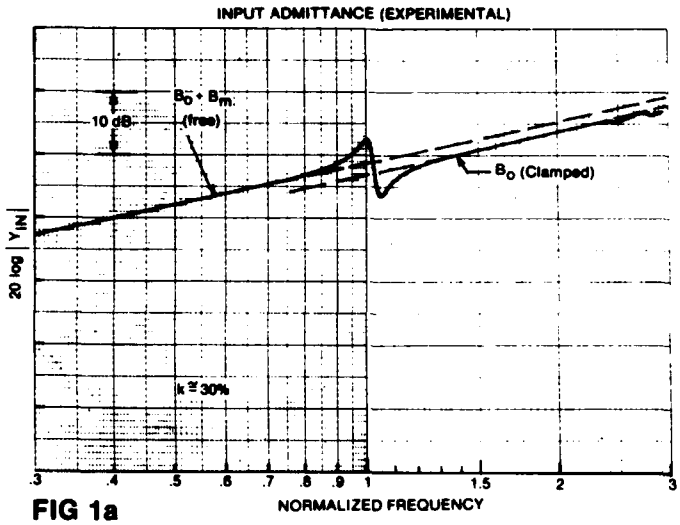

FIG 1a

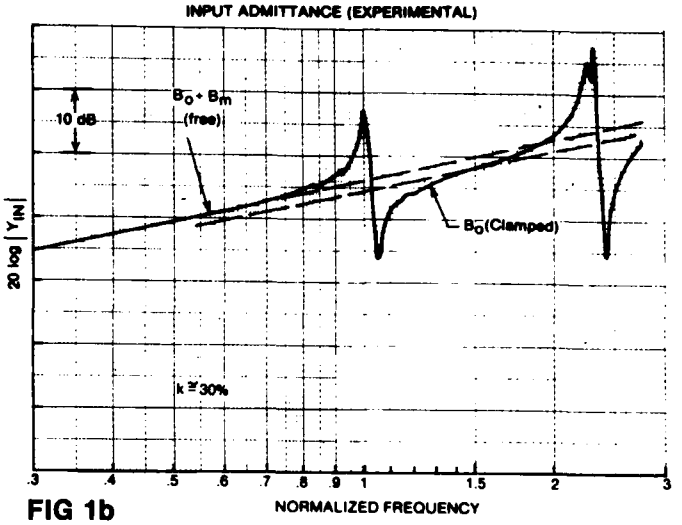

FIG 1b

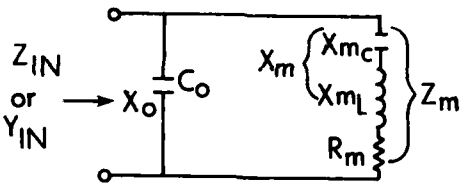

FIG 1c

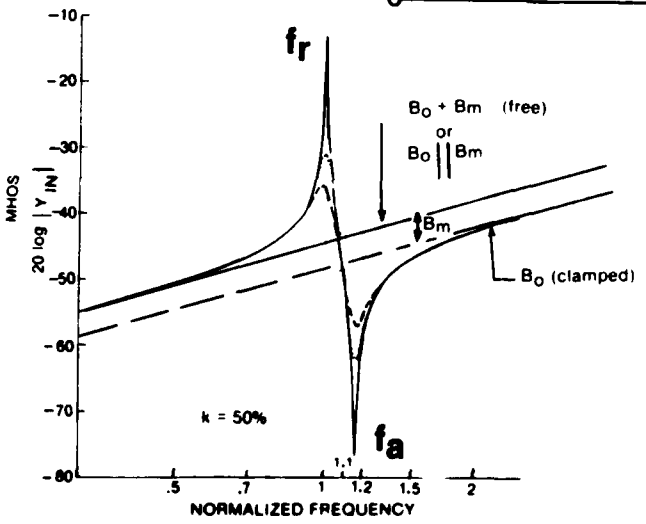

FIG 1d

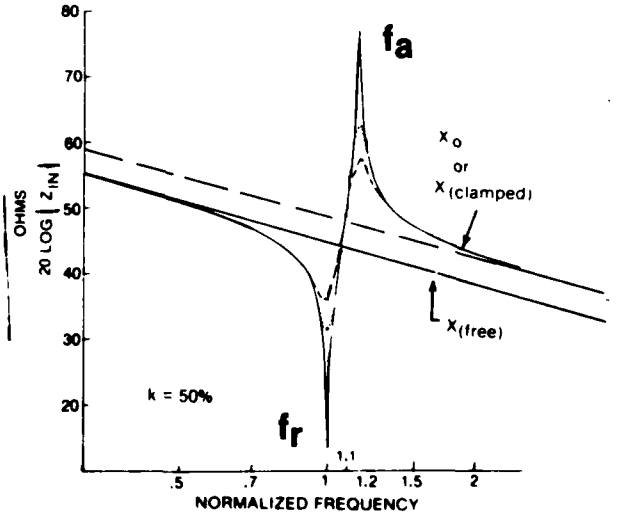

FIG 1e

If we had ignored the term $-\left(\frac{\Delta f}{f_a}\right)^2$ and simply used $k^2 = \frac{2\Delta f}{f_a}$, then $\underline{k} \geq 0.305$. In any event the error is less than 2%.

Figure 1b shows the input admittance of a competitive transducer, similar to that of Figure 1a. In Figure 1b it is very difficult to draw the B_o asymptote since the next overtone (nominally the 3rd harmonic) distorts the slope of B_o. This is because Q_m is high for the overtone as well as for the fundamental. (We note, in passing, that a high air-Q around any resonance implies a high efficiency at that resonance.) But in spite of the difficulty in finding B_o (which is $B_{clamped}$) and hence ΔdB, we can easily obtain Δf. Here $\Delta f/f_a$ is clearly 0.047. So again $\underline{k}$ = 0.30+.

Figs. 1d and 1e show a computer-simulation of a transducer comprised of a stack of PZT rings in the 33 mode. (Three different values of radiation resistance were used.) The value of dynamic k_{33} from Δf is $\simeq$ 0.50.

The value of static k_{33} using the measured value $B_m \simeq$ -3.3dB in the admittance curve of Fig 1d (i.e. log $B_{clamped}$ - log B_{free}), gives static $k_{33} \simeq 0.56$. Equally true, using $\Delta X \simeq$ -3.3dB in the impedance curve of Fig 1e (i.e. log X_{free} - log $X_{clamped}$) gives static $k_{33} \simeq 0.56$. The dynamic k_{33} is thus about 90% of the static k_{33} value, in this case. For future reference:

static $k^2 = \frac{C_m}{C_o + C_m} = \frac{B_m}{B_o + B_m} = \frac{\left(B_{free} - B_{clamped}\right)_{mhos}}{B_{free}\ mhos}$ from Fig 1d by inspection. Using dB: 20 log $(1-k^2) = B_{clamped}$ (dB) - B_{free} (dB) = ΔdB.

If we try to do an analogous derivation for k^2 using Figure 1e and reactances, we run into a problem. It is true that a similar form shows up,

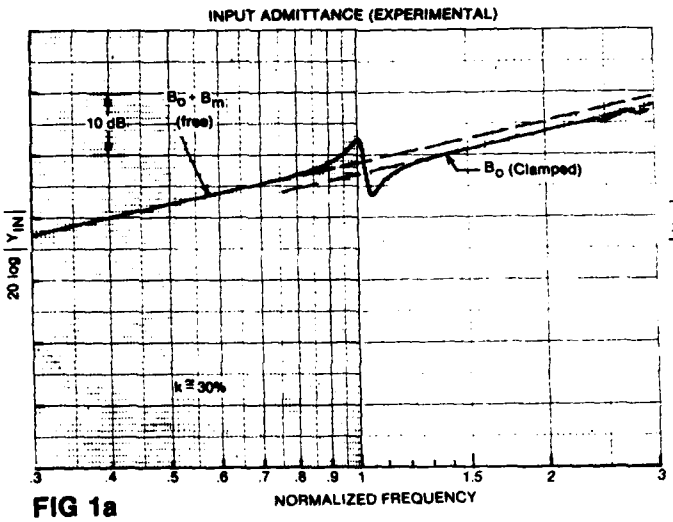

FIG 1a

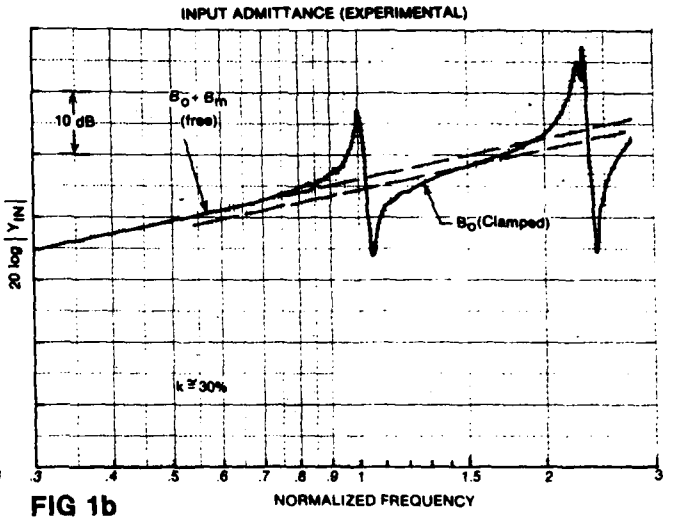

FIG 1b

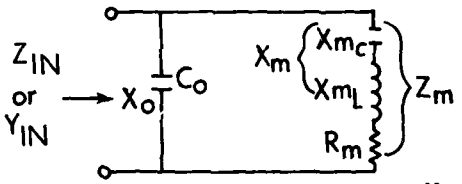

FIG 1c

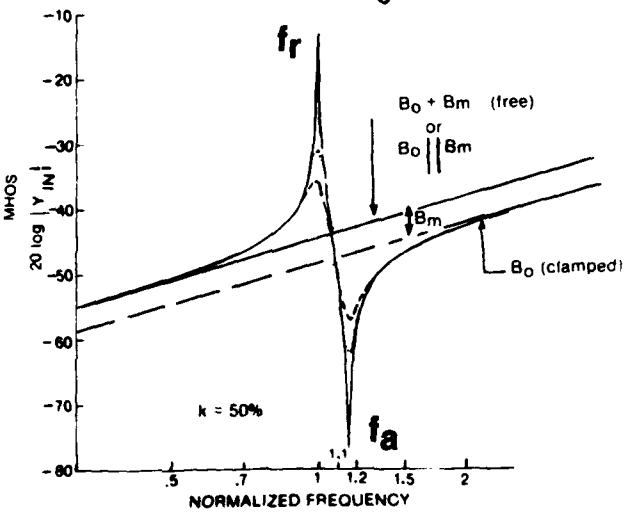

FIG 1d

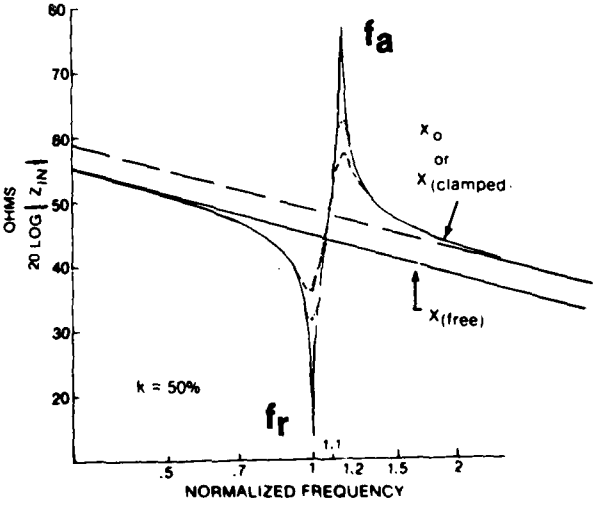

FIG 1e

namely $k^2 = \left(\frac{X_{clamped} - X_{free}}{X_{clamped}} \right)_{ohms}$ *

But the numerator implies a <u>series</u> arrangement for $X_{clamped}$ and X_{free}. Figure 1c, however, shows only a parallel arrangement. What is needed is another <u>form</u> of Figure 1c. This is discussed at length in Chapter 3, where we use the terminology

$$k^2 = \frac{X'_{m_c}}{X'_o + X'_{m_c}}$$

Here X'_{m_c} is indeed the isolated "mechanical" (i.e. motional) reactance, analogous to B_m above. And Xo' is identical with X_{free}.

---

* $1-k^2 = \frac{B_{clamped}}{B_{free}} = \frac{X_{free}}{X_{clamped}}$

$$k^2 = \frac{X_{clamped} - X_{free}}{X_{clamped}}_{ohms}$$

Chapter 2. Further Information Obtainable from $|Z_{in}|$

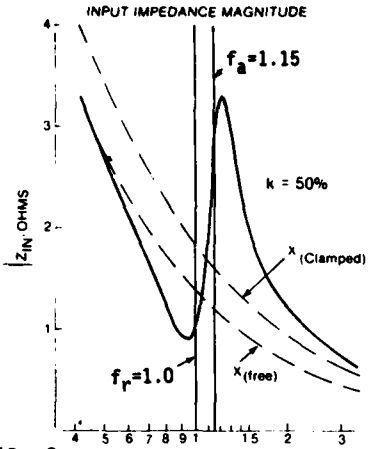

FIG. 2a

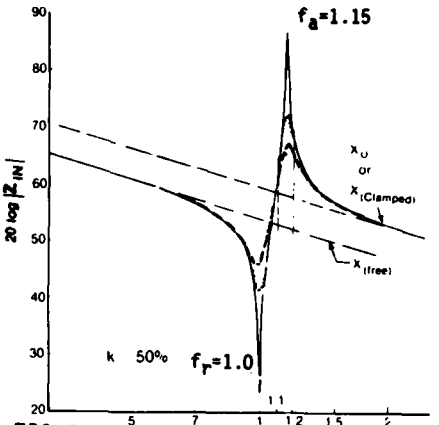

FIG 2b

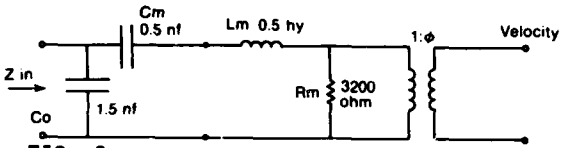

FIG. 2c

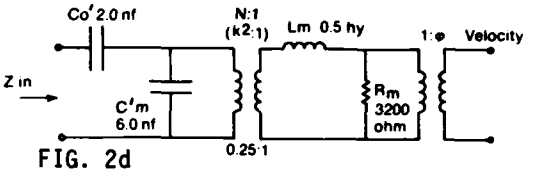

FIG. 2d

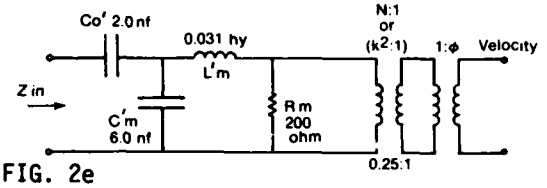

FIG. 2e

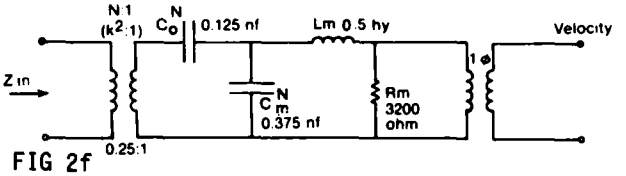

FIG 2f

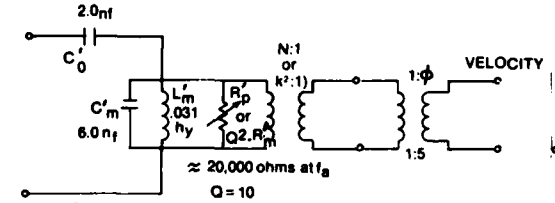

FIG. 2g

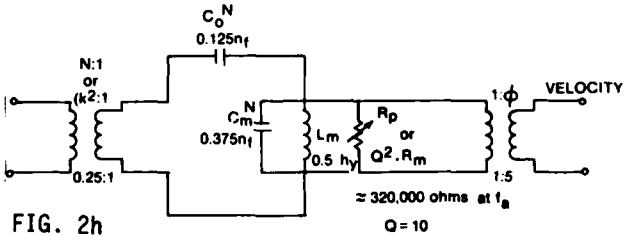

FIG. 2h

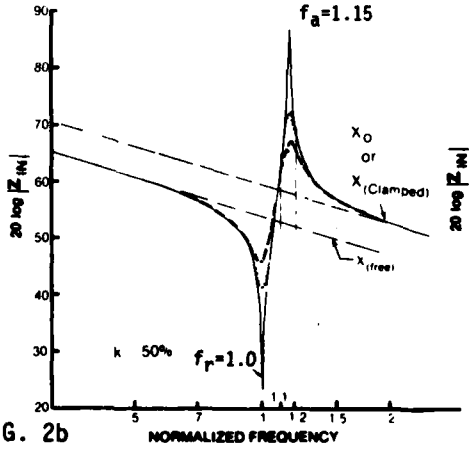

FIG. 2b

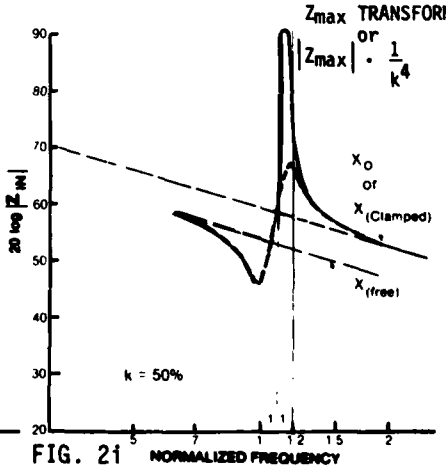

FIG. 2i

Chapter 2. Further Information Obtainable from $|Z_{in}|$.

The Figures illustrate:

a. Input Impedance magnitude, shown both as 20 log $|Z|$ vs. log frequency and as linear-scale $|Z|$ vs. log frequency.
b. Foster's Equivalent Circuits.
c. Determination of Q_m from $|Z|$ curve.

Preliminary Note: The operator $||$ (parallel), when used with impedance elements, will mean for example: $Z_1||Z_2 = \frac{Z_1 \cdot Z_2}{Z_1 + Z_2}$. With admittance elements it means: $Y_1||Y_2 = Y_1 + Y_2$. Likewise the operator $\$$ (series), when used with admittance elements, will mean for example: $Y_1 \$ Y_2 = \frac{Y_1 \cdot Y_2}{Y_1 + Y_2}$. With impedance elements it means: $Z_1 \$ Z_2 = Z_1 + Z_2$.

Introduction. Chapter 2 has two main purposes. (1) The first is to familiarize the reader with "the other Basic Circuit" (seen in Fig 2e). This is different in form from "the Basic Circuit" of Fig 2c, which is, in effect, Mason's modification of the Van Dyke-circuit of Figure 1c. Nevertheless the circuits of Fig 2c and Fig 2e are interchangeable. The reader should practice converting rapidly from Fig 2c to Fig 2e or vice versa. The numbers and ratios are very simple in our repeating examples, often being 3/4 (from $1-k^2$) or 3/1 (from $\left[1-k^2\right]/k^2$), since our $\underline{k} = 0.50$. Hence the converting can be done in one's head. The pay-off to the reader will be large. For, all the difficult manipulations required when the circuit of Fig 2c must handle impedance problems in addition to the admittance problems it is especially suited to—all this becomes greatly simplified as soon as the second circuit is available. The Appendix 2-A shows the general method of converting, following the approach of Shea, "Transmission Networks and Wave Filters".

(2) The second purpose of this chapter is to give an intuitively reasonable derivation of the relation of the mechanical Q, or Q_m, to the

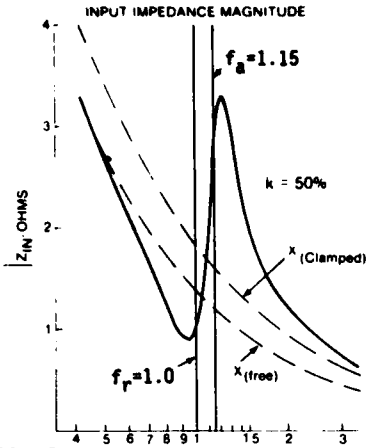

FIG. 2a

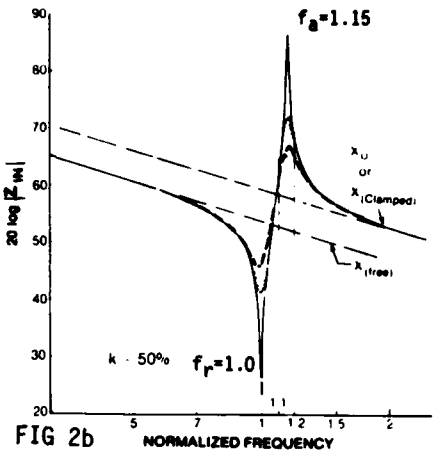

FIG 2b

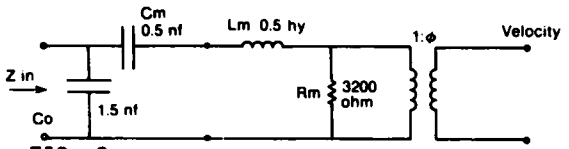

FIG. 2c

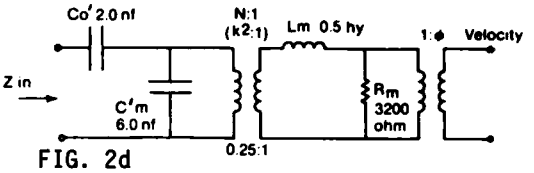

FIG. 2d

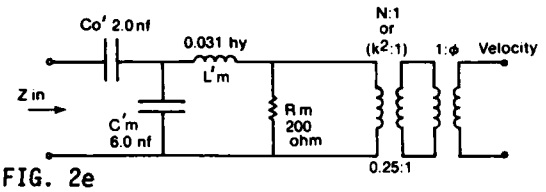

FIG. 2e

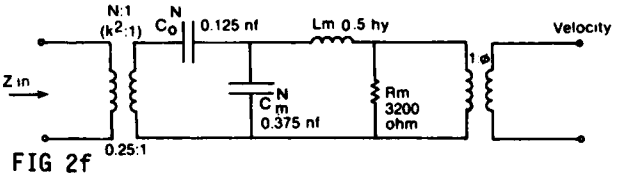

FIG 2f

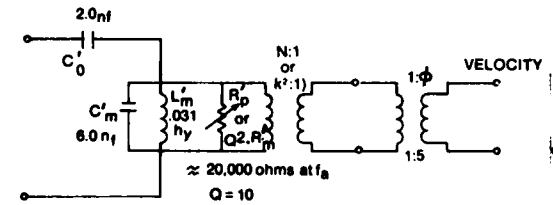

FIG. 2g

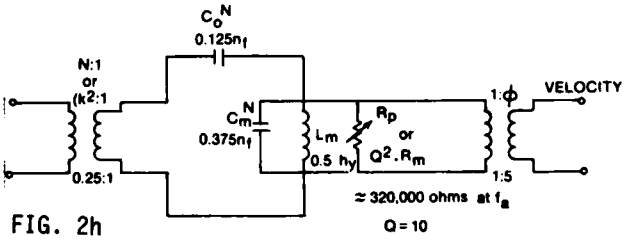

FIG. 2h

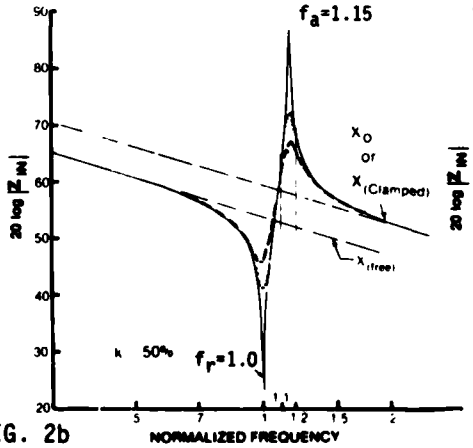

FIG. 2b

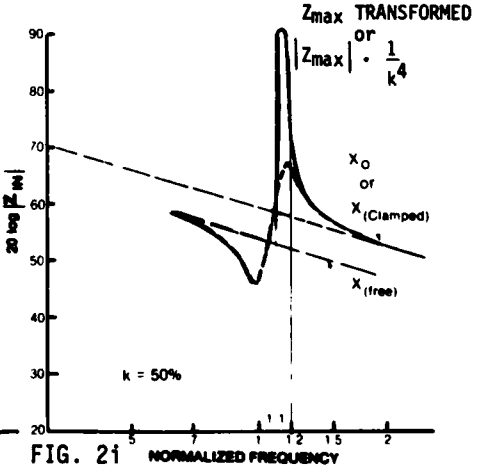

FIG. 2i

ratio $|Z_{max}| / |Z_{min}|$. The standard derivations are much more complicated and not much more accurate. The present derivation is worth the learning effort.

Figure (2a) shows linear $|Z_{in}|$ vs log frequency for a low-Q transducer. Figure (2b) shows log |Z in| vs log frequency for this transducer when the Q's are much higher. If the frequency scale were linear in Fig. (2a) the converging asymptotes $X_{clamped}$ and X_{free} would be true hyperbolas. The log scale compresses the frequency axis and slightly distorts the hyperbolas. But we will retain a log frequency scale throughout this handbook because the shape of a curve, thereby, is invariant as the resonance frequency is moved around. In Fig 2b the asymptotes are two parallel straight lines.

To show some further differences in <u>appearance</u> of things on a linear scale vs. a log scale: In Fig (2a) a linear impedance curve is shown, corresponding to one given value of Q_m; and in Fig. (2b) log impedance curves are shown corresponding to three different values of Q_m. These three curves intersect at a point close to the mean frequency, viz. $\sqrt{f_r \cdot f_a}$, where f_r is the resonance frequency and f_a is the anti-resonance frequency, as discussed in Chapter 1. The point of intersection is seen, in Fig. (2b), to be located (along the ordinate) more or less midway between log $|Z_{min}|$ and log $|Z_{max}|$. In Fig. (2a), linear $|Z_{min}|$ and $|Z_{max}|$ are clearly <u>not</u> symmetrically disposed about this point (interpolated). And indeed, if Q_m approaches infinity, $|Z_{min}|$ is $\simeq 0$ and $|Z_{max}|$ is $\simeq \infty$ and the asymmetry is all the clearer. But the two asymptotes are unaffected by Q_m and always enclose this point of intersection.

It has long been observed that a close relation exists between the ratio $|Z_{max}| / |Z_{min}|$ and the mechanical "quality factor" or selectivity

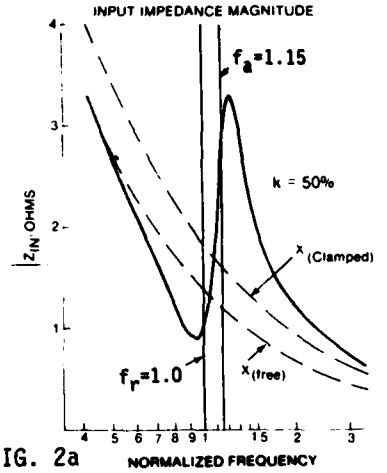

FIG. 2a

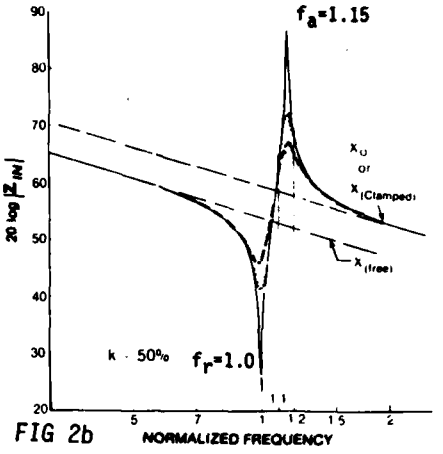

FIG 2b

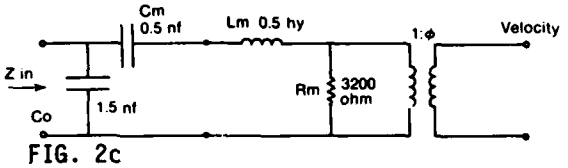

FIG. 2c

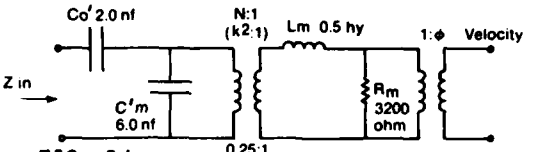

FIG. 2d

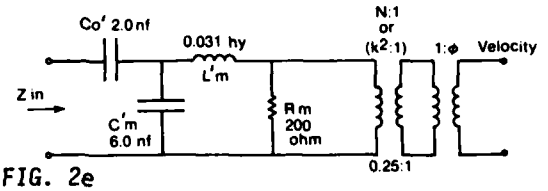

FIG. 2e

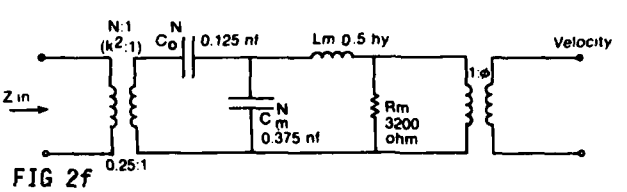

FIG 2f

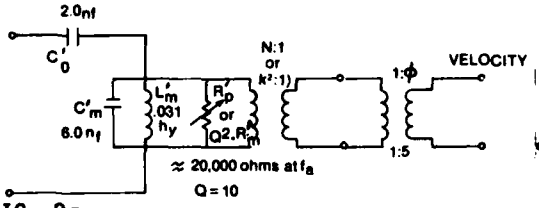

FIG. 2g

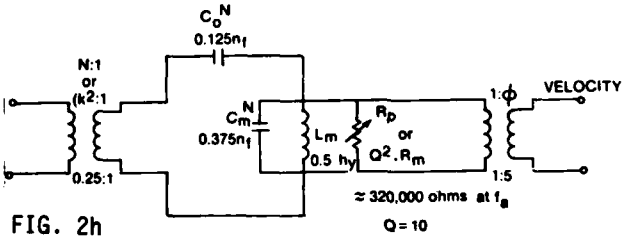

FIG. 2h

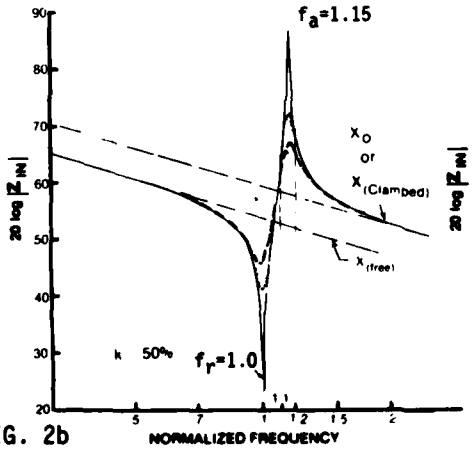

FIG. 2b

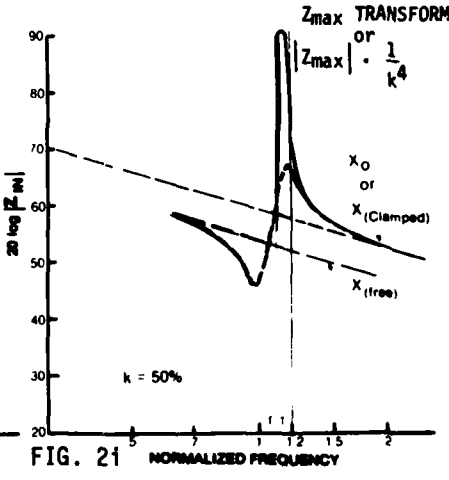

FIG. 2i

factor Q_m. The desired relation can be found in the connection between Fig. (2c) and Fig. (2e). Figure 2c is often taken (arbitrarily)as "the Basic Circuit" of a transducer.

1. Foster's Equivalent Circuits

Figure (2e) is an alternate form of Fig. (2c). The two are exactly equivalent and are discussed in detail (when $R_m = 0$) in Foster's paper "A Reactance Theorem, and in writings by Shea, and Norton.* We will refer to Fig. (2c) as the Half-Pi circuit and Fig. (2e) as the Half-Tee circuit. In both circuits, ϕ is the electro-mechanical transformer (which is not needed by Foster et al). Calculations made with either circuit will give the correct and same impedance values over the whole frequency band.

Now if we reserve Fig (2c) for the band around the mechanical resonance frequency f_r (electric terminals short-circuit) and reserve Fig. (2e) for the band around the "anti-resonance" frequency f_a (the mechanical resonance frequency for open-circuit electric terminals), the Z_{in} calculations become greatly simplified for the the two regions, resonance and anti-resonance. We have converted a Half-Pi input to a Half-Tee input in changing Fig. (2c) to Fig (2e). The additional (purely electrical) transformer N:1 is merely implied by Foster, but is explicitly used by Shea, Norton, and others. It turns out that their N is exactly the same quantity as our k^2, as shown in Appendix 2-A. The equivalence of the circuits of Figs. 2c and 2e can be confirmed by testing the open-circuit and short-circuit input immittances, looking first into the left port and then into the right port. Thus impedances like R_m transform as k^4 to become R_m'. (Cf. the conversion of Fig 2d into Fig. 2e.)

*See Appendix 2-A

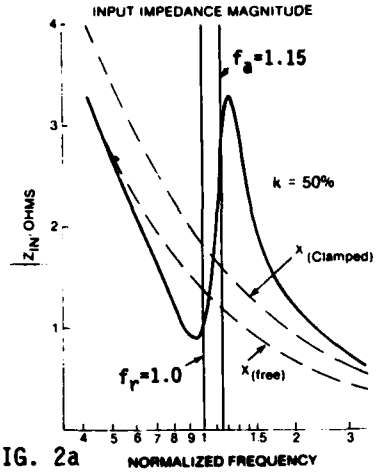

FIG. 2a

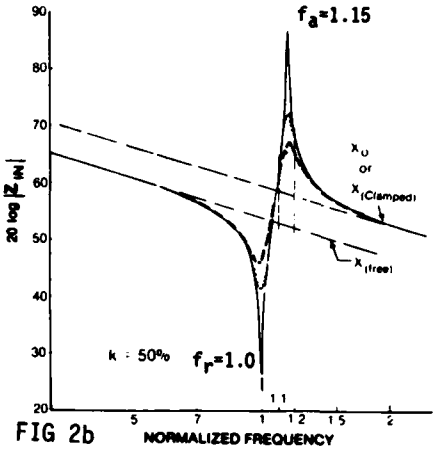

FIG 2b

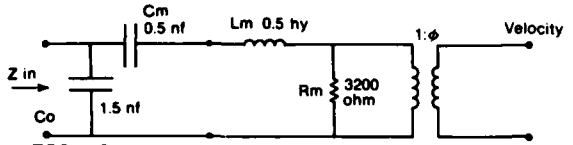

FIG. 2c

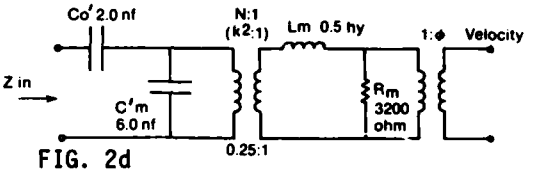

FIG. 2d

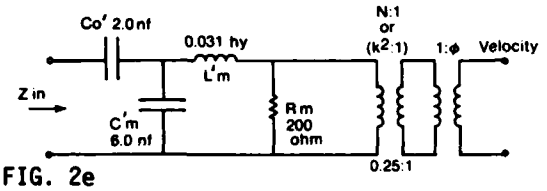

FIG. 2e

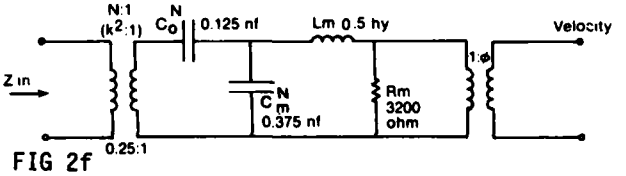

FIG 2f

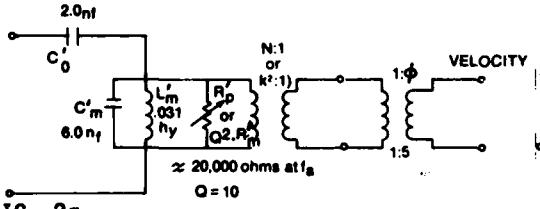

FIG. 2g

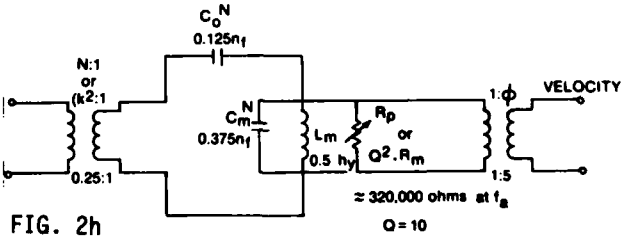

FIG. 2h

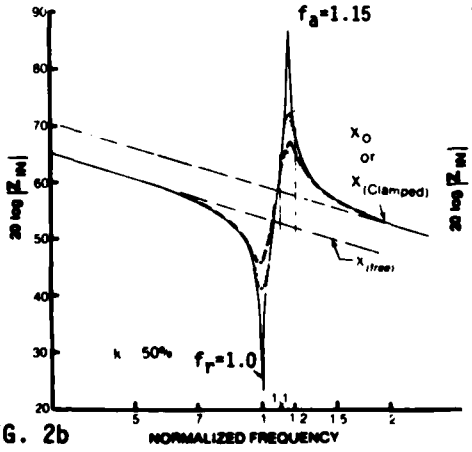

FIG. 2b

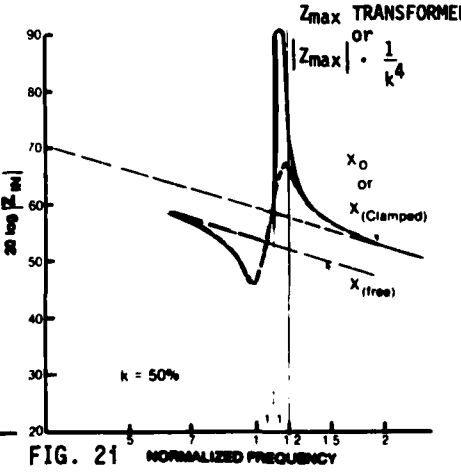

FIG. 21

As an example, let us consider a transducer with k=0.50 and f_r = 10 kHz. The specific value of ϕ is unimportant, but happpens to be 5N/volt. Referring to Fig. (2c), let C_o = 1.5nF, C_m = 0.5nF, L_m ≃ 0.5H, X_{m_L} = 32,000 ohms at the f_r of 10 kHz, and R_m = 3200 ohms.

Then for constant-voltage drive $Q_m^E = \frac{X_{m_L}}{R} = 10$.

Moving over to Fig. (2d): C_o' = 2.0nF, C_m' = 6.0nF, and N^2:1 or k^4:1 is 1/16:1. L_m and R_m are unchanged as yet. Then progressing to Fig. (2e), C_o' and C_m' are unchanged; but L_m' and R_m' are *now divided by 16*. Thus R_m' = 200 ohms, L_m' = .031 H and X_{m_L}' ≃ 2000 ohms at either f_r or f_a. [This is an approximate reactance value that an observer at the electric terminals sees at the "anti-resonance" f_a of 11.5 kHz. It is more useful for the moment than the exact value of 2300 ohms which, under constant-current drive, would give a Q_m^I of 11.5.]

The two transformers in Fig. (2e), N:1 and 1:ϕ, are usually combined (multiplied) into a single transformer N/ϕ or k^2/ϕ which is then called N':1. In the present example this would be .05:1, since $k^2 = \frac{1}{4}$ and ϕ = 5, giving $\frac{1}{20}$. But this combining conceals some useful information; so we will keep them uncombined.

Note that Q_m^E is still = 10, even though the (X_L, R) impedance level has dropped by 16 to one, or -24 dB on a 20 log scale. Alternatively, we can retain the original (X_L, R) impedance level by sending C_o' and C_m' through the N:1 transformer thus multiplying by k^4, to become C_o^N and C_m^N as

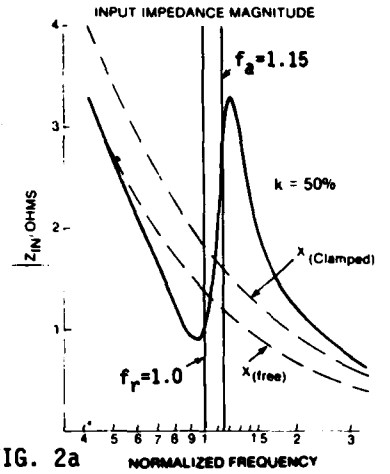

FIG. 2a

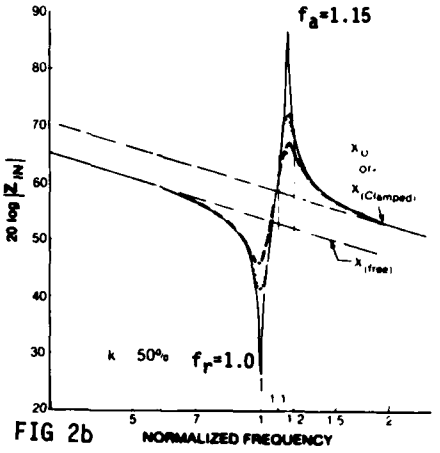

FIG 2b

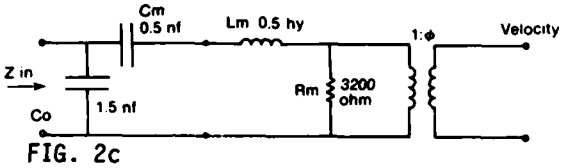

FIG. 2c

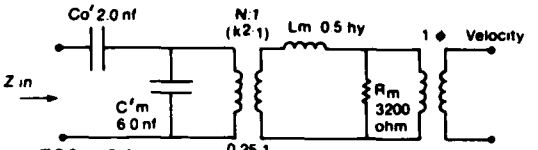

FIG. 2d

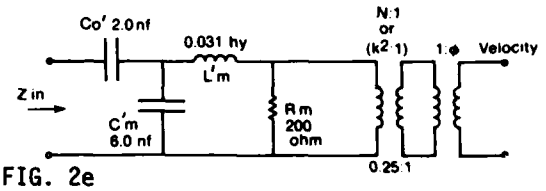

FIG. 2e

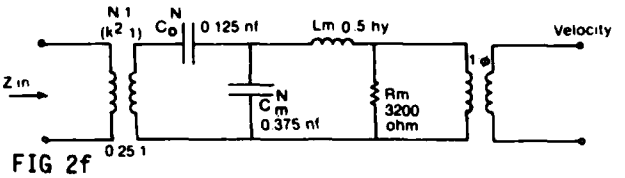

FIG 2f

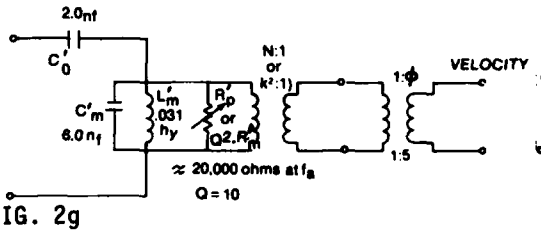

FIG. 2g

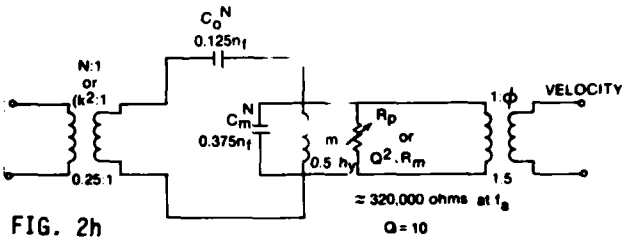

FIG. 2h

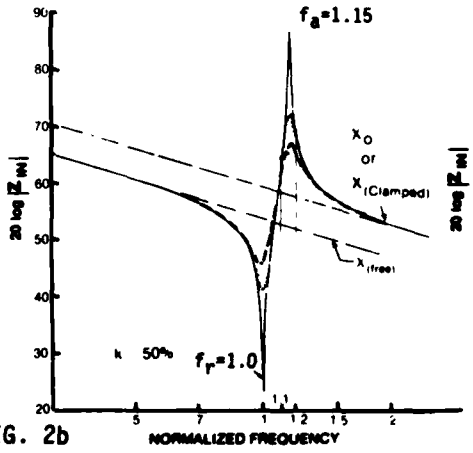

FIG. 2b

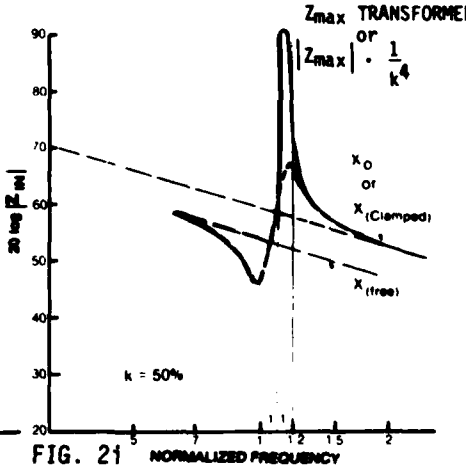

FIG. 21

shown in Fig. (2f). Then C_o^N = 0.125 nF and C_m^N = 0.375 nF. This clearly shows how to compare the resonance frequency f_r, at sight, with the anti-resonance frequency f_a, using C_m^N = 0.375 nF in Fig. (2f). The anti-resonance f_a (electric open-circuit) must therefore occur at a higher frequency than the resonance f_r (electric short-circuit) which uses C_m = 0.5 nF in Fig. (2c). The frequency ratio is $\sqrt{0.5/0.375}$ or $\sqrt{4/3}$ or about 1.15:1. [This of course is one reason for having Foster's <u>two</u> forms always in mind.] In this handbook the values of 1.15 for f_a, and 1.0 for f_r will be used in every chapter, along with $\underline{k}$ = 0.50. Also the Q_m^E (for constant-voltage drive) will usually be arranged to be 10, in sample calculations. The Q_m^I (for constant-current drive) would then be 11.5. But for convenience we will sometimes let $Q_m^I \simeq Q_m^E$, giving the value 10 for both the constant-current and the constant-voltage situations. And we will then give it the undifferentiated name Q_m.

It is sometimes useful to make one more conversion of Fig. (2e), into an equivalent represented by Fig. (2g). C_o' and C_m' are unaffected. And if Q_m^I is 10 or greater, L_m' is approximately constant with frequency and has the same value as in Fig. (2e). Then the only variable element is R_p', a variable parallel resistance which has replaced the invariant series R_m' of Fig. (2e). R_p' is called the inverse conductance of the "tank circuit".

2. Derivation of "quality factor" Q_m^I from $|Z_{max}|$ and $|Z_{min}|$

From prior knowledge we know that $Q_m^I \simeq 10$. Now however we will try to find this value by measurement, at the input terminals, pretending that it is unknown. To derive Q_m^I, the "quality-factor" around f_a for

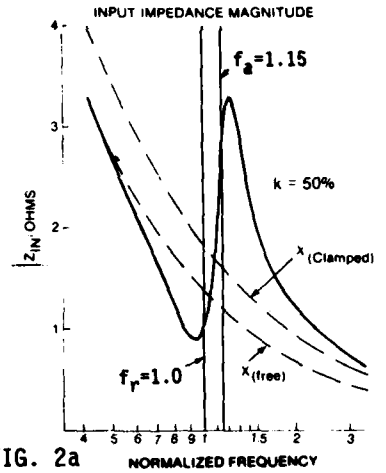

FIG. 2a

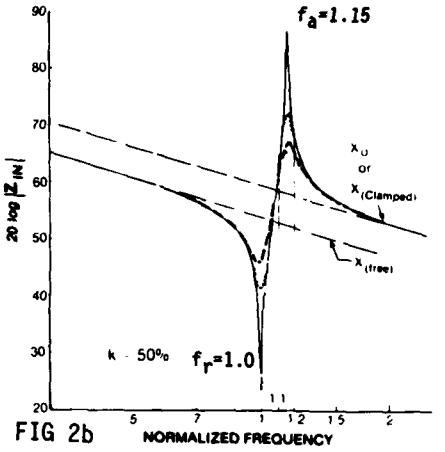

FIG 2b

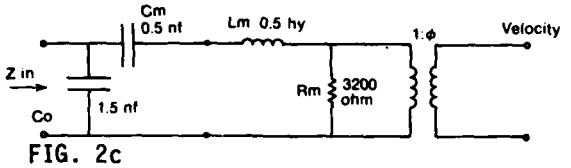

FIG. 2c

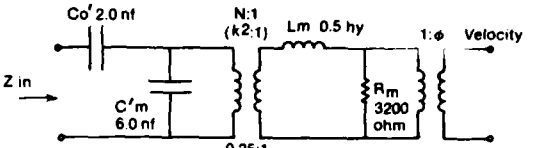

FIG. 2d

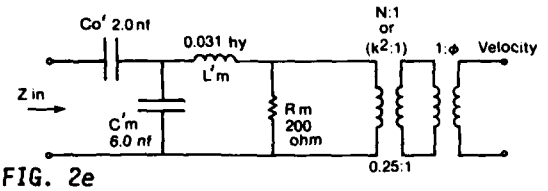

FIG. 2e

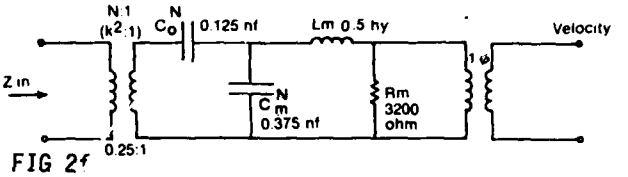

FIG 2f

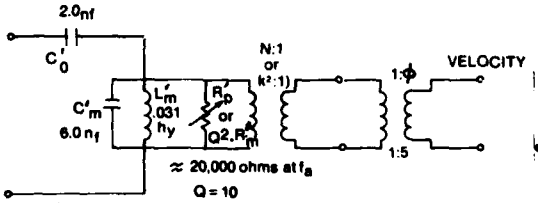

FIG. 2g

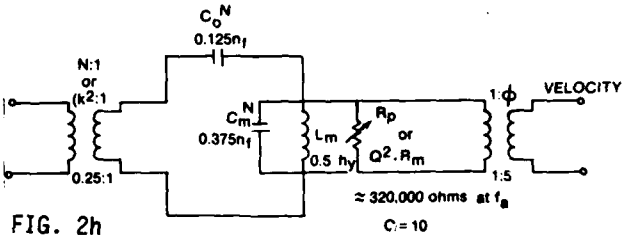

FIG. 2h

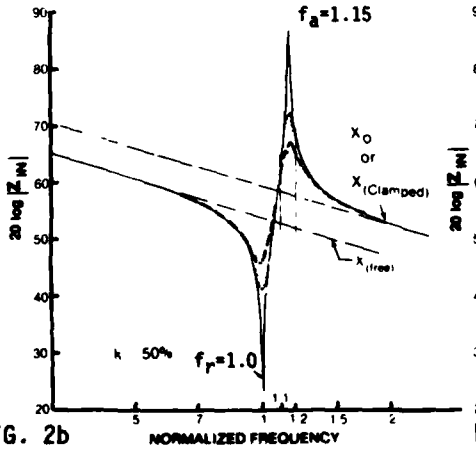

FIG. 2b

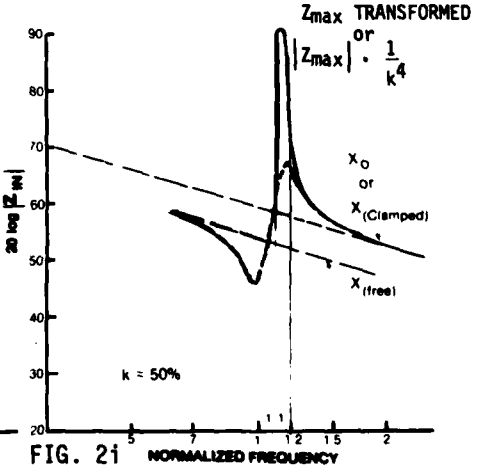

FIG. 2i

constant-current drive, we will work with R_p'. Now

$$R_p' = (1 + Q_m^{I^2}) \times R_m' \simeq Q_m^{I^2} \times R_m'. \tag{2.11}$$

From Fig. 2g this is seen to be 100 x 200 or 20,000 ohms, for the specific example. Then at anti-resonance f_a

$$Z_{in} \simeq jX_o' + R_p' \tag{2.12}$$

But the contribution of jX_o' is usually small enough so that we can say

$$|Z_{in}|_{f_a} \simeq R_p' \simeq Q_m^{I_2} \times R_m'. \tag{2.13}$$

If now we take the ratio $|Z_{in}|_{f_a} \Big/ |Z_{in}|_{f_r}$ which is also known as $|Z_{max}| \Big/ |Z_{min}|$ (as seen in Fig. 2a) we get

$$|Z_{max}| \Big/ |Z_{min}| \simeq \frac{Q_m^{I^2} \times R_m'}{R_m} \qquad \text{(neglecting the small contribution of } jB_o\text{).} \tag{2.2}$$

But this equation is <u>not</u> what we are looking for in order to isolate $Q_m^{I_2}$. It uses both R_m from Fig. 2c, and R_m' from Figs. 2e and 2g. So we must go further.

If we proceed from Fig. 2g to Fig. 2h by sending all impedances to the right through the turns-ratio $\frac{1}{k^2}$, we multiply $|Z_{max}|$ by $\frac{1}{k^4}$. From input measurements we can determine that $\underline{k} = 0.50$ and that hence $\frac{1}{k^4}$ is 16 in this case. Then

$$|Z_{max}| \cdot \frac{1}{k^4} = |Z_{max}| \cdot 16 \simeq R_p' \cdot 16 \simeq Q_m^{I_2} (R_m' \cdot 16) = Q_m^{I^2} \cdot R_m. \tag{2.3}$$

The value of $|Z_{max}|$ transformed is thus about 320,000 ohms in this case.

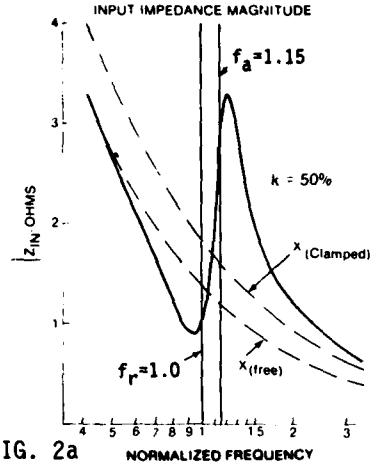

FIG. 2a

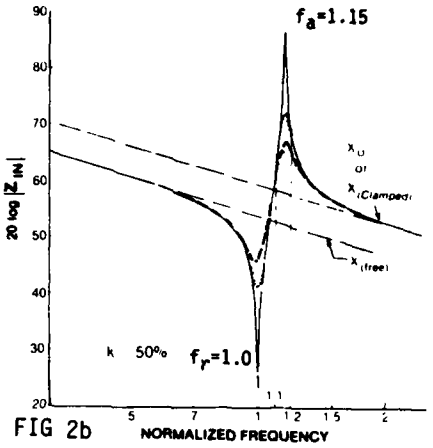

FIG 2b

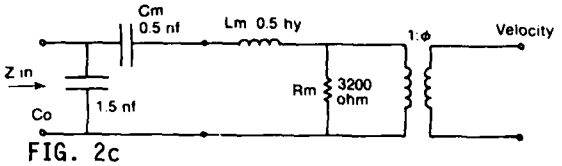

FIG. 2c

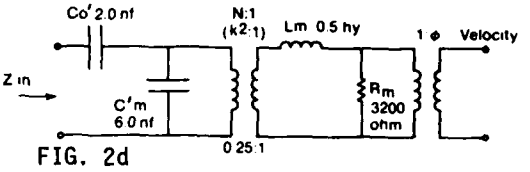

FIG. 2d

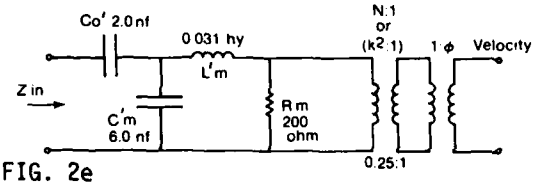

FIG. 2e

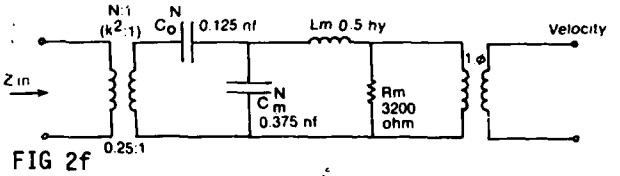

FIG 2f

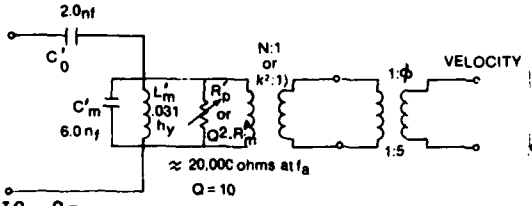

FIG. 2g

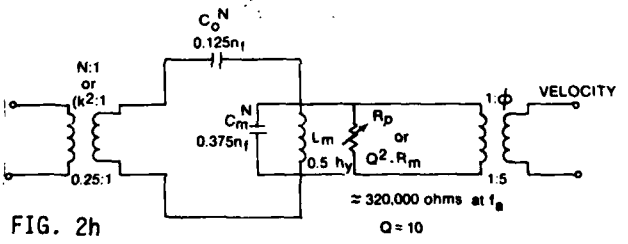

FIG. 2h

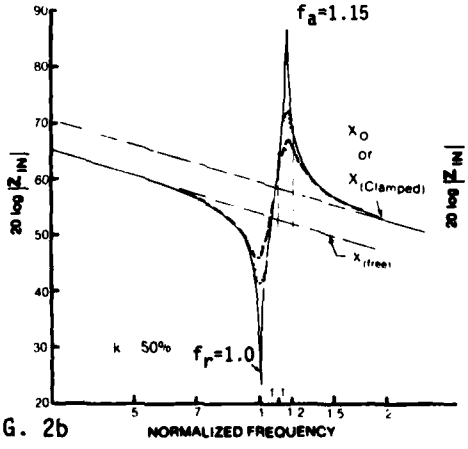

FIG. 2b

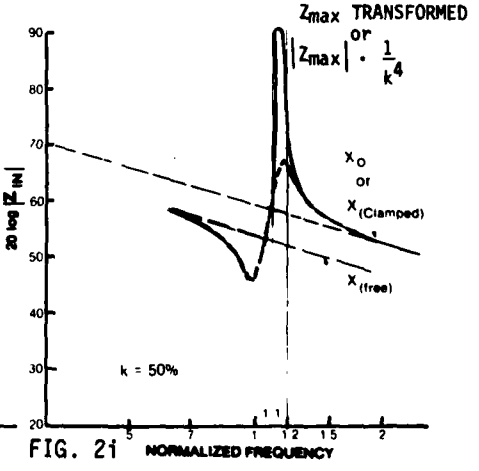

FIG. 2i

And then for the general case, $|Z_{max}| \times 1/k^4$ or $|Z_{max}|$ transformed divided by $|Z_{min}|$ gives:

$$|Z_{max}| \times \frac{1}{k^4} \Big/ |Z_{min}| = \frac{Q_m^{I^2} \times R_m}{R_m} = Q_m^{I^2} . \qquad (2.4)$$

A geometrical meaning of $|Z_{max}| \times 1/k^4$ is shown in Fig. 2i, where the transformed $|Z_{max}|$ is superposed on the simple $|Z_{max}|$ of the lowest-Q curve of Figure 2b. The transformed $|Z_{max}|$ is increased by 24 dB, as will be shown.

If we convert Eq. 2.4 to dB (using a 20 log scale for our dB) and if we also use some numbers; then, recalling that $1/k^4$ or 16/1 is +24 dB:

$$20 \log |Z_{max}| + 24 \text{ dB} - 20 \log |Z_{min}| = 40 \log Q_m^I. \qquad (2.51)$$

or

$$|Z_{max}| \text{ dB} - |Z_{min}| \text{ dB} + 24 \text{ dB} = 2\, Q_m^I \text{ dB} \qquad (2.52)$$

or

$$\frac{\Delta dB}{2} + 12 \text{ dB} = Q_m^I \text{ dB} \qquad (2.53)$$

where ΔdB refers to $|Z|^{dB}$ at f_a minus $|Z|^{dB}$ at f_r; and the 12 dB is the value of $1/k^2$.

Then in the general case, using a 20 log scale:

$$\frac{\Delta dB}{2} + (1/k^2)dB = Q_m^I \text{ dB}. \qquad (2.6)$$

Or, on a linear scale:

$$Q_m^I = \sqrt{\frac{|Z_{max}|}{|Z_{min}|}} \times \frac{1}{k^2} \cdot \left(\text{Formerly } \sqrt{\frac{|Z_{max}| \cdot \frac{1}{k^4}}{|Z_{min}|}} . \right) \qquad (2.71)$$

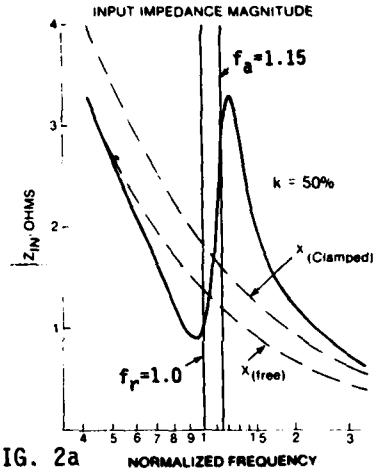

FIG. 2a

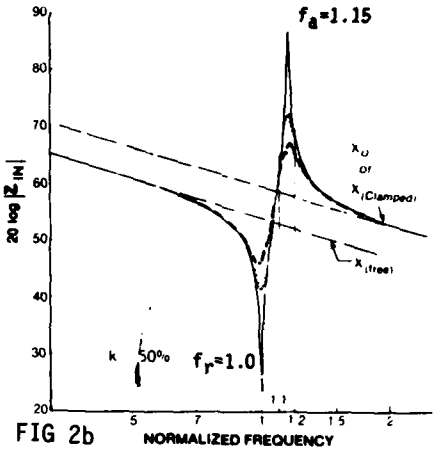

FIG 2b

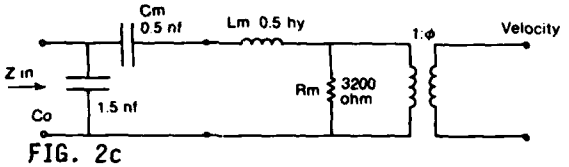

FIG. 2c

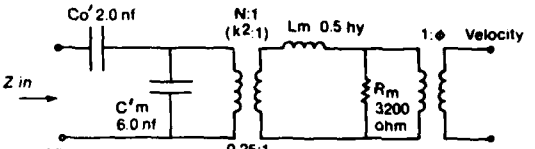

FIG. 2d

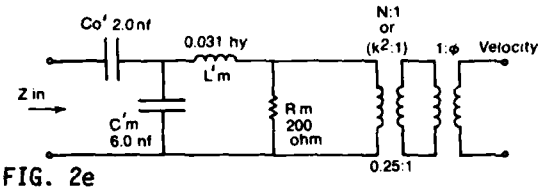

FIG. 2e

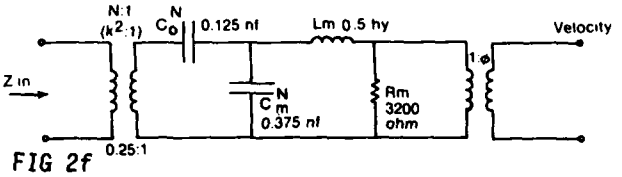

FIG 2f

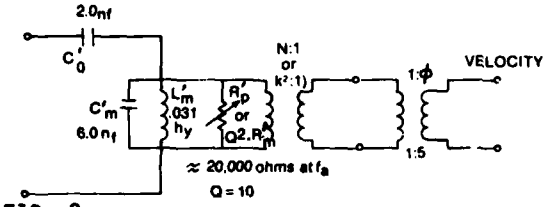

FIG. 2g

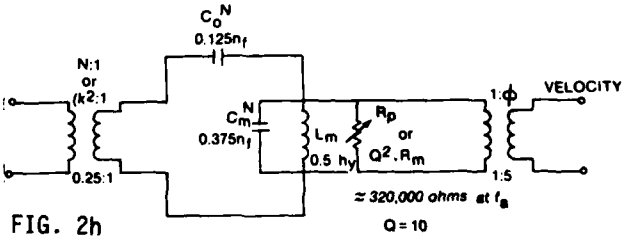

FIG. 2h

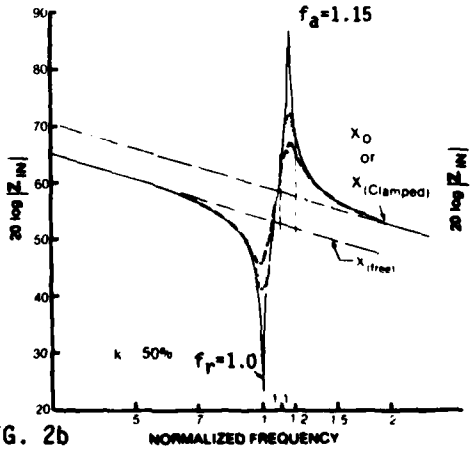

FIG. 2b

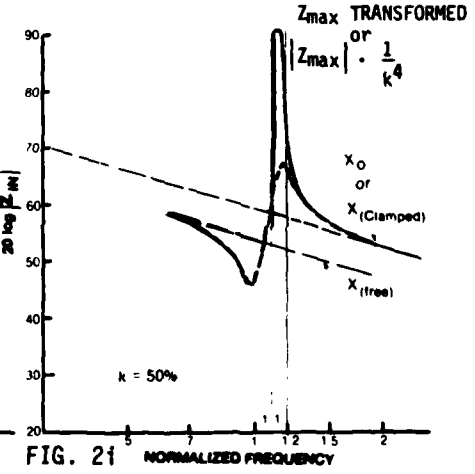

FIG. 2i

This equation sometimes occurs in the literature as:

$$k^2 Q_m^I = \sqrt{\frac{|Z_{max}|}{|Z_{min}|}} \tag{2.72}$$

And since $Z_{max} = 1/Y_{min}$ (at f_a) and $Z_{min} = 1/Y_{max}$ (at f_r),

$$k^2 Q_m^I = \sqrt{\frac{|Y_{max}|}{|Y_{min}|}} \text{ , also.} \tag{2.73}$$

Now if we wish to find an expression for Q_m^E, the quality factor around f_r, we must modify (Eq. 2.71). We could have used only the circuit of Fig. 2c in deriving Q_m^I. It was simply more convenient to use Figs. 2g and 2h in addition. We will now make further use of Figure 2c. We will short the electric terminals, in order to find f_r; and we will observe that R_m = 3200 ohms at both f_a and f_r (and indeed over the whole band). Hence the only factor that changes from f_a to f_r is the reactive term.

Now $Q_m^E = \frac{\omega_r L_m}{R_m}$. And $Q_m^I = \frac{\omega_a L_m}{R_m}$. So $Q_m^E / Q_m^I = \omega_r / \omega_a$.

But from Fig. 2c, $\omega_r = \frac{1}{\sqrt{C_m \cdot L_m}}$ and $\omega_a = \frac{1}{\sqrt{(C_m \parallel C_o) \cdot L_m}}$.

$$\left.\begin{aligned} \text{So } \omega_r/\omega_a &= \sqrt{\frac{C_m \parallel C_o}{C_m}} = \sqrt{\frac{C_o}{C_m + C_o}} \\ \text{or} \quad & \\ & \sqrt{\frac{0.375}{0.5}} = \sqrt{\frac{1.5}{2.0}} \end{aligned}\right\} = \sqrt{1 - k^2} \text{ ,} \tag{2.81}$$

as can be easily seen from Eq. I.2 .

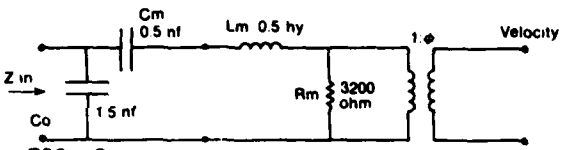

FIG. 2c

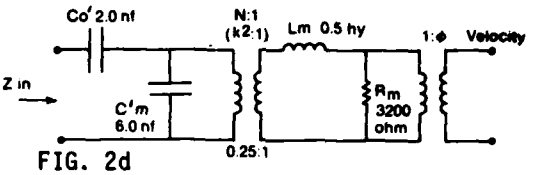

FIG. 2d

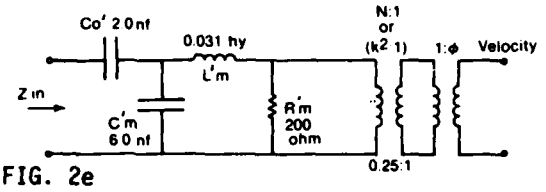

FIG. 2e

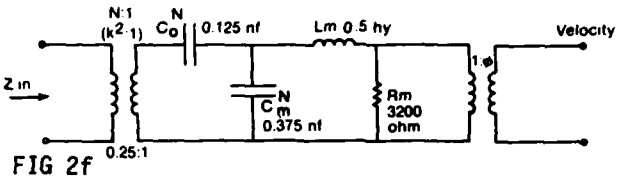

FIG 2f

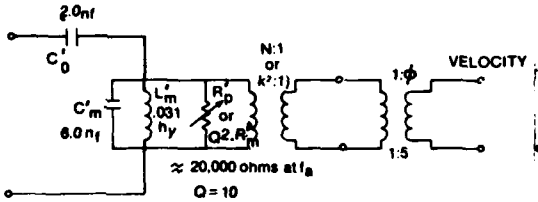

FIG. 2g

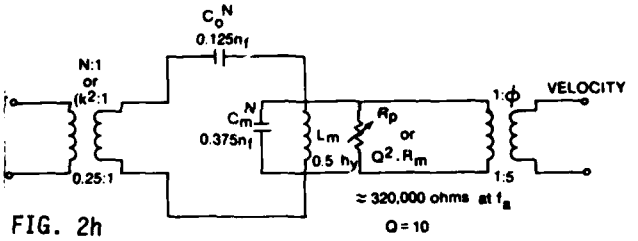

FIG. 2h

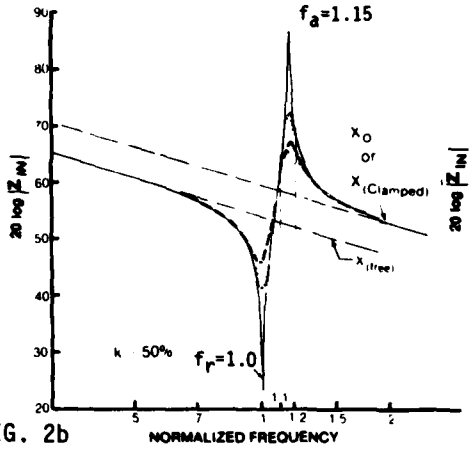

FIG. 2b

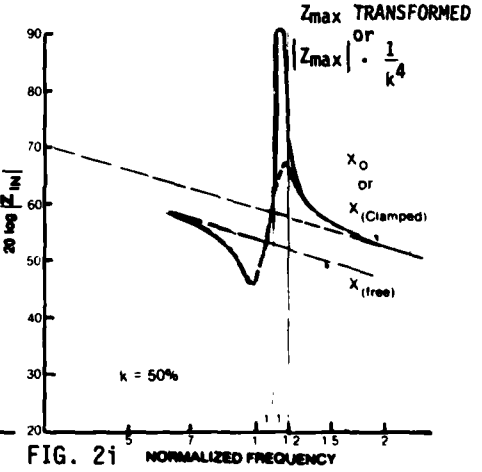

FIG. 2i

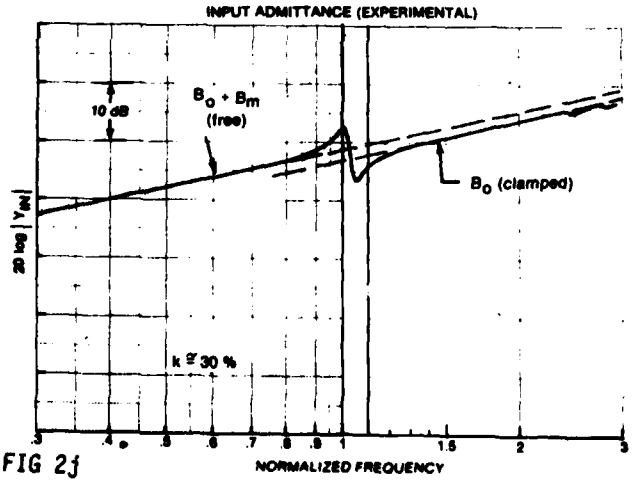

FIG 2j

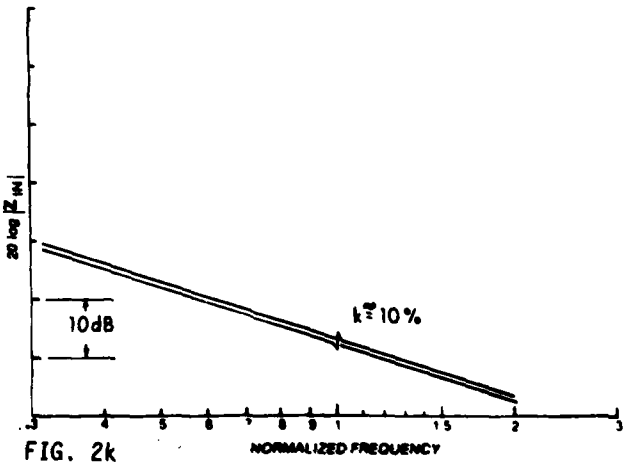

FIG. 2k

Then $Q_m^E = Q_m^I \times \omega_r/\omega_a = Q_m^I \cdot \sqrt{1 - k^2}$. (2.82)

And from Eq. 2.71, $Q_m^E = \sqrt{\frac{|Z_{max}|}{|Z_{min}|}} \cdot \frac{\sqrt{1 - k^2}}{k^2}$. (2.91)

Now in Appendix 2-A, references are given to alternative derivations of Q_m^E, rather more difficult, which finally give:

$$Q_m^E \simeq \sqrt{\frac{|Y_{max}|}{|Y_{min}|}} \cdot \frac{\omega_a}{\omega_r} \cdot \frac{1 - k^2}{k^2} \quad . \tag{2.92}$$

But $\omega_a/\omega_r = \frac{1}{\sqrt{1 - k^2}}$. So we get

$$Q_m^E \simeq \sqrt{\frac{|Y_{max}|}{|Y_{min}|}} \cdot \frac{\sqrt{1 - k^2}}{k^2} \quad . \tag{2.93}$$

And we see that this is the same as our Eq. 2.91. $\left(\text{Since } \frac{Ymax}{Y\,min} \simeq \frac{Zmax}{Z\,min}\right)$

Returning to Eq. 2.6 *and* Q_m^I *in* dB:

$$Q_m^I \text{ (dB)} = \frac{\Delta dB}{2} + (1/k^2)dB \quad . \tag{2.6}$$

Now, the relatively small $1/k^2$ factor of 12 dB (in Eq. 2.53) or 4:1, was due to the relatively large $\underline{k}$ of 0.50. *Thus in Fig. 2b,* the lowest-Q curve shows a ΔdB of about 21.5 dB. This results in a Q_m^I(dB) of only about 22.75 dB or $Q_m^I \simeq 13.7$.

But when the $\underline{k}$ is reduced to 0.30, as in Fig. 1a (repeated here as Fig. 2j), the $1/k^2$ factor is 11:1 or 21 dB. And then although ΔdB is only 9 dB, this results in a Q_m^I(dB) of 25.5 dB or $Q_m^I \simeq 19$.

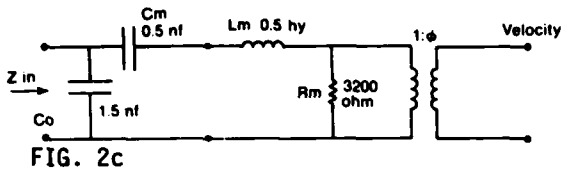

FIG. 2c

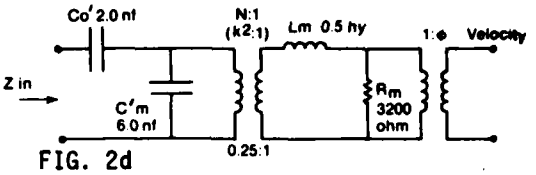

FIG. 2d

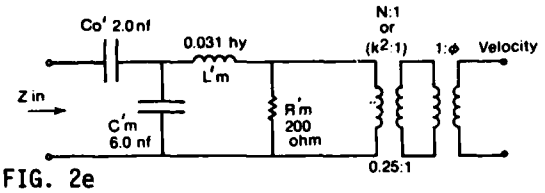

FIG. 2e

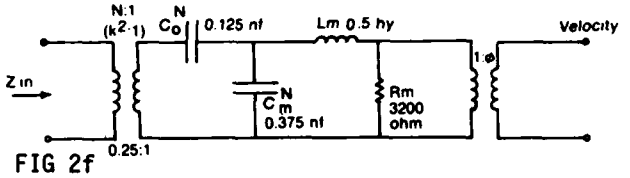

FIG 2f

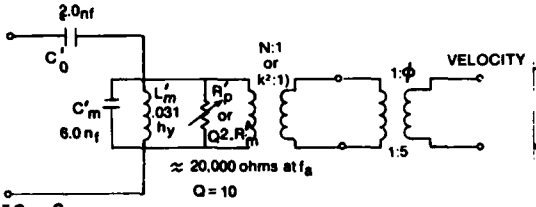

FIG. 2g

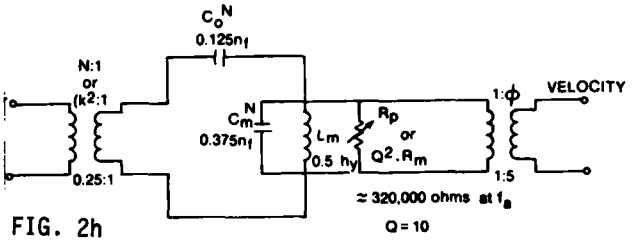

FIG. 2h

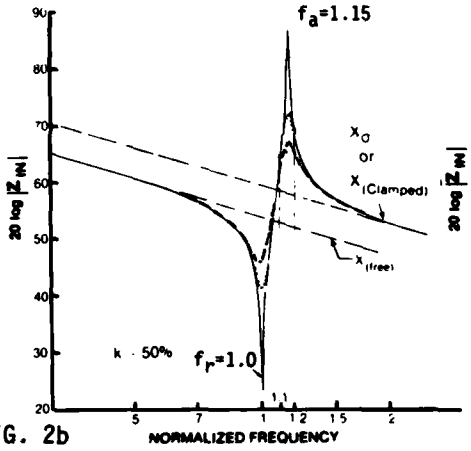

FIG. 2b

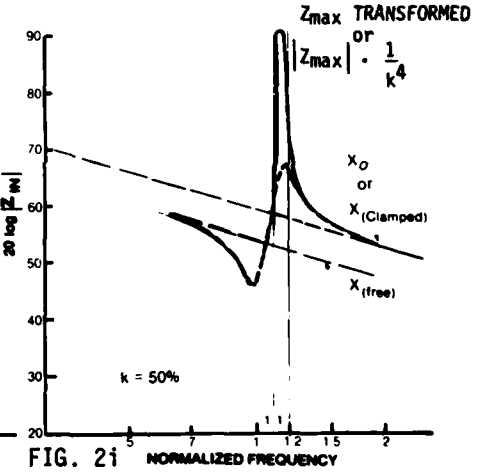

FIG. 2i

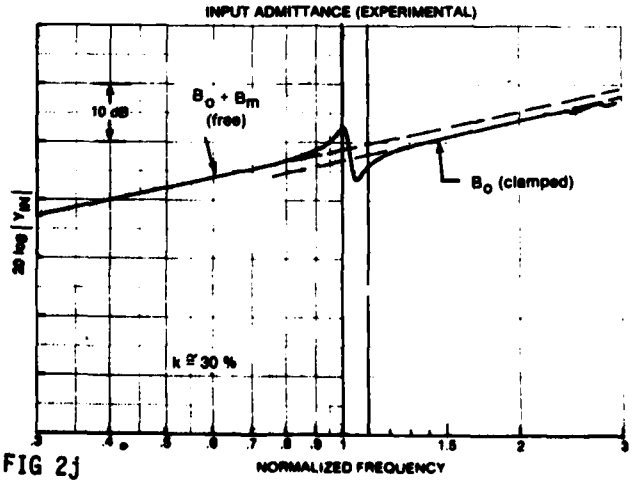

FIG 2j

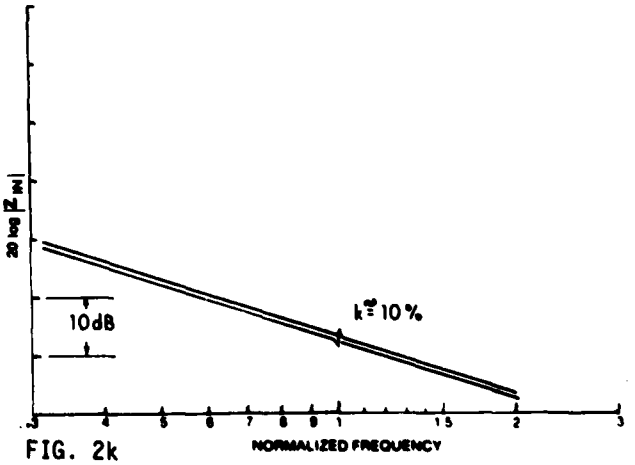

FIG. 2k

The point is that when the coupling coefficient is fairly low, 30% in this case, the decoupling (of the mechanical branch from the electrical branch) is high. Hence even a slight bump from the mechanical branch becomes significant. It means that Q_m(dB) is > 0 dB + 21 dB; and hence that $Q_m > 11$.

This is shown in Fig. 2k, where the $|Z_{in}|$ of a quartz resonant bar is given. Quartz has a $\underline{k}$ of about 10%, so $k^2 \simeq 0.01$. Observe that for such a small k^2 the two asympototes are almost touching; ΔdB is very small; and $f_a - f_r$ is very small. That is, the "rectangular window" enclosing f_a, f_r, $|Z_{max}|$, and $|Z_{min}|$ has shrunk on all sides. Then even if we call $\Delta dB \simeq 0$ dB, $1/k^2 = +40$ dB and so $Q > 100$. In such an example another indication is usually given that Q is high: the tiny peak and tiny dip are very sharp.

TABLE I

EXAMPLE OF THE MEASUREMENT OF Q_M^I

$\left|\text{when } k = 0.50;\ \ 1/k^2 = 4{:}1 \ \text{ or } +12 \text{ dB}\right|$

Using Δf from Reactance Curve	Using ΔdB from Impedance Magnitude Curve
$Q_m^I = \frac{f_4 - f_3}{f_a}$	(1) R_{mech} = 100 ohms MKS
	ΔdB = +77.5 dB −+13.5 dB +64.0 dB
	ΔdB/2 = +32 dB
	Q(dB) = +32 dB + 12 dB = 44 dB
$Q_m^I \simeq 91$	$Q_m^I \simeq 160$
	(2) R_{mech} = 5000 ohms MKS
	ΔdB = +62.5 dB −+31.0 dB +31.5 dB
	ΔdB/2 = +15.8 dB
	Q(dB) = +15.8 dB + 12 dB = +27.8 dB
$Q_m^I \simeq 26$	$Q_m^I \simeq 25$
	(3) R_{mech} = 10,000 ohms MKS
	ΔdB = +57.5 dB −+36.0 dB +21.5 dB
	ΔdB/2 = +10.8 dB
	Q(dB) = +10.8 dB + 12 dB = +22.8 dB
$Q_m^I \simeq 13$	$Q_m^I \simeq 14$

Table I shows a comparison between Q_m^I via Δf, from the reactance curves of Chap. 6; and Q_m^I via ΔdB between $|Z_{max}|$ and $|Z_{min}|$. The transducer under consideration is a realistic computer-simulated transducer whose impedance-magnitude response is shown in Fig. 2b. A number of reactance-response curves are shown in Figs. 6l, 6m, and 6n. The large detailed originals of these were used in preparing the Δf portion of Table I (where $\Delta f = f_4 - f_3$). For Q_m^I values $\gtrsim$ 100, the Δf was more difficult to read than the ΔdB. For lower values the two methods seem equally reliable.

The Δf method has the attraction that it does not require a determination of $1/k^2$; it can be read off directly from a reactance curve, or from an impedance circle diagram (see Fig. 7.2).

On the other hand the ΔdB method has the attraction that it is quick and requires no sophisticated instrumentation such as a vector impedance analyzer which automatically resolves Z into R and X. This method is then convenient when only a voltmeter and an oscillator are available.

Appendix 2-A

Reversing an L-Network

FIG 2-A.1

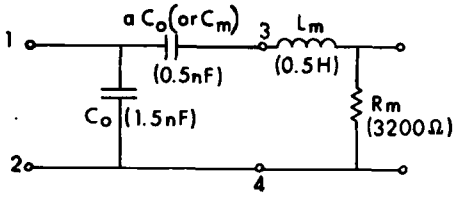

k = 0.50

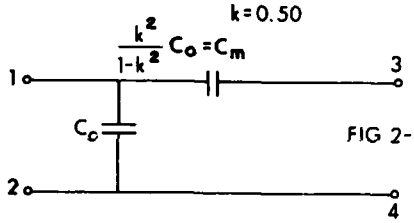

FIG 2-A3

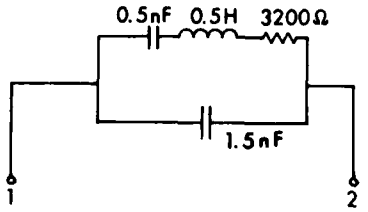

FIG 2-A.5

FIG 2-A.2

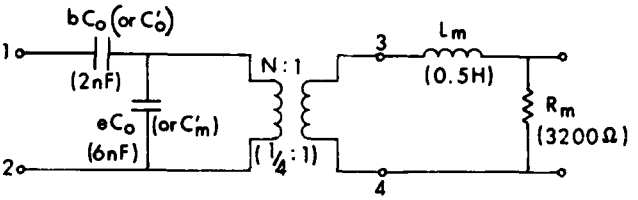

k = 0.50

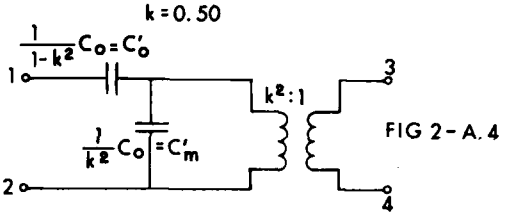

FIG 2-A.4

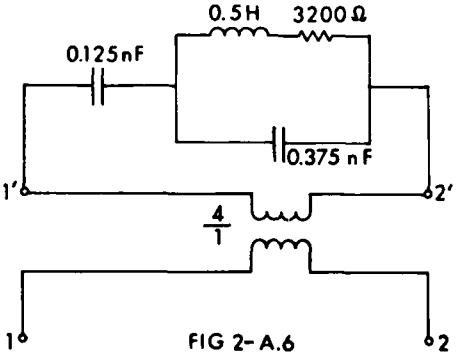

FIG 2-A.6

Appendix 2-A

Reversing an L-Network

Figure 2-A.1 shows the basic network we will work with. We wish to reverse only the C_o and C_m portion, and not touch the L and R portion. The solution requires adding a transformer with turns-ratio N:1. (Note that we are allowed to reverse merely the central portion of a network, without disturbing the elements to the left or the right of it.)

To find the desired relationships, we would ordinarily equate the open-circuit and short-circuit impedances Z from each end of Fig. 2-A.3, to the respective open-circuit and short-circuit impedances of Fig. 2-A.4. Or equally well, we could work with the admittances Y. But since the Y of a capacitive network is ωC, we can drop ω and equate the various capacitances C.

We will use C_o as our reference capacitance (Fig. 2-A.1), and express all other capacitances as fractions of C_o. In Fig. 2-A.1 we are <u>given</u> the value of <u>a</u>, since we have measured the ratio of C_m/C_o. We will solve for the other values <u>b</u>, <u>e</u>, and <u>N</u> in terms of <u>a</u>. (We have written in the answers, however, to allow the reader to check things as we proceed.)

1. Open-circuit condition. (We use only terminals 1-2, 3-4.)

$$C^{oc}_{(1-2)} = C_o = \frac{be}{b+e} \cdot C_o \qquad (2\text{-A1})$$

$$C^{oc}_{(3-4)} = \frac{a}{a+1} \cdot C_o = eN^2 \cdot C_o \qquad (2\text{-A2})$$

2. Short-circuit condition. (We use only terminals 1-2, 3-4.)

$$C^{sc}_{(1-2)} = (a+1) \cdot C_o = bC_o \qquad (2\text{-A3})$$

$$C^{sc}_{(3-4)} = aC_o = (b+e)N^2 \cdot C_o \qquad (2\text{-A4})$$

FIG 2-A.1

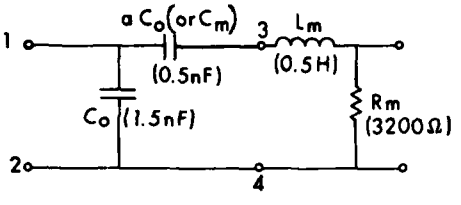

k = 0.50

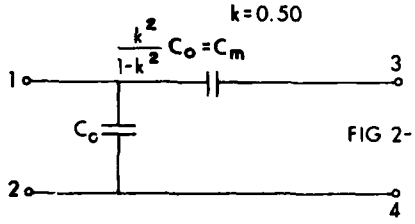

FIG 2-A3

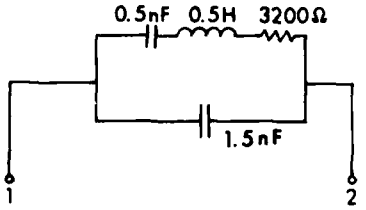

FIG 2-A.5

FIG 2-A.2

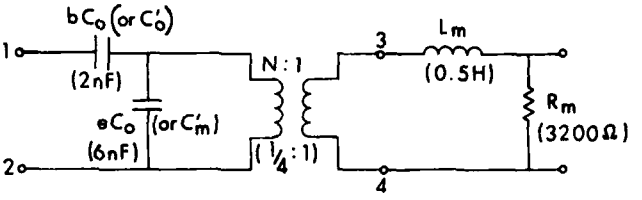

k = 0.50

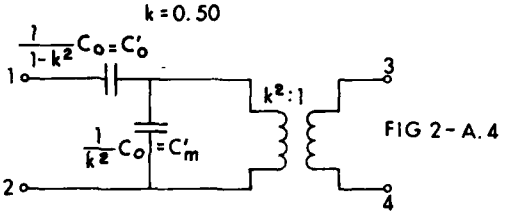

FIG 2-A.4

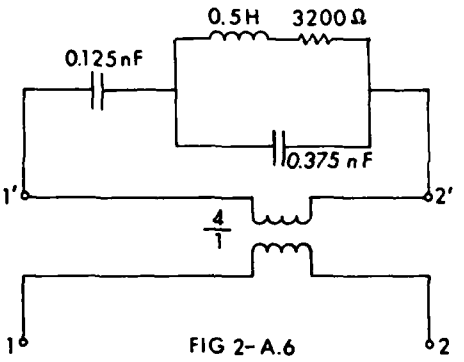

FIG 2-A.6

We can use any three of these four equations. Thus:

$$b = a+1 \tag{2-A5}$$

$$b + e = be; \quad e = \frac{b}{b-1}; \quad e = \frac{a+1}{a} \tag{2-A6}$$

$$eN^2 = \frac{a}{a+1}\ ; \quad N^2 = \frac{a}{a+1} \cdot \frac{1}{e} = \left(\frac{a}{a+1}\right)^2 \tag{2-A7}$$

$$\text{So} \quad N = \frac{a}{a+1} \tag{2-A8}$$

But our definition of k^2 has been $\frac{C_m}{C_m+C_o}$ which equals $\frac{aC_o}{(a+1)C_o}$. (cf. Eq. I.1)

$$\text{So} \quad N \equiv k^2 = \frac{a}{a+1} \tag{2-A9}$$

We will now rework the a formulas in terms of k^2.

$$a = \frac{k^2}{1-k^2} \tag{2-A10}$$

$$b = a+1 = \frac{1}{1-k^2} \tag{2-A11}$$

$$e = \frac{a+1}{a} = \frac{1}{k^2} \tag{2-A12}$$

In the present example since a = 1/3 (Fig. 2-A.1)

$$k^2 = \frac{1}{4} = N$$

Then $\frac{k^2}{1-k^2} = \frac{1}{3} = a$

$$\frac{1}{1-k^2} = \frac{4}{3} = b$$

$$\frac{1}{k^2} = 4 = e$$

FIG 2-A.1

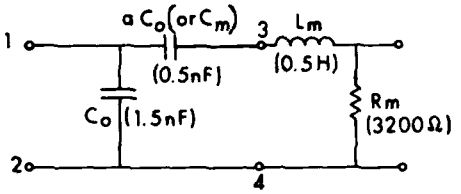

FIG 2-A.2

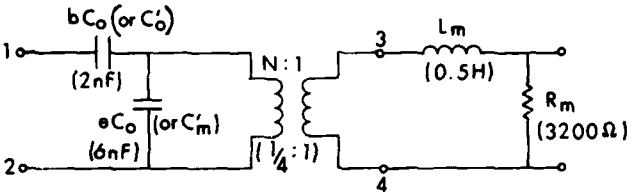

k = 0.50

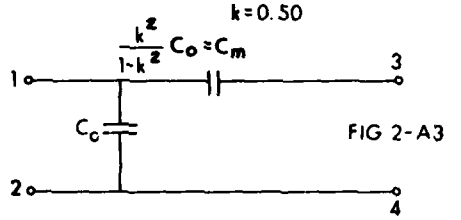

FIG 2-A3

k = 0.50

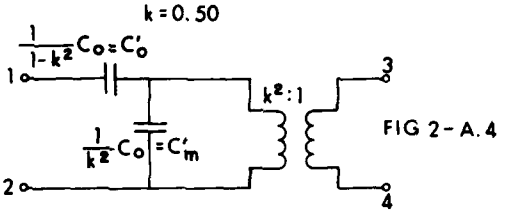

FIG 2-A.4

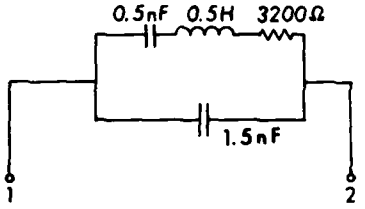

FIG 2-A.5

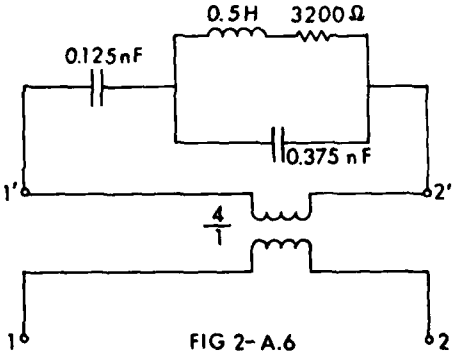

FIG 2-A.6

Note also that the relation of the two shunt elements is

$$\frac{C_o}{C_m} = k^2.$$

And the relation of the two series elements is

$$\frac{C_m}{C_o} = k^2.$$

Figures 2-A.5 and 2-A.6 show the two networks drawn as 2-terminal rather than 4-terminal networks. (This is somewhat the way Foster might draw them.) In addition we have sent all elements through the transformer.

Figure 2-A.5 high-lights the resonance frequency f_r of the networks.

Figure 2-A.6 high-lights the anti-resonance frequency f_a of the network. A simple mental calculation gives the ratio of f_a/f_r, thus again showing the usefulness of using the <u>two</u> Foster forms.

References:

Shea, T. E.: "Transmission Networks and Wave Filters", Van Nostrand. 1929; 1938. pp. 135-6.

Norton, E. L.: U.S. Patent 1,681,554 (1928)

Foster, R. M.: "A Reactance Theorem", Bell System Technical Journal. p. 259, (1924)

Chapter 3. The reactance curves of the two basic circuits; and how to sketch them "at sight".

Circuit useful for analysis of behavior around resonance, fr; and for admittance components.

Fig 3a

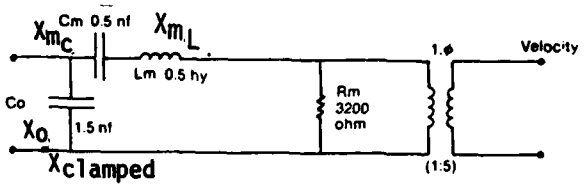

At low frequencies:

X_o is clamped reactance ($R_m = \infty$).

$X_o \,||\, X_{m_c}$ is free reactance ($R_m = 0$).

X_{m_c} is "motional" reactance.

——— ——— ——— $Q = \infty$

..... $Q = 100$

_____ $Q = 20$

Fig 3b

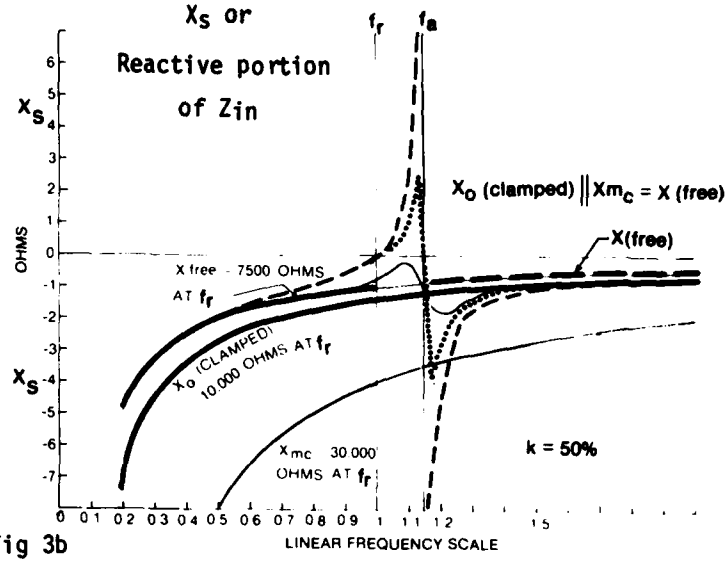

Circuit useful for analysis of behavior around antiresonance, fa; and for impedance components.

Fig 3c

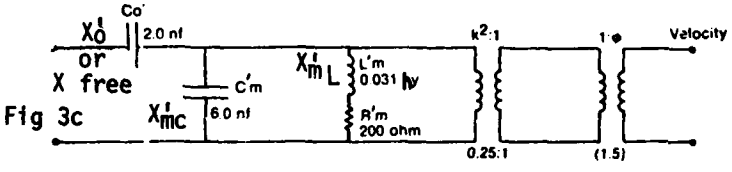

At low frequencies:

$X'_o \,\$\, X'_{m_c}$ is clamped reactance($R'_m = \infty$).

X'_o is free reactance ($R'_m = 0$).

X'_{m_c} is "motional" reactance.

Fig 3d

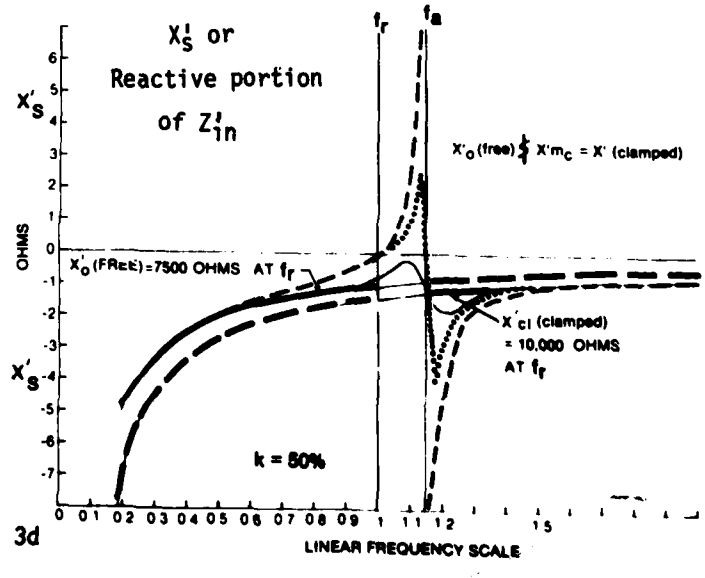

CHAPTER 3. The Reactance Curves of the Two Basic Circuits; and how to Sketch Them "at sight".

We will arbitrarily select the circuit of Fig. 3a as our Basic Circuit and derive all the other circuits from it. We could as well have chosen Fig 3c as our basic circuit; and some writers do. This is merely another form of Fig 3a, i.e. a Half-Tee instead of a Half-Pi, as shown in Foster's Reactance Theorem paper for the case of infinite Q; and as discussed by Shea, Norton, and others. Fig 3a, the Half-Pi, is especially useful when behavior around the resonance region f_r is explicitly asked for. Fig 3c, the Half-Tee, is especially useful when behavior around the anti-resonance region f_a is explicitly asked for. Both circuits give identical values for Z_{in} and Z'_{in}, Z^{oc}, Z^{sc}, Y_{in} and Y'_{in}, the series reactances X_s and X'_s, etc.

$$\text{In Fig 3a, } Z_{in} = jX_o \,||\, Z_m = \frac{jX_o \cdot (R_m + jX_m)}{jX_o + (R_m + jX_m)} \approx R_s + jX_s \ . \qquad (3.1)$$

Here, $+ jX_m$ will mean $+ j(X_{m_L} + X_{m_C})$, where $X_{m_L} = \omega L_m$ and $X_{m_C} = \frac{-1}{\omega C_m}$. That is, we use $+ jX_{m_C}$ for $- j\frac{1}{\omega C_m}$. We therefore never expect to see a term $- jX_{m_C}$. This is the A.S.A. convention. (Some books use $- jX_{m_C}$ for $- j\frac{1}{\omega C_m}$. To convert to the convention used here, simply multiply X_{m_C}, every time it appears, by (-1).)

Now the analysis of Z_{in} by Equation 3.1 gives unsatisfying results when $R_m > 0$, and especially when Q is very low. However, the analysis becomes clear when $R_m = 0$ and hence $Q = \infty$. Figure 3b, dashed curve, is then the resultant of the series-resonance circuit $X_{m_C} \lessgtr X_{m_L}$ connected in parallel with $X_{clamped}$. Thus, the series-resonance branch goes to zero at the resonance frequency f_r, shorts out $X_{clamped}$, and makes the total X_s

Circuit useful for analysis of behavior around resonance, fr; and for admittance components.

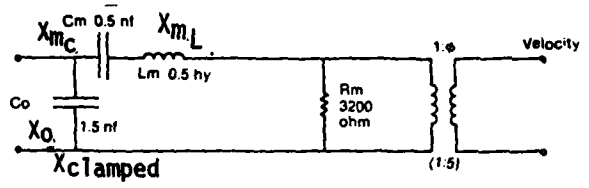

Fig 3a

At low frequencies:

X_o is clamped reactance ($R_m = \infty$).

$X_o \,||\, X_{m_c}$ is free reactance ($R_m = 0$).

X_{m_c} is "motional" reactance.

——— ——— ——— $Q = \infty$

..... $Q \approx 100$

——————— $Q \approx 20$

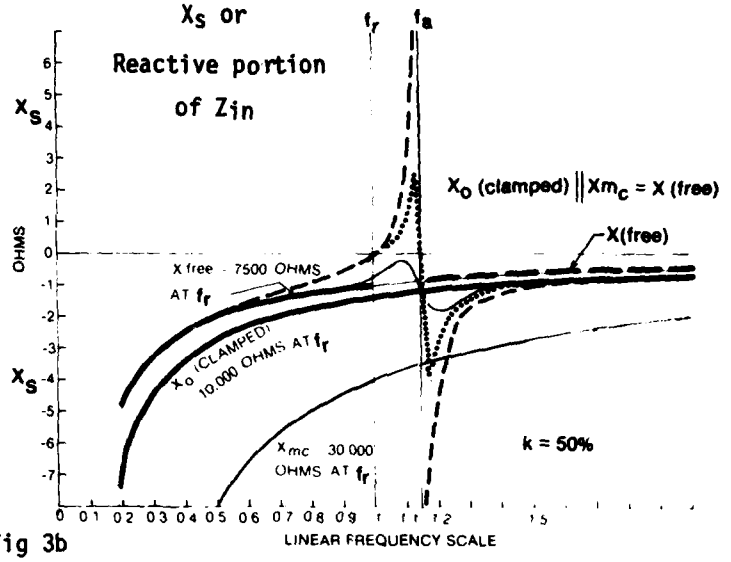

Fig 3b

Circuit useful for analysis of behavior around antiresonance, fa; and for impedance components.

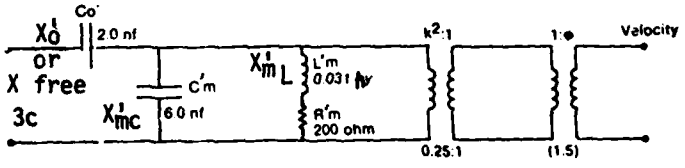

Fig 3c

At low frequencies:

$X'_o \,\$\, X'_{m_c}$ is clamped reactance($R'_m = \infty$).

X'_o is free reactance ($R'_m = 0$).

X'_{m_c} is "motional" reactance.

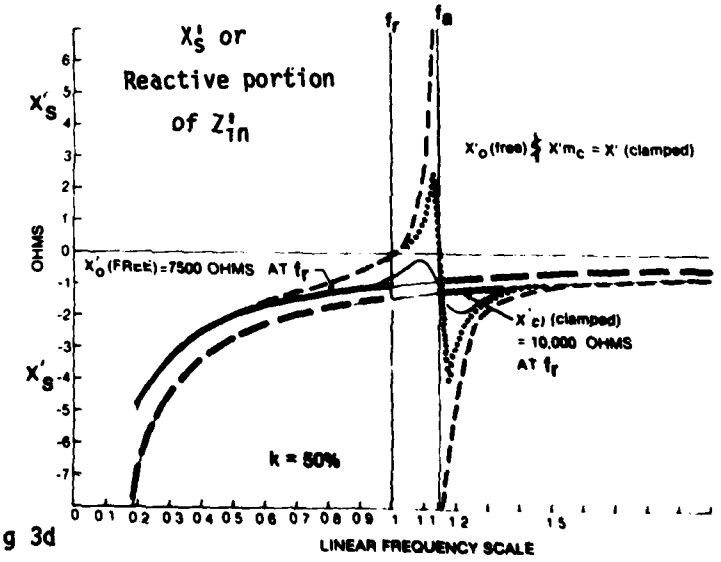

Fig 3d

equal zero at f_r. As the frequency increases, the series-resonance branch changes from capacitive to inductive and soon anti-resonates with $X_{clamped}$ at the anti-resonance frequency f_a, making the total X_s equal infinity at f_a. It then becomes capacitive again and follows the $X_{clamped}$ asymptote.

But when R > 0 and Q is low the reactive response curve X_s (Fig 3b, thin Solid Curve) in the region of resonance f_r and of anti-resonance f_a, has no simple intuitive explanation from this network. Indeed it is not obvious how this purely reactive curve (derived from Fig 3a) manages to stay below the axis both at f_r and also in the vicinity of f_a. The reactive behavior of Figs. 3a and 3b is discussed in greater depth at a later point.

Their susceptance behavior is discussed in Chapter 4. For, it turns out that in the analysis of the circuit of Fig 3a, it is more useful and instructive to convert Z_{in} to Y_{in} and work with the admittance components.

$$\text{Then } Y_{in} = \frac{1}{Z_{in}} = \frac{1}{(jX_o \,||\, Z_m)} = \frac{1}{jX_o} + \frac{1}{Z_m}. \quad \textit{Thus } Y_{in} = jB_o + Y_m. \qquad (3.2)$$

The resultant variable <u>parallel</u> resistance R_p (in parallel with C_o); or better, variable parallel conductance G, its inverse, which is the real component of Y_m (see Chap. 4), will then be independent of such variables as cable capacitance added in parallel to the electrical capacitance C_o. Such independence will not exist for the variable resistance R_s (a <u>series</u> component; see Chap. 5) which is the real component of total Z_{in} in Eq. 3.1 and also (with identical values) of total Z'_{in} in Eq. 3.3. This equation pertains to Figures 3c and 3d.

$$Z'_{in} = jX'_o \not\$ Z_{tank} = jX'_o + \left\{(R'_m + jX'm_L) \;||\; jX'm_C\right\} = R'_s + jX'_s \text{ (or } R_s + jX_s). \qquad (3.3)$$

In both Z equations, 3.1 and 3.3, the effective variable <u>series</u> resistance R_s will change every time the cable capacitance changes. This is easily

At low frequencies:
X_o is clamped reactance ($R_m = \infty$).

$X_o \,||\, X_{m_c}$ is free reactance ($R_m = 0$).

X_{m_c} is "motional" reactance.

——— ——— ——— $Q = \infty$

..... $Q = 100$

——————— $Q = 20$

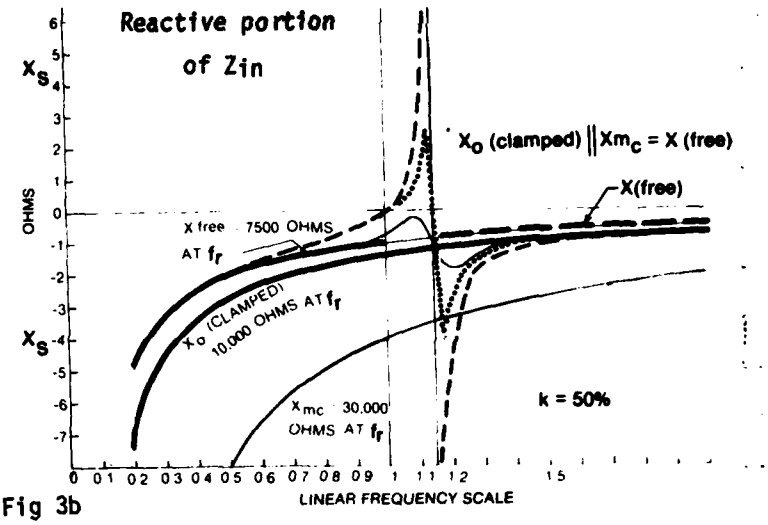

Fig 3b

Circuit useful for analysis of behavior around antiresonance, fa; and for impedance components.

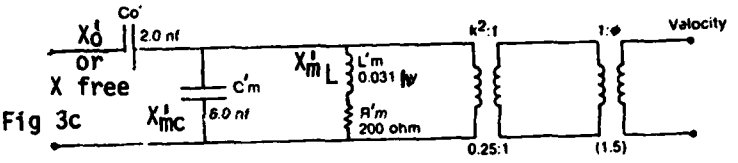

Fig 3c

At low frequencies:

$X'_o \,\$\, X'_{m_c}$ is clamped reactance ($R'_m = \infty$).

X'_o is free reactance ($R'_m = 0$).

X'_{m_c} is "motional" reactance.

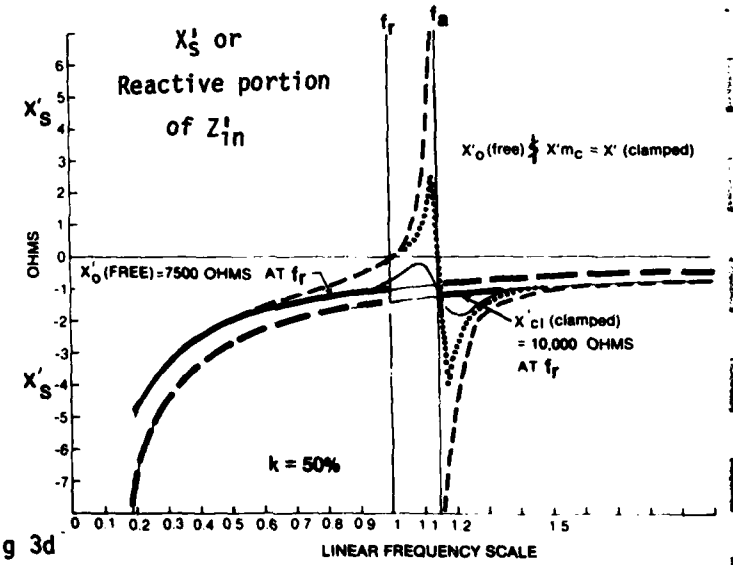

Fig 3d

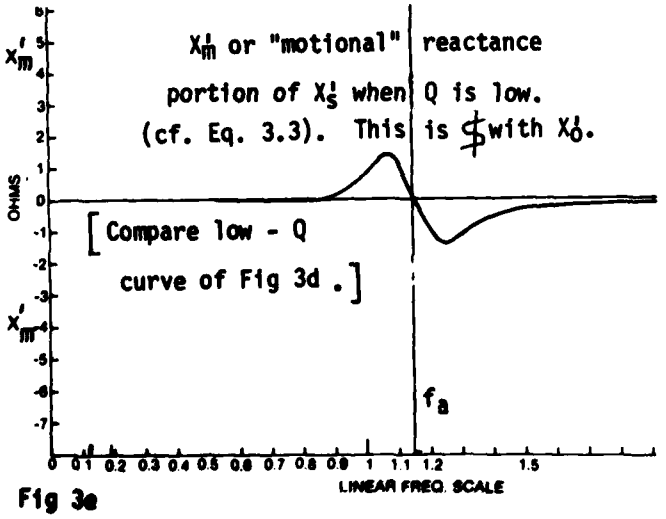

Fig 3e

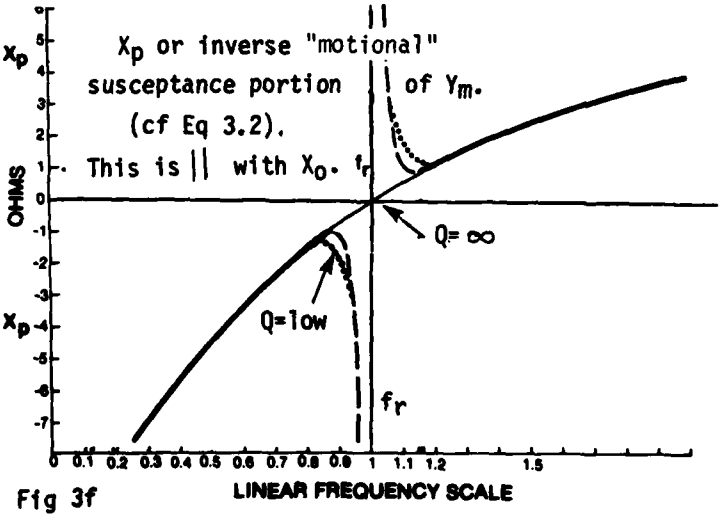

Fig 3f

seen in Eq. 3.1, where an added cable capacitance modifies X_o (e.g., in the denominator) and hence modifies the resultant R_s. It is less easily seen in Eq. 3.3, but we know that it must be so here also. [Mechanism: the cable capacitance modifies not only X'_o but also X'_{m_c} (by changing the value of the coupling coefficient k); thence the Q of the tank (Fig. 3c) and thence R'_s.]

The components of Y_{in} and Z'_{in} will be analyzed in Chapters 4 and 5.

We now turn again to the illustrations of Chapter 3.

Figures 3b and 3d look alike ___ grossly. But many details are different.

1. In Figs. 3c and 3d, $X'_{clamped}$ must be derived, from $X'_o \not\$ X'_{m_c}$.

2. But in Figs 3a and 3b, $X_{clamped}$ exists alone, as X_o.

3. In Fig 3d the operator $\not\$$ ("series") tells us to add $\pm X'_m$ to the hyperbolic baseline X'_o (free), thereby first raising and then lowering the position of the curve; which also means first lowering and then raising the value of the curve. This distinction arises during inversions, as from G to R_p, B to X_p, etc. The factor X'_m is discussed in Chapter 5. It is shown here in Fig 3e.

4. But in Fig 3b the operator || ("parallel") calls for something more complicated than adding. For the sake of illustration, we will work here only with impedance components rather than admittance components. We must start with the other hyperbolic baseline X_o (clamped) and then "parallel" the contribution of the reactive portion of Z_m or of $(R_m \not\$ jX_m)$ after it has been transformed to the equivalent parallel representation $(R_p||jXp)$. [See Chap. 4 and Fig. 4i.] A plot of Xp is shown in Fig. 3f. We then represent total Z_{in} as $R_p \,||\, \left[jX_o \,||\, jX_p\right]$. Note that the parallel motional component X_p is quite different from the series motional component X'_m which is shown in Fig. 3e. In fact for the OO-Q case they would be duals

At low frequencies:

X_o is clamped reactance ($R_m = \infty$).

$X_o \,||\, X_{m_c}$ is free reactance ($R_m = 0$).

X_{m_c} is "motional" reactance.

——— ——— ——— $Q = \infty$

..... $Q = 100$

——————— $Q = 20$

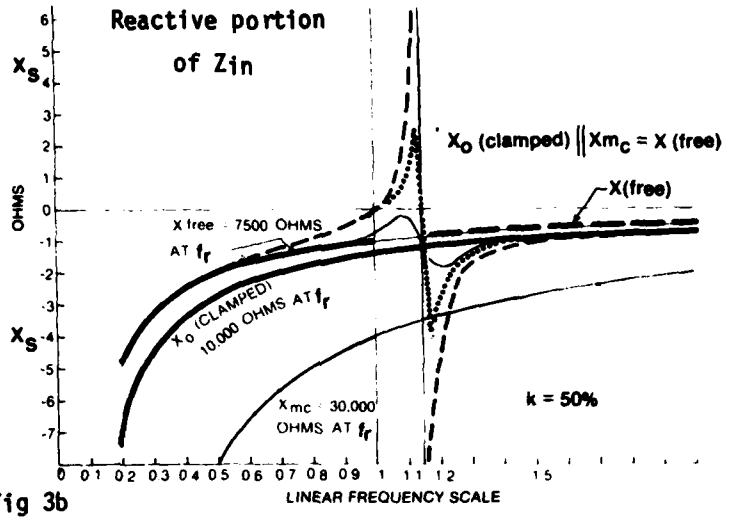

Fig 3b

Circuit useful for analysis of behavior around antiresonance, fa; and for impedance components.

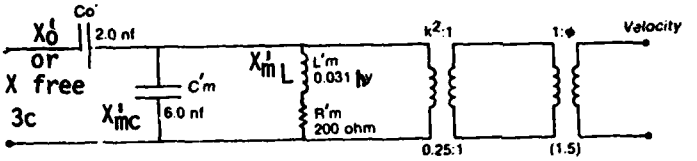

Fig 3c

At low frequencies:

$X'_o \,\$\, X'_{m_c}$ is clamped reactance($R'_m = \infty$).

X'_o is free reactance ($R'_m = 0$).

X'_{m_c} is "motional" reactance.

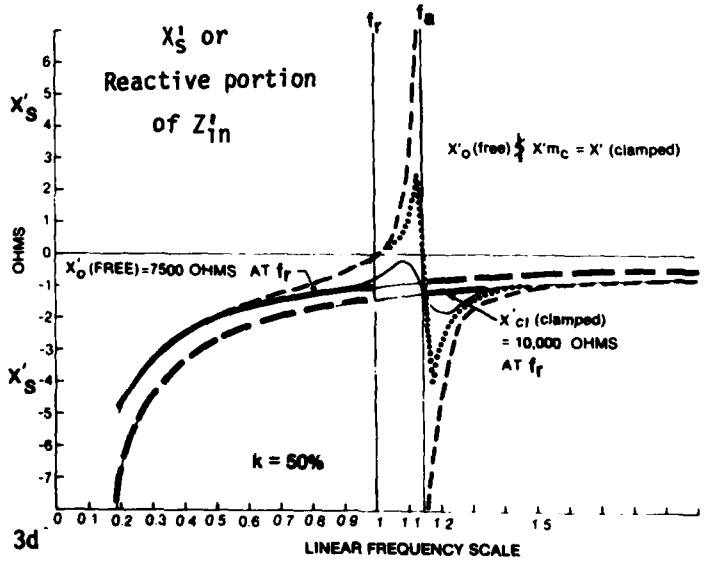

Fig 3d

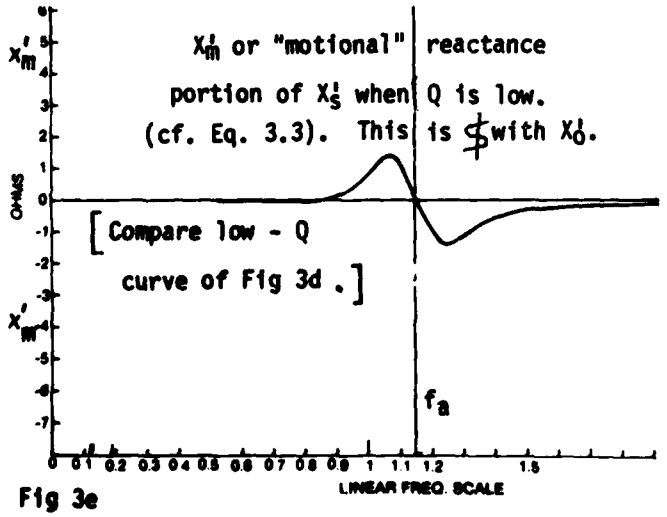

Fig 3e

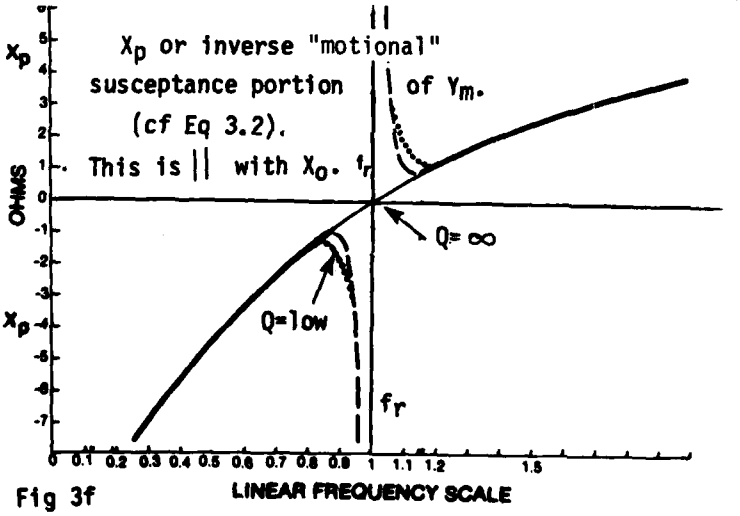

Fig 3f

if only they were centered about the same reference frequency. This can be seen from Fig 3f, which itself will be discussed further at a later point.

Now, $X_o||X_p$ still does not give us the X_s of Fig 3b, although paralleling any curve of Fig 3f with the X_o (clamped) curve of Fig 3b gives a resultant curve which, for the first time, somewhat resembles the family of curves in Fig 3b. (In fact, away from f_r and f_a agreement is perfect.) As the final step, we must now "parallel" R_p with $\left[jX_o||jX_p\right]$ and convert <u>this</u> (which of course is total Z_{in}) into the series form $R_s \lessgtr X_s$ or identically, $R_s' \lessgtr X_s'$. We will then have, explicitly, the exact reactance curves shown equally correctly in either Fig 3b or Fig 3d.

The above exercise helps explain why it is easier to deal with Fig 3a via parallel susceptance and conductance components rather than via parallel reactance and resistance components; except when Q is ∞. The analysis via the admittance components is treated in Chapter 4. We will now elaborate on Fig 3b and discuss how to sketch out the paralleling of X_o with X_p "at sight".

(a) We start at the low-frequency region by paralleling C_o and C_m. We travel up the X(free) hyperbola until we approach f_r. (b) At f_r if Q is high (dotted curve and dashed curve), the Net X must $\simeq 0$ since X_o has been shorted out by X_m. But if Q is low, the Net $X \neq 0$ at f_r (solid curve). {This low-Q case is not easily handled by the Fig 3a-approach. But it is very easily handled by the Fig 3c-approach.} (c) Jumping to the region far above

At low frequencies:

X_o is clamped reactance ($R_m = \infty$).

$X_o \,||\, X_{m_c}$ is free reactance ($R_m = 0$).

X_{m_c} is "motional" reactance.

——— ——— ——— $Q = \infty$

..... $Q = 100$

——— $Q = 20$

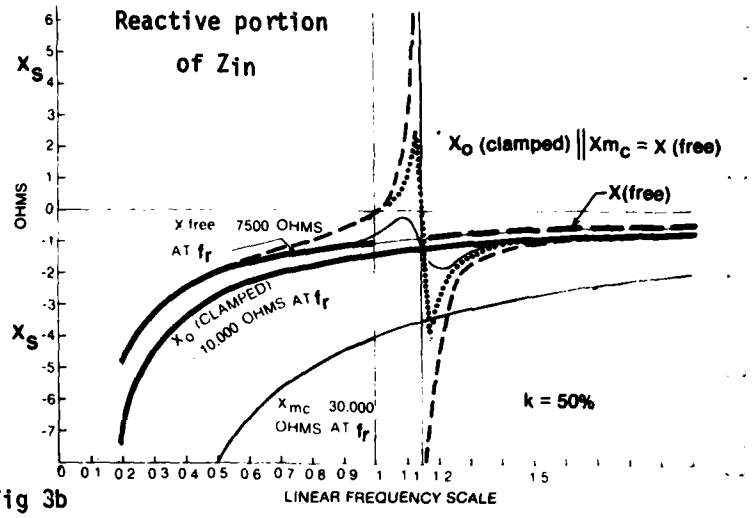

Fig 3b

Circuit useful for analysis of behavior around antiresonance, fa; and for impedance components.

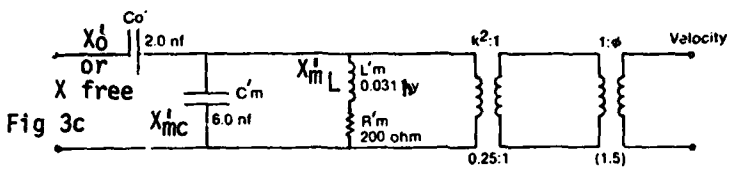

Fig 3c

At low frequencies:

$X'_o \,\$\, X'_{m_c}$ is clamped reactance ($R'_m = \infty$).

X'_o is free reactance ($R'_m = 0$).

X'_{m_c} is "motional" reactance.

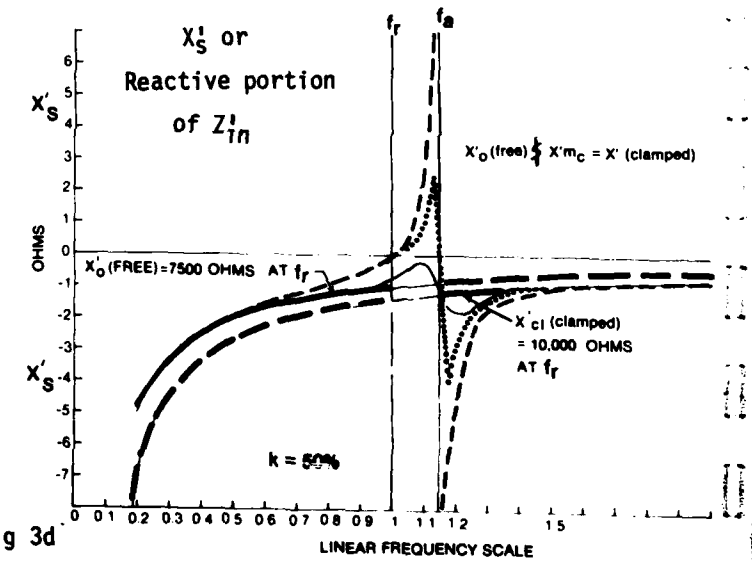

Fig 3d

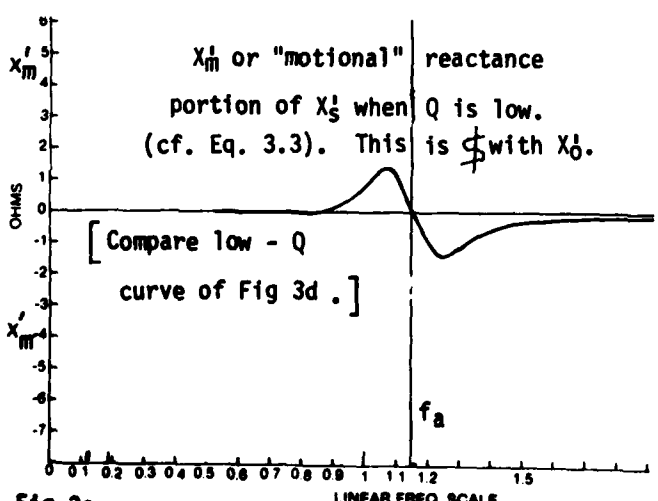

Fig 3e

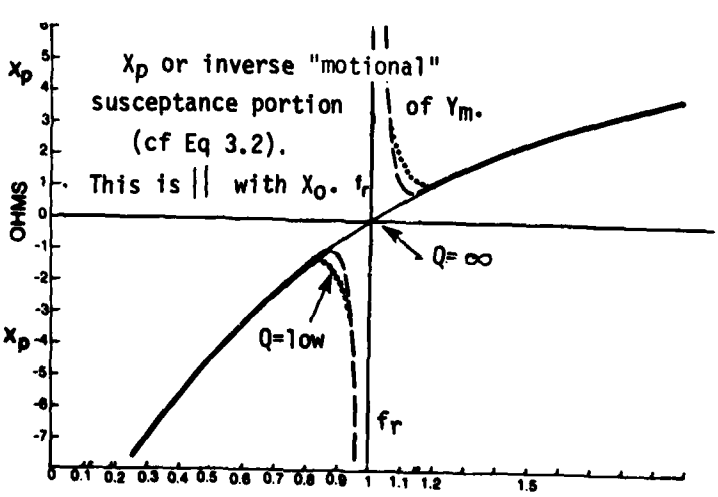

Fig 3f

f_a we see that the parallel branch, X_m, (Fig 3a) has jammed and that only the X_o branch is functioning. So we are now traveling up the $X_{clamped}$ hyperbola, namely X_o. (d) Now we back up. We know from Foster's Reactance Theorem that the resonance at f_r must be followed by an anti-resonance at f_a. How to locate f_a? One man's anti-resonance is another man's resonance. We look from the mechanical terminals toward the open-circuited electrical terminals, and see a "mechanical" resonance caused by $X_{m_\ell} \$ X_{m_c} \$ X_o$. This is f_a, made higher than f_r because of X_o in series. Using numbers: $C_m \$ C_o$ is 0.375 nf = C_{net}. Then C_m/C_{net} = 0.5/0.375 = 1.33/1. Then the square root is 1.15/1. And this is indeed the ratio of f_a to f_r.

We now add a comment on Figs. 3c and 3d. If we were to take all components through the transformer k^2:1; as shown in Fig 2f, we would get at once $C_m \$ C_o$, with the value 0.375 nf. This combination would now appear as the single "motional condenser" C_m^N. These circuits of Fig 3c and Fig 2f will give quantitative answers around f_a more readily than will the circuit of Figure 3a.

Chapter 4. Derivation of the Susceptance and Conductance curves.

Chapter 4. Derivation of the Susceptance and Conductance curves.

Fig 4a

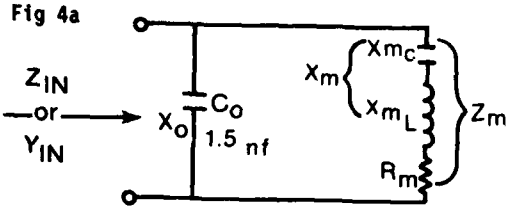

$Z_{IN} = jX_o \,||\, Z_m$

$Y_{IN} = \frac{1}{jX_o} + \frac{1}{Z_m} = jB_o + Y_m$

FIG 4b The B_o component of input susceptance of "clamped" transducer

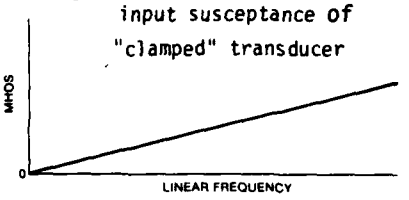

FIG 4c

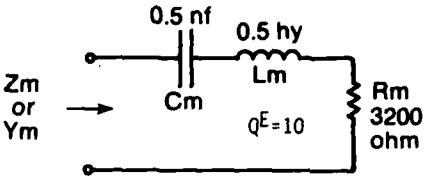

NUMERATOR TERM or N:

NEGATIVE SERIES RESONANCE RESPONSE

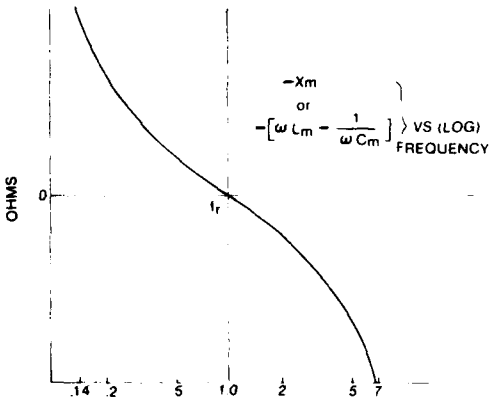

FIG 4e.1

NEGATIVE SERIES RESONANCE RESPONSE ($-X_m$) AND POSITIVE SERIES RESONANCE RESPONSE ($+X_m$)

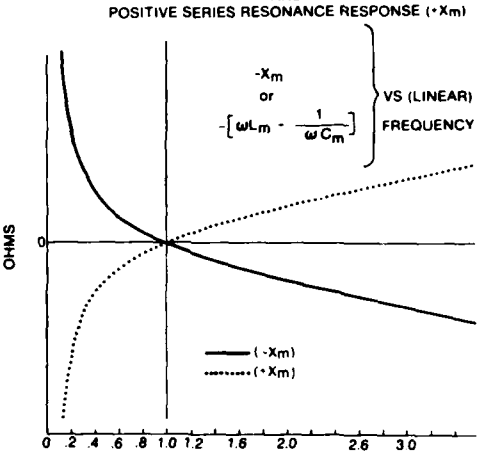

FIG 4e.2

(1/DENOMINATOR) TERM: ADMITTANCE SQUARED OF "MOTIONAL" BRANCH, $|Y_m|^2$ (ALSO $|Y_m|$)

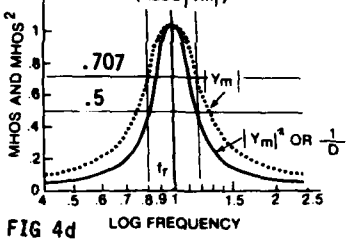

FIG 4d

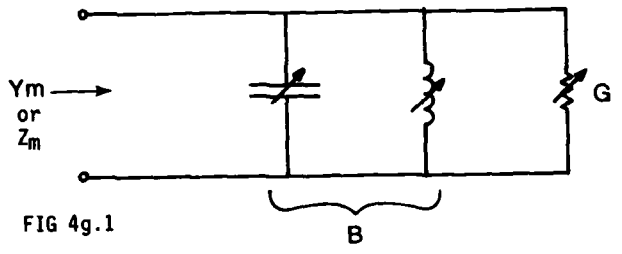

FIG 4g.1

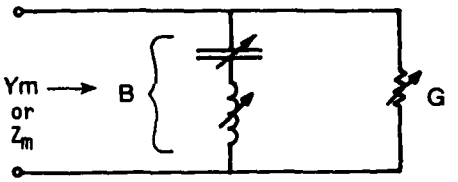

FIG 4g.2

"motional" SUSCEPTANCE B_m
— LOW Q
--- ∞ Q

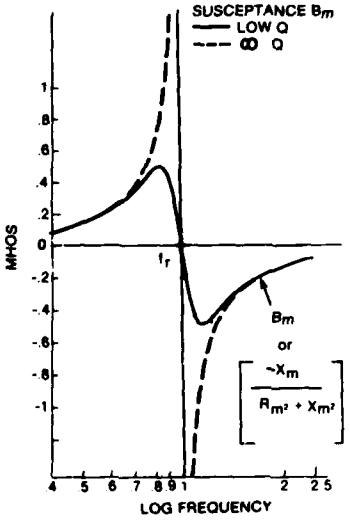

FIG 4f

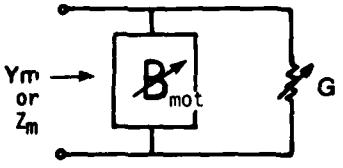

FIG 4h

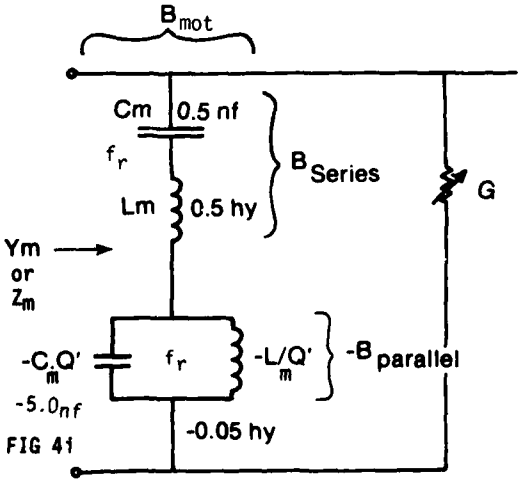

FIG 41

RECTIFIED SUSCEPTANCE B_m
CONDUCTANCE G (= to Y m)^2

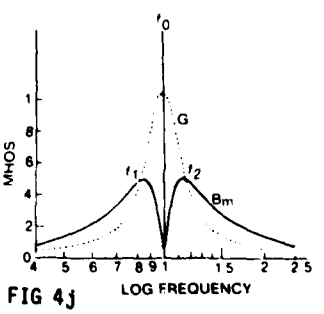

FIG 4j

CHAPTER 4. Derivation of the Susceptance and Conductance Curves.

Preliminary Note: The operator || (parallel), when used with impedance elements, will mean for example: $Z_1||Z_2 = \frac{Z_1 \cdot Z_2}{Z_1 + Z_2}$. With admittance elements it means: $Y_1||Y_2 = Y_1 + Y_2$. Likewise the operator $\oint$ (series), when used with admittance elements, will mean for example: $Y_1 \oint Y_2 = \frac{Y_1 \cdot Y_2}{Y_1 + Y_2}$ With impedance elements it means: $Z_1 \oint Z_2 = Z_1 + Z_2$.

Figure 4a shows the simplified Basic Circuit that we will work with for susceptance and conductance. All "mechanical" quantities have been transformed to the electrical side, where they are now called "motional" quantities. They are now components of Z_m, the "motional impedance".

The term $\left| \frac{1}{jX_o} \right|$ or B_o, the clamped susceptance, is plotted in Fig. 4b. It will act as a bias or a new baseline for the motional susceptance term B_m of the "motional admittance" Y_m. A linear frequency plot was chosen, to show how simple the bias function is. In general, we will use log frequency plots.

The term $Y_m = \frac{1}{Z_m} = \frac{1}{R_m + jX_m}$ resolves into G + jB. It is shown in Fig. 4c, which is equally valid for Y_m or Z_m.

$$Y_m = \frac{1}{R_m + jX_m} \cdot \frac{R_m - jX_m}{R_m - jX_m} = \frac{R_m}{R_{m^2} + X_{m^2}} + j \frac{-X_m}{R_{m^2} + X_{m^2}} \qquad (4.1)$$

$$\text{Thus } G_m = \frac{R_m}{R_{m^2} + X_{m^2}} \text{ and } B_m = \frac{-X_m}{R_{m^2} + X_{m^2}} \qquad (4.2)$$

Chapter 4. Derivation of the Susceptance and Conductance curves.

Fig 4a

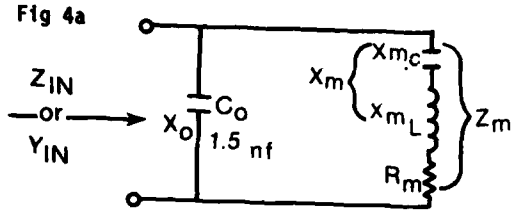

FIG 4b The B_o component of input susceptance of "clamped" transducer

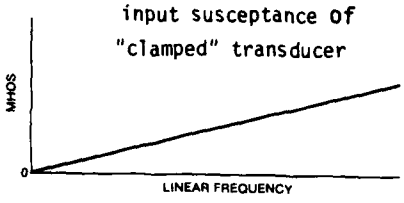

FIG 4c

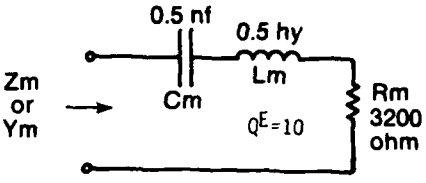

$$Z_{IN} = jX_o \,||\, Z_m$$

$$Y_{IN} = \frac{1}{jX_o} + \frac{1}{Z_m} = jB_o + Y_m$$

NUMERATOR TERM or N:

NEGATIVE SERIES RESONANCE RESPONSE

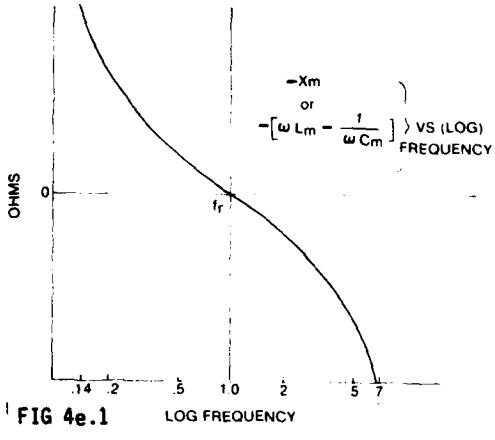

FIG 4e.1

NEGATIVE SERIES RESONANCE RESPONSE ($-X_m$) AND POSITIVE SERIES RESONANCE RESPONSE ($+X_m$)

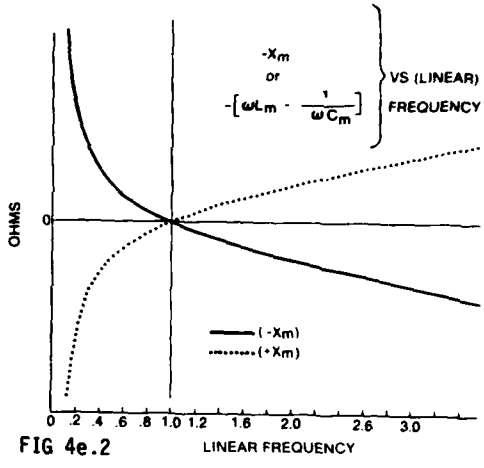

FIG 4e.2

(1/DENOMINATOR) TERM: ADMITTANCE SQUARED OF "MOTIONAL" BRANCH, $|Ym|^2$ (ALSO $|Ym|$)

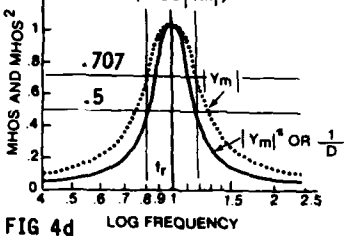

FIG 4d

"motional" SUSCEPTANCE B_m

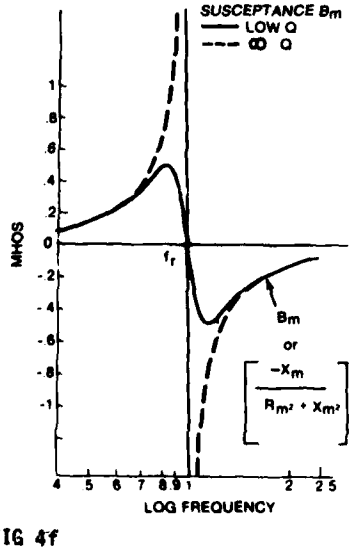

FIG 4f

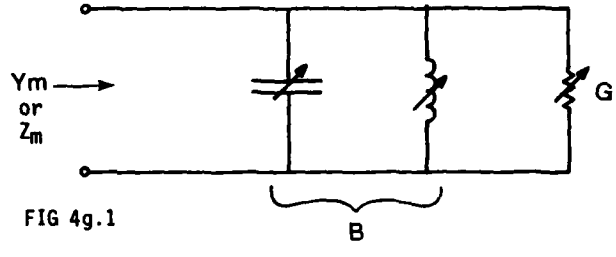

FIG 4g.1

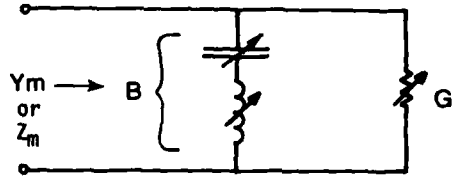

FIG 4g.2

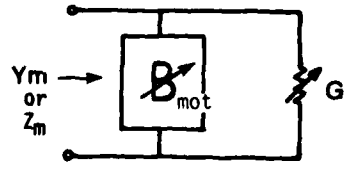

FIG 4h

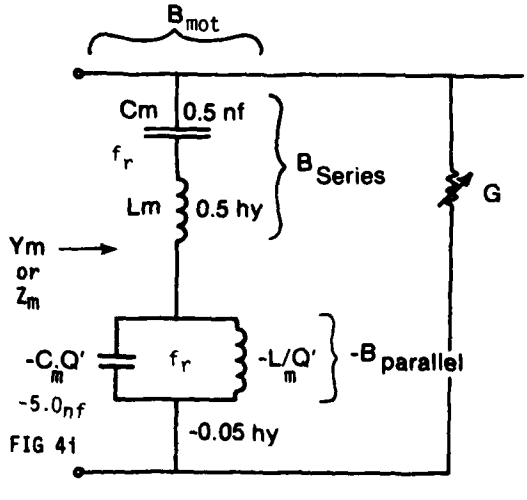

FIG 4i

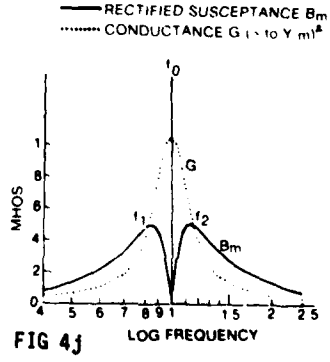

FIG 4j

We will ignore G_m for the moment and concentrate on B_m.

B_m = Numerator/Denominator = N/D. D is $|Z_m|^2$ and $\frac{1}{D} = |Y_m|^2$. It plots as shown in Fig. 4d: normalized$(\text{mhos})^2$ vs. log frequency. The "log" reveals the left-right symmetry which is obscured in a linear frequency plot.

N is - $X_m = -(\omega L_m - \frac{1}{\omega C_m})$. Now this describes a negative L and a negative C in series. So $-X_m$ is the reactance of a negative series-resonance circuit. It plots as shown in Fig 4e.1 and is merely the mirror-image of the usual plot. This becomes clearer if we look at Fig 4e.2 which uses the familiar linear frequency axis.

When N of Fig 4e is multiplied by 1/D of Fig 4d, we get Fig 4f. Note that this multiplication automatically produces at f_r the negative slope which always shows up, except when Q is infinite, as the curve crosses the axis. Most textbooks fail to comment on this negative slope, probably because of concern about violating Foster's Reactance Theorem (which is actually not violated). This curve is found also in plots of the hyperbolic tangent function, tanh $(\alpha+j\beta)$, which describes a lossy transmission line. It should be noted that negative elements are not a mathematical fiction. They can actually be built now, and they are stable.

In detail: Figure 4f shows, dashed curve, the typical susceptance plot of a series-resonance circuit having infinte Q. This curve goes from $+\infty$ to $-\infty$ without passing through zero at f_r. But when the Q is finite the curve, instead of having the value infinity at the susceptance "pole" f_r, has the value zero——a rather drastic exchange. Multiplying N by 1/D gives the solid curve of Fig 4f when $Q<\infty$. Thus for a low Q, the $|Y_m|^2$ curve or $\frac{1}{R_m^2 + X_m^2}$ of Fig 4d has a finite peak at f_r. But the $-X_m$ curve, which will

Chapter 4. Derivation of the Susceptance and Conductance curves.

Fig 4a

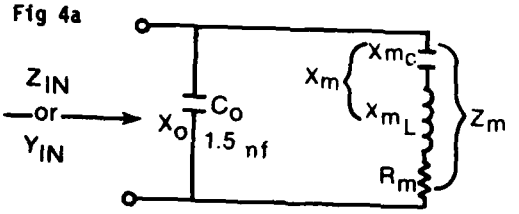

$$Z_{IN} = jX_o \,||\, Z_m$$

$$Y_{IN} = \frac{1}{jX_o} + \frac{1}{Z_m} = jB_o + Y_m$$

FIG 4b The B_o component of input susceptance of "clamped" transducer

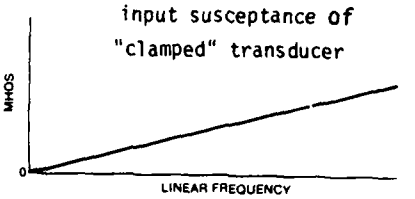

FIG 4c

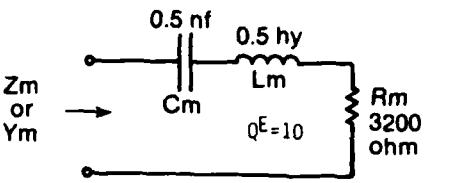

NUMERATOR TERM or N:

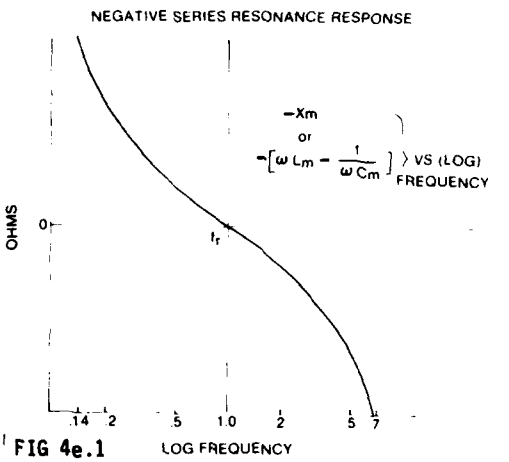

FIG 4e.1

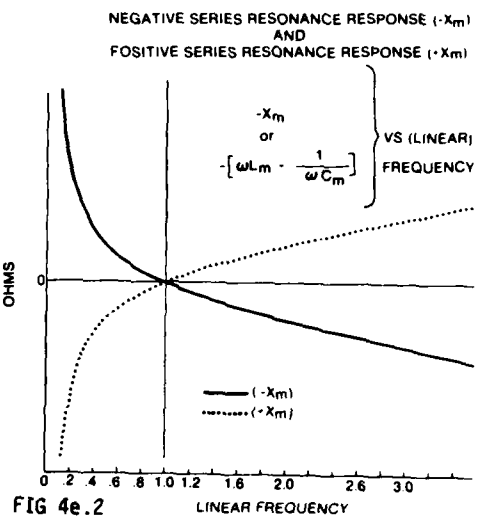

FIG 4e.2

(1/DENOMINATOR) TERM:
ADMITTANCE SQUARED OF "MOTIONAL" BRANCH, $|Y_m|^2$
(ALSO $|Y_m|$)

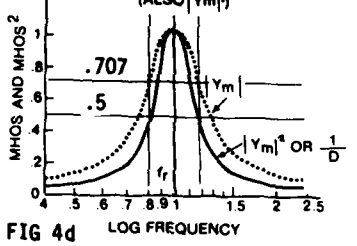

FIG 4d

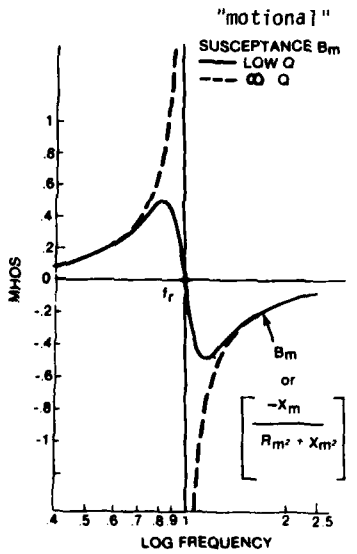

FIG 4f

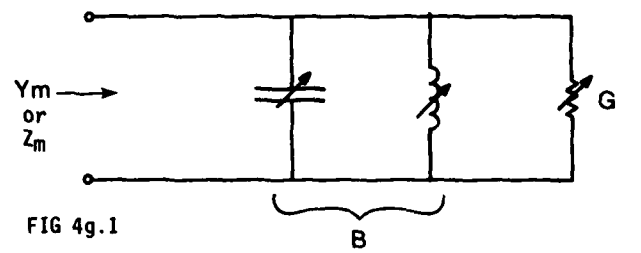

FIG 4g.1

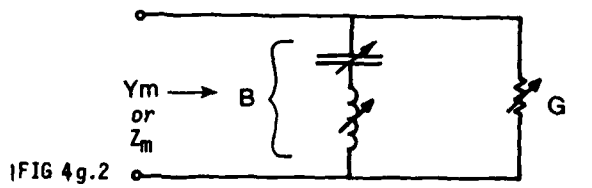

FIG 4g.2

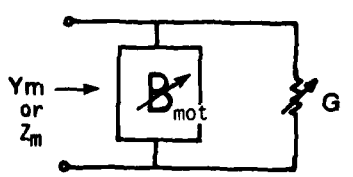

FIG 4h

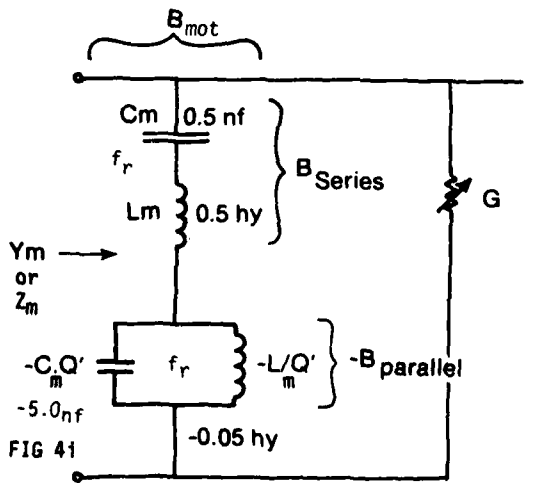

FIG 4i

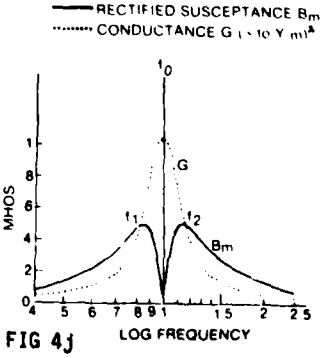

FIG 4j

multiply with it, has a zero precisely at f_r. The zero term wins out. So the product is zero.

If now we let R go to 0 and Q go to ∞, $-X_m$ is of course zero at f_r. But $|Y_m|^2$ is ∞^2 at f_r. The square term wins out; so the product, or net B, is ∞ rather than zero at f_r when Q is ∞.

The other way to show this is: $B = \frac{-X_m}{0 + X_m^2} = \frac{1}{(-X_m)}$. And this gives a simple ∞ at f_r. This ∞ - Q curve is of course merely the inverse of the negative series-resonance curve ($-X_m$) of Fig 4e.1. [Inverting the j-operator in $\frac{1}{Zm} = \frac{1}{jXm}$ produced the desired negative sign; i.e. $\frac{1}{(+X_m)}$ would be all wrong.]

Another circuit equivalent to the "motional branch" of Fig 4a and commonly used for analysis of Y functions is shown in Fig 4g.1. This looks much like the dual of the circuit for Z_m shown in Fig 4c; but of course it must not be! [A circuit and its dual cannot both represent the same Z.] Since all the elements must be variable anyway, we cannot call it wrong. But is is not terribly useful, except right at resonance. A more useful equivalent circuit is probably that of Fig 4g.2. This at least hints at the proper response at very low frequencies and very high frequencies. It fails to be useful at resonance, however.

Actually the equation $G + jB = G + j \frac{-X_m}{R_m^2 + X_m^2}$ demands only the equivalent circuit of Fig 4h. But the equation certainly implies that a better equivalence might exist.

And indeed a good approximate equivalent circuit for the B_m component alone of the Y_m of Fig 4h does exist. It is shown in Fig 4i and it contains only fixed elements. It is a lossless series-resonance circuit in series with

Chapter 4. Derivation of the Susceptance and Conductance curves.

Fig 4a

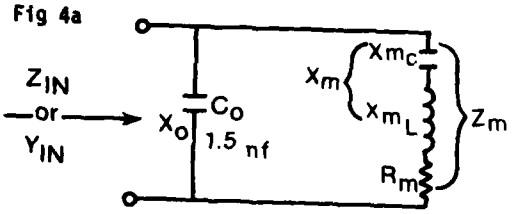

FIG 4b The B_o component of input susceptance of "clamped" transducer

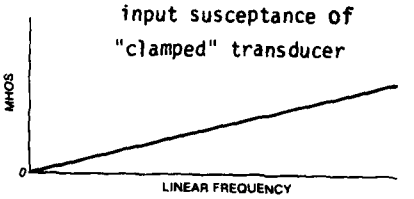

FIG 4c

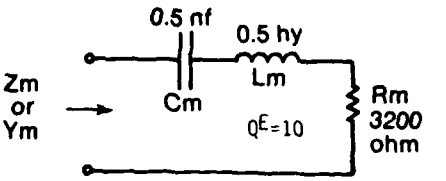

$$Z_{IN} = jX_o \,||\, Z_m$$

$$Y_{IN} = \frac{1}{jX_o} + \frac{1}{Z_m} = jB_o + Y_m$$

NUMERATOR TERM or N:

NEGATIVE SERIES RESONANCE RESPONSE

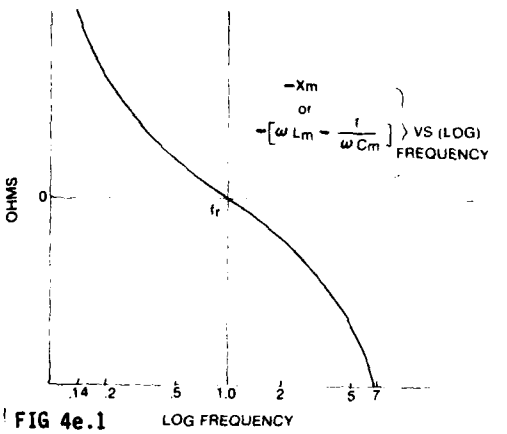

FIG 4e.1

NEGATIVE SERIES RESONANCE RESPONSE ($-X_m$)
AND
POSITIVE SERIES RESONANCE RESPONSE ($+X_m$)

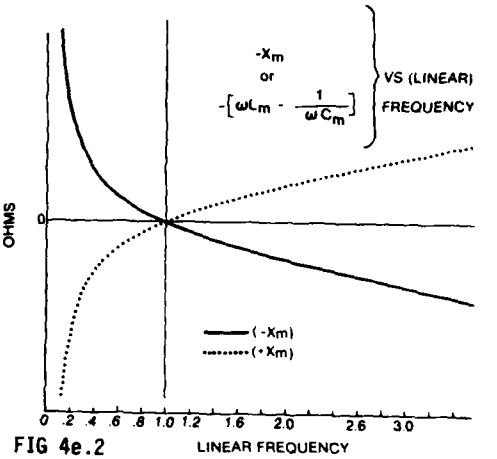

FIG 4e.2

(1/DENOMINATOR) TERM:
ADMITTANCE SQUARED
OF "MOTIONAL" BRANCH, $|Ym|^2$
(ALSO $|Ym|$)

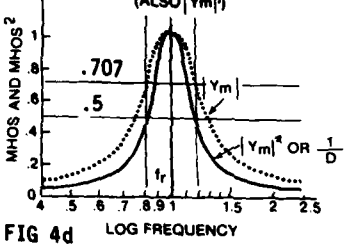

FIG 4d

"motional"

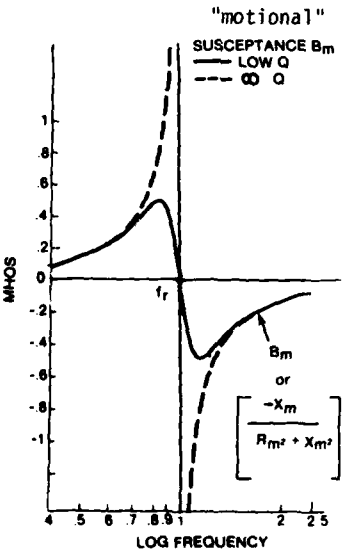

FIG 4f

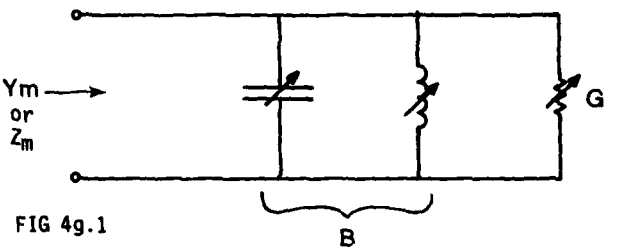

FIG 4g.1

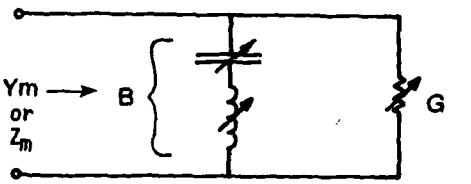

FIG 4g.2

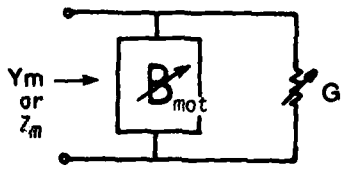

FIG 4h

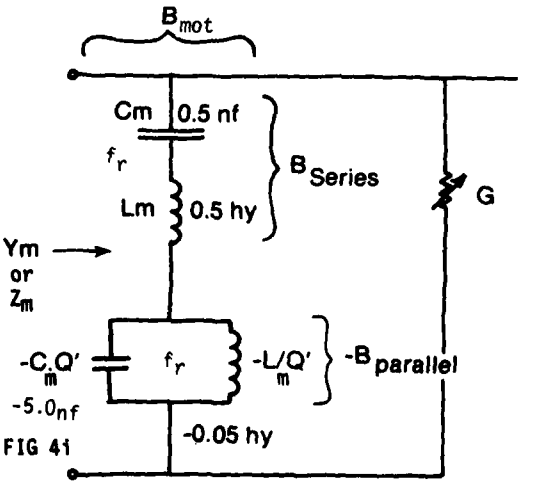

FIG 4i

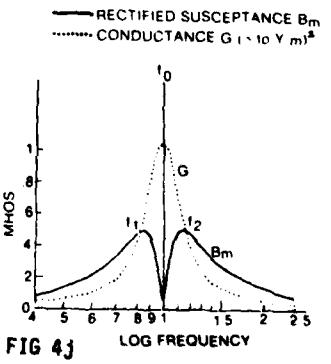

FIG 4j

a lossless negative parallel-resonance circuit. Hence $B_m = B_s \oint (-B_p)$ or $B_m = \frac{-B_p \cdot B_s}{-B_p + B_s}$. These terms B_{series} and $B_{parallel}$ are obtainable from Fig 4c. [The mechanism by which Fig 4f's low-Q curve is obtained, is a little different this time from above. Although the curve for $-B_p$ is practically identical with the $-X_m$ of Fig 4e, we do not multiply the curve this time with $|Y_m|^2$. Instead, we multiply it with B_s, obtaining a constant value for the numerator. We then divide by $(-B_p + B_s)$ This sum, the denominator term, has a shape somewhat like one cycle of a cosecant curve; hence its inverse or 1/D will look somewhat like one cycle of a sine curve: it starts with zero value at d-c, rises to a peak below f_r, goes to zero at f_r, proceeds to a negative peak, and then heads up toward zero value. Furthermore, the higher the value of Q' in Fig 4i, the more the "sine curve" is distorted, the peak moving closer to f_r, and the slopes conforming better to Fig 4f's solid curve. And this is just what we need.]

Actually, mentally sketching out the current through $-B_p \oint B_s$ (cf. Fig 4i) is the preferred way, whenever possible. Thus: at the resonance frequency, where $B_s = \infty$ (calling for an ∞ current) B_m reduces to $-B_p$. This equals 0 and calls for a 0 current; which is what we observe in Fig. 4f. At very low frequency and very high frequency, where $-B_p$ is very large, B_m reduces to B_s; so $-B_p$ has no effect. This also is apparent in Fig 4f. The effect of the coefficient Q' is to control the slope of the $-B_p$ curve and hence the size of the positive peak and negative peak of B_m itself. This $-B_p$ curve is practically identical to the $-X_m$ curve of Fig 4e. As $Q' \rightarrow \infty$, the curve becomes steeper and steeper by rotating clockwise toward the ordinate axis. This Q' is closely related to the true Q, which is

Chapter 4. Derivation of the Susceptance and Conductance curves.

Fig 4a

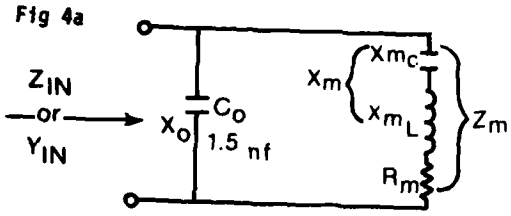

$$Z_{IN} = jX_o \,||\, Z_m$$

$$Y_{IN} = \frac{1}{jX_o} + \frac{1}{Z_m} = jB_o + Y_m$$

FIG 4b The B_o component of input susceptance of "clamped" transducer

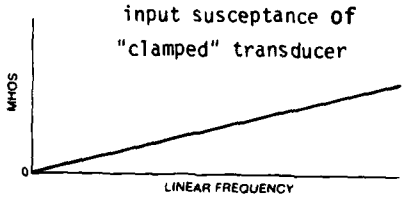

FIG 4c

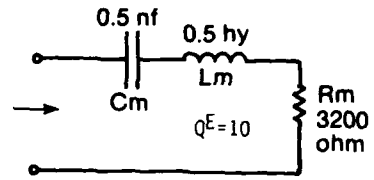

NUMERATOR TERM or N:

NEGATIVE SERIES RESONANCE RESPONSE

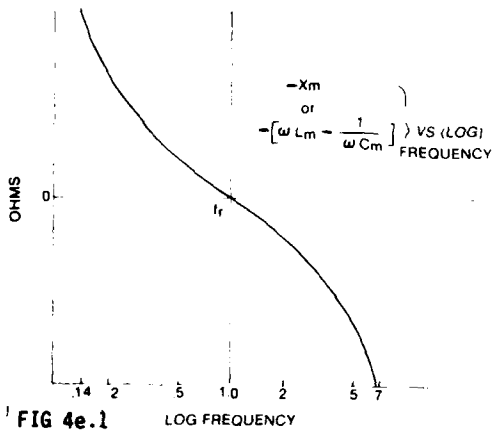

FIG 4e.1 LOG FREQUENCY

NEGATIVE SERIES RESONANCE RESPONSE ($-X_m$)
AND
POSITIVE SERIES RESONANCE RESPONSE ($+X_m$)

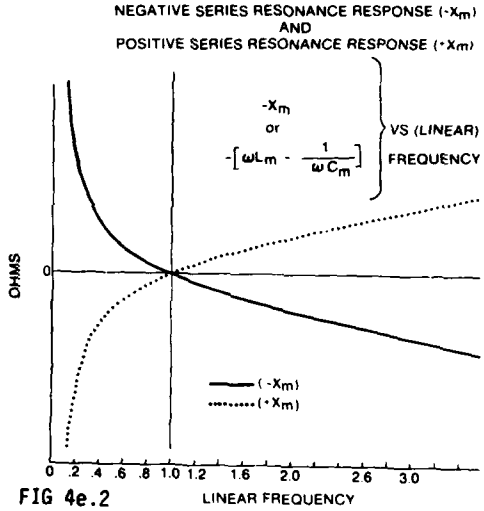

FIG 4e.2 LINEAR FREQUENCY

(1/DENOMINATOR) TERM:
ADMITTANCE SQUARED
OF "MOTIONAL" BRANCH, $|Y_m|^2$
(ALSO $|Y_m|$)

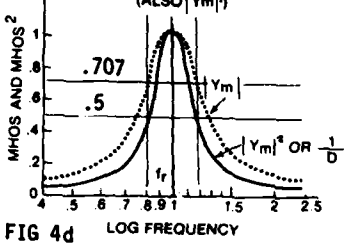

FIG 4d

"motional"
SUSCEPTANCE B_m
LOW Q
∞ Q

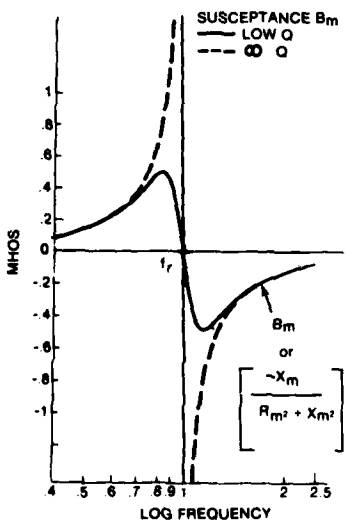

FIG 4f

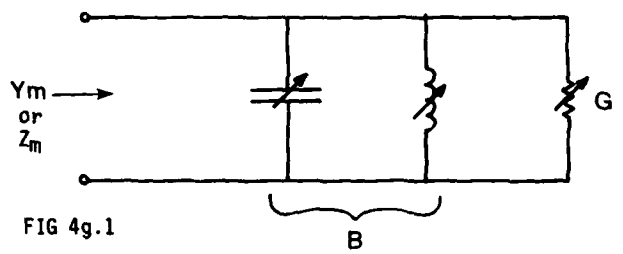

FIG 4g.1

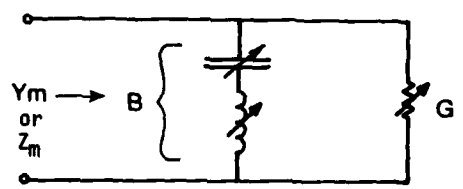

FIG 4g.2

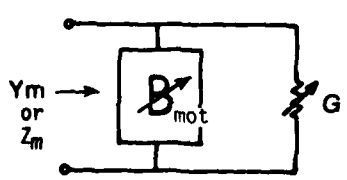

FIG 4h

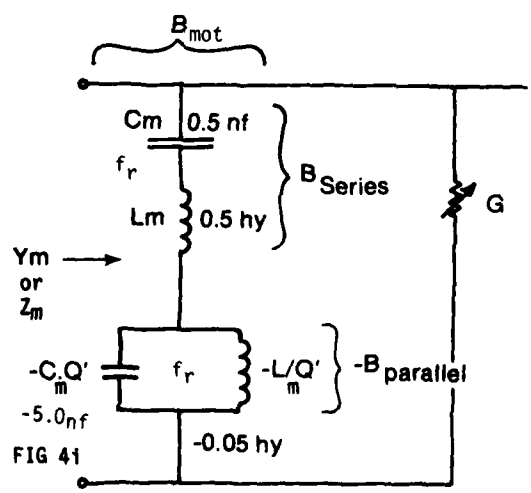

FIG 4i

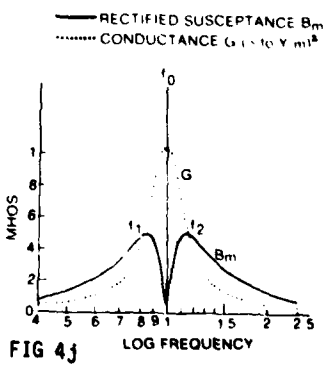

FIG 4j

related to R_m. [As an aid to working with these susceptances, it is permissible to construct the dual circuit and work with its reactances. The curves are the same. The dual circuit to Fig 4i is shown in Fig 5i and its response curves are shown in Fig 5f.]

One term remains to be discussed: $\not{G}$ of Fig 4i. No useful equivalent circuit using constant elements has appeared yet. The plot of G appears in Fig 4j, dotted curve. The curve is, in effect, the same sharp curve $|Y_m|^2$ that appears in Fig 4d, solid curve. For, $G = \frac{R_m}{R_{m^2} + X_{m^2}}$ or $R_m \cdot |Y_m|^2$. So R_m is just a scale factor; and it is a constant. The d-c value of G is zero. The maximum value is 1/Rm; 0.31×10^{-3} mhos in this example.

Note that the dotted curve in Fig 4d for $|Y_m|$ or $1/\sqrt{R_{m^2} + X_{m^2}}$ is much less sharp. This curve acts as the envelope for the rectified B curve shown in Fig 4j, solid curve. For, $B = \frac{-X_m}{R_{m^2} + X_{m^2}}$ or $-X_m \cdot |Y_m|^2$; and the $-X_m$ factor (shown in Fig 4e) acts to "fatten up" the $|Y_m|^2$ curve at low frequencies and high frequencies, into $|Y_m|$ (using rectification appropriately). This is seen alternatively if we let R_m go to zero (hence ∞ Q). Then $B = \frac{-1}{X_m}$ Which is merely the inverse of Fig 4e, (namely the ∞ - Q curve of Fig 4f). And this of course, when rectified, must follow the $|Y_m|$ envelope except near resonance.

The two peaks of the rectified B curve (Fig 4j) intersect the G curve at exactly half the maximum value of G. (This can be proved analytically.) The two associated frequencies f_1 and f_2 are thus the half-power frequencies. And these determine Q^E, since $Q^E = \frac{f_r}{f_2 - f_1}$. That is, at these two frequencies,

Chapter 4. Derivation of the Susceptance and Conductance curves.

Fig 4a

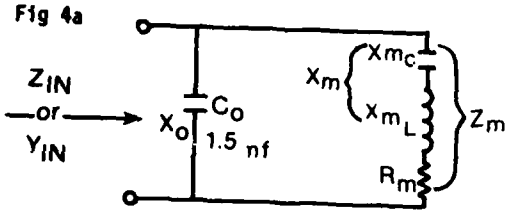

$Z_{IN} = jX_o \,||\, Z_m$

$Y_{IN} = \frac{1}{jX_o} + \frac{1}{Z_m} = jB_o + Y_m$

FIG 4b The B_o component of input susceptance of "clamped" transducer

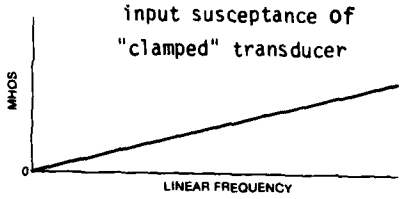

FIG 4c

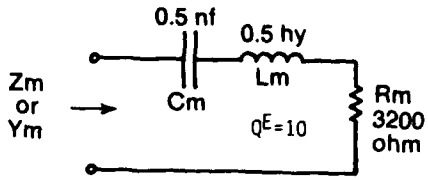

NUMERATOR TERM or N:

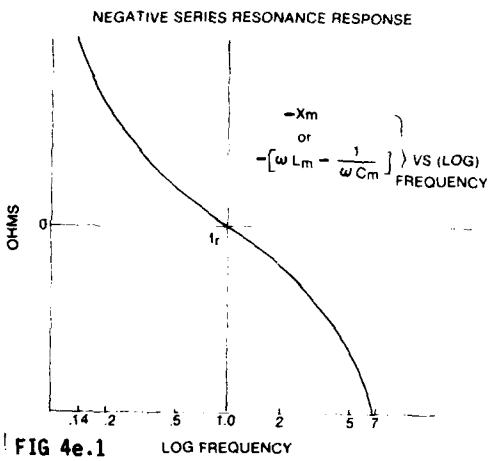

FIG 4e.1

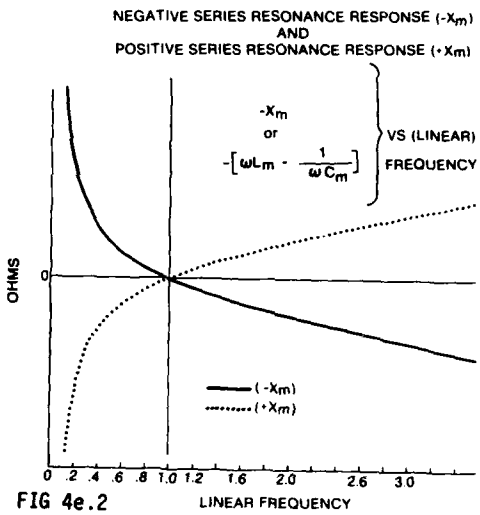

FIG 4e.2

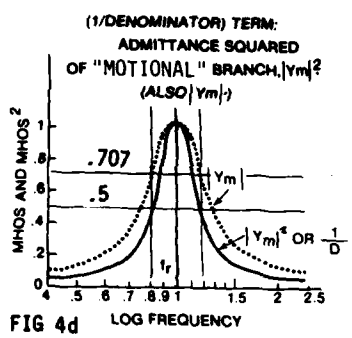

FIG 4d

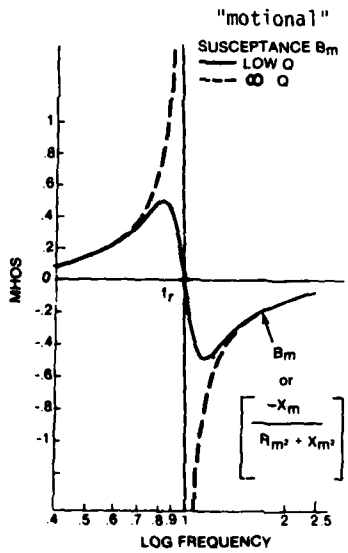

FIG 4f

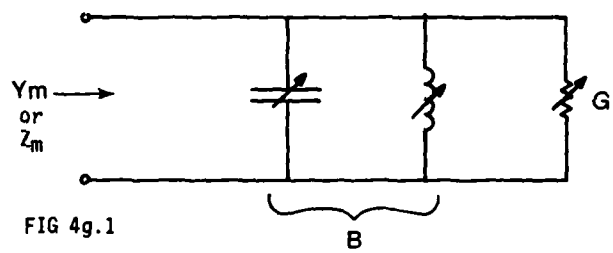

FIG 4g.1

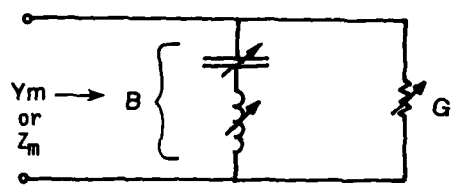

FIG 4g.2

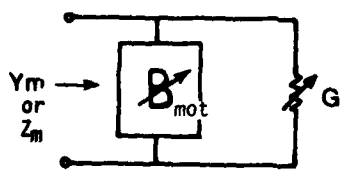

FIG 4h

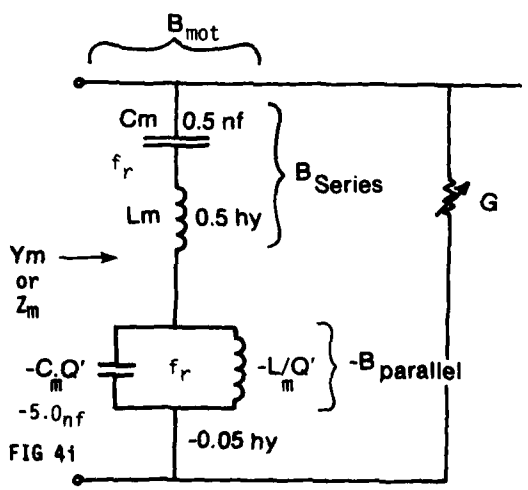

FIG 4i

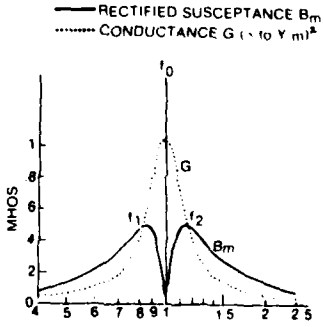

FIG 4j

$|Y_m|$ or I is 0.707 of $|Y_m|$ max or I max (see Fig 4d); and these are thus called the -3dB frequencies (using a 20 log scale). Since power at these frequencies equals E_{in}x(0.707 I max) x cos 45^{o}, the power is 0.50 of maximum power. But alternatively, at these two frequencies the G value is 0.50 of G max. And since power also equals E_{in}^{2} x G, the power is clearly reduced here to 0.50 of maximum power. Hence again, -3dB; this time using a 10 log scale. A study of Fig 4d will clarify these points.

Chapter 5. Derivation of the Reactance and Resistance curves.

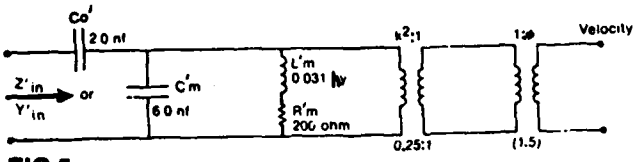

FIG 5a

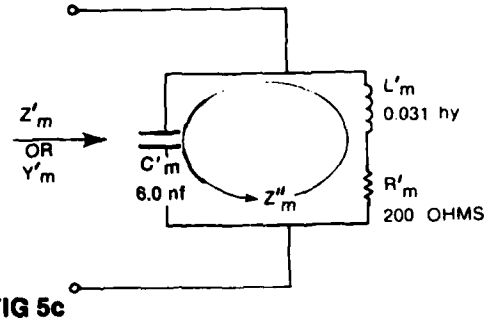

FIG 5c

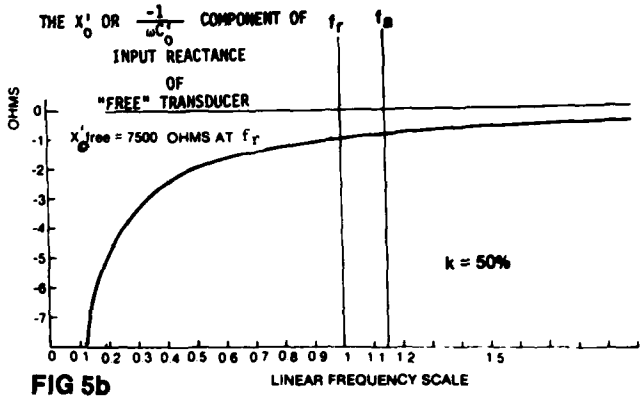

FIG 5b

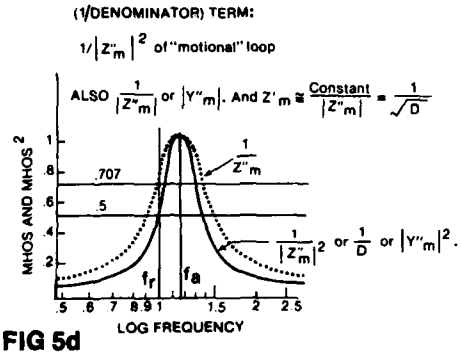

FIG 5d

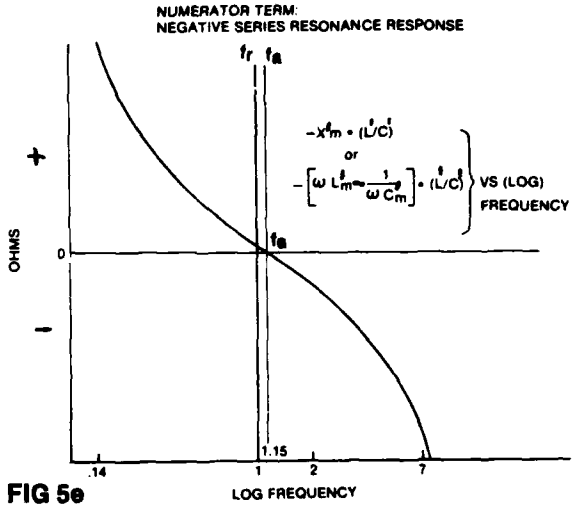

FIG 5e

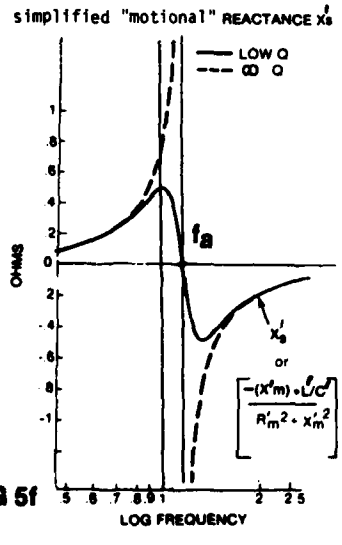

FIG 5f

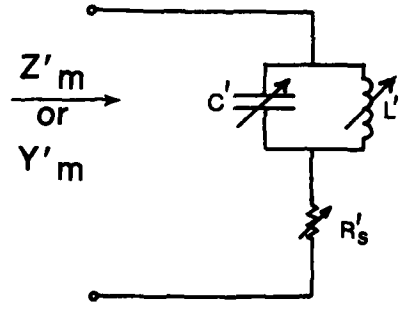

FIG 5g

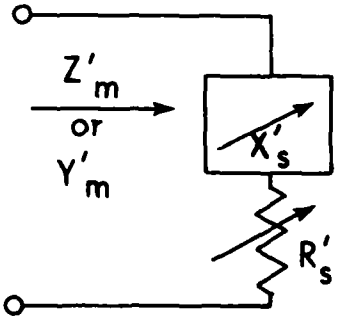

FIG 5h

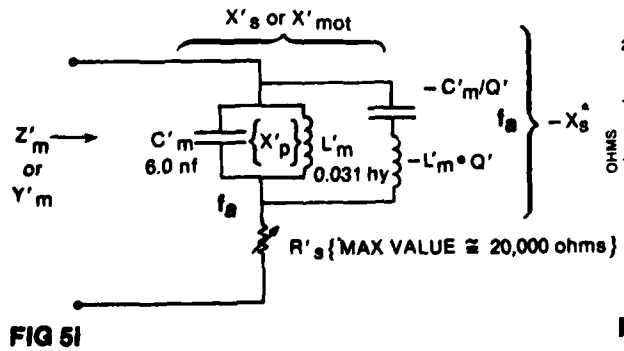

FIG 5i

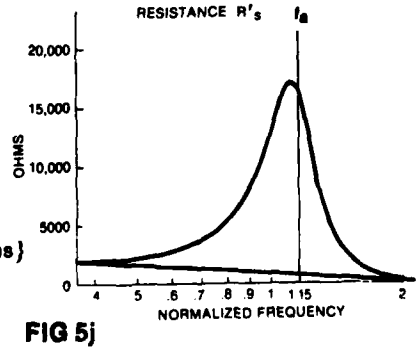

FIG 5j

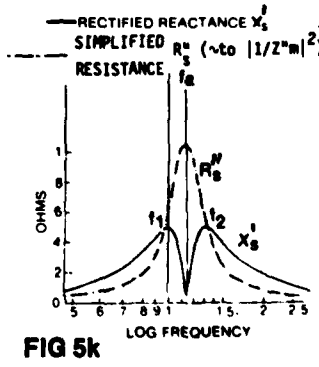

FIG 5k

CHAPTER 5. Derivation of the Reactance and Resistance curves.

Figure 5a shows the simplified Basic Circuit that we will work with for reactance and resistance. All "mechanical" quantities have been transformed to the electrical side, where they are now called "motional" quantities. They are now components of Z_m', the "motional impedance". Then Z_{in}' equals $jX_o' + Z_m'$.

The term X_o', the "free" reactance, is plotted in Fig 5b. It is a hyperbola. It will act as a bias or a new baseline for the motional reactance component of Z_m'.

The term Z_m' consists of a resistance and a reactance and is $jX_{m_c}' \,||\, (R_m' + jX_{m_\ell}')$. By inspection Z_m' is seen to be a simple damped "tank circuit", as seen in Fig 5c.

$$\text{Then: } Z_m' = \frac{jX_c'(R_m' + jX_\ell')}{jX_c' + (R_m' + jX_\ell')} = \frac{jX_c' \cdot R_m' - X_c' \cdot X_\ell'}{R_m' + jX_m'} \cdot \frac{R_m' - jX_m'}{R_m' - jX_m'} \qquad (5.1)$$

Note that jX_m' is the series reactance $j(X_\ell' + X_c')$, obtained by going around the loop in Fig 5c.

$$Z_m' = \frac{-X_c' \cdot X_\ell' \cdot R_m' + X_c'(X_\ell' + X_c') \cdot R_m'}{R_m'^2 + X_m'^2} + j\,\frac{X_c' \cdot X_\ell' \cdot X_m' + X_c' \cdot R_m'^2}{R_m'^2 + X_m'^2} \qquad (5.2)$$

$$Z_m' = \overbrace{\frac{R_m' \cdot (X_c')^2}{D}}^{R' \text{ series or } R_s'} + j\,\overbrace{\frac{-(L'/C') \cdot X_m' + R_m'^2(-1/\omega C')}{D}}^{+jX' \text{ series or } jX_s'} \qquad (5.3)$$

And the denominator $D = R_m'^2 + X_m'^2$.

This compares quite closely with Chapter 4's formulation for Y_m.

$$Y_m = \underbrace{\frac{R_m}{D}}_{G \text{ parallel}} + j\,\underbrace{\frac{-X_m}{D}}_{+jB \text{ parallel}} \quad ; \text{ but here } D = R_m^2 + X_m^2 \qquad (5.4)$$

SOME DIFFERENCES:

Z always has the terms

$$\text{Ohms}^3/|Z|^2 + j\ \text{Ohms}^3/|Z|^2 = R_s \text{ ohms} + jX_s \text{ ohms}.$$

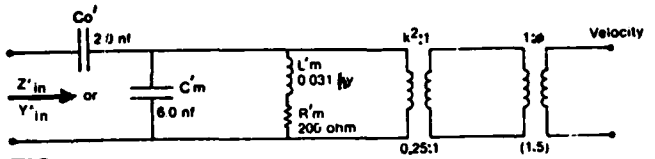

FIG 5a

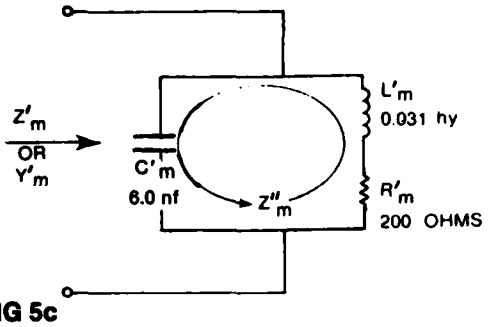

FIG 5c

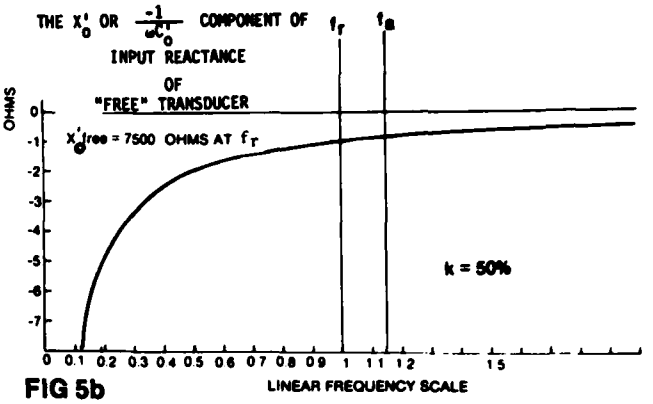

FIG 5b

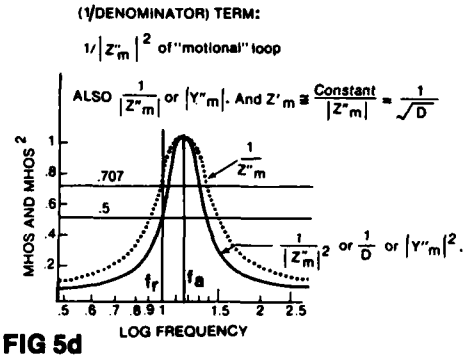

FIG 5d

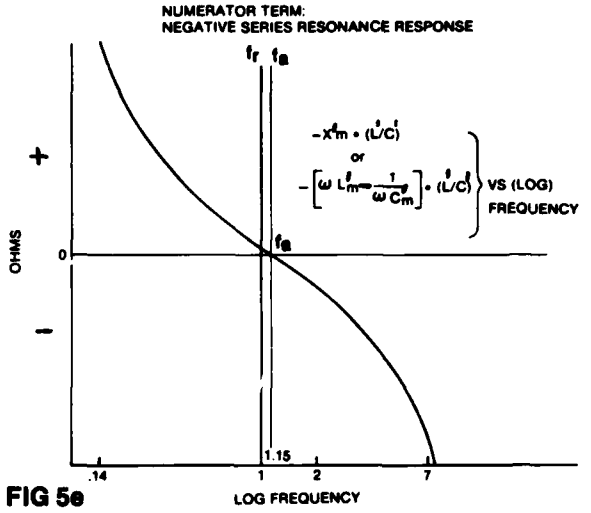

FIG 5e

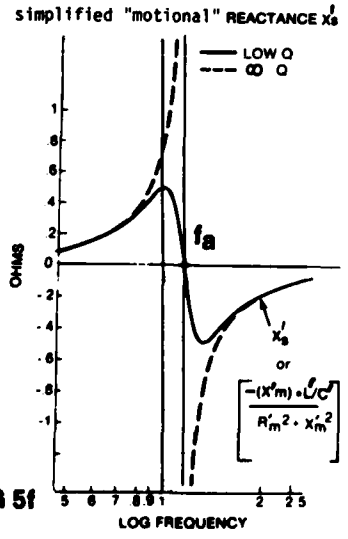

FIG 5f

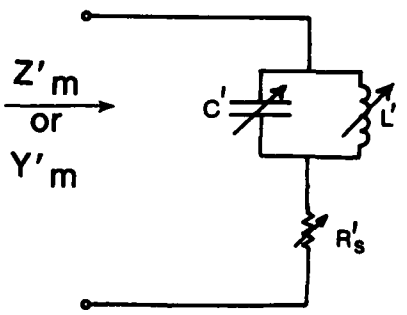

FIG 5g

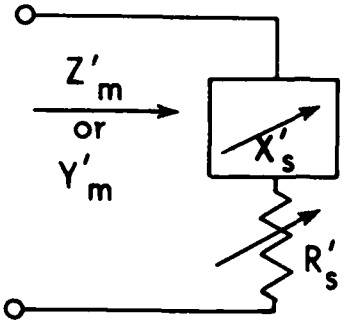

FIG 5h

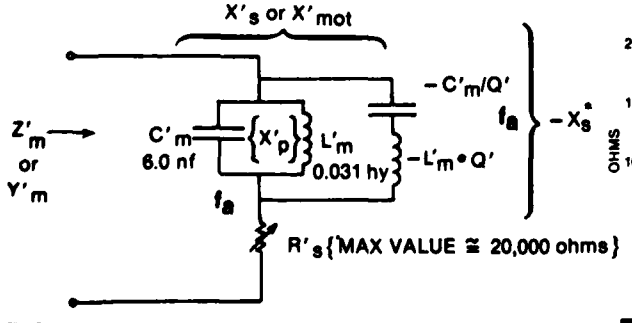

FIG 5i

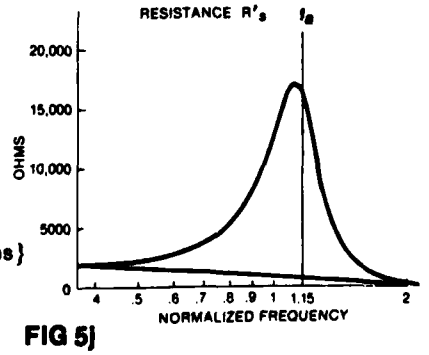

FIG 5j

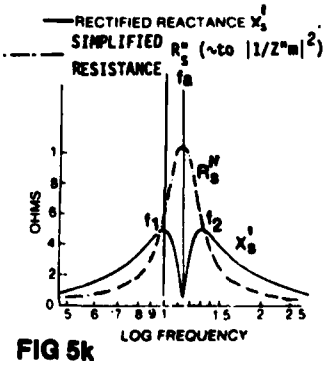

FIG 5k

Y always has the terms

Ohms $/|Z|^2$ + j Ohms$/|Z|^2$ = G mhos + jB mhos.

G goes to zero at d-c, as seen in Eq. 5.4.

R_s' goes to R_m' at d-c, due to the factor $(X_c')^2$, as seen in Eq. 5.3 and in Figs 5a and 5c.

X_s' has an additional factor, $(-1/\omega C_m')\cdot R_m'^2$, which perturbs the X_s' curve slightly, as seen in Eq. 5.3 .

[The mechanism of the perturbation is as follows: the curve of the factor $-X_m'\cdot(L'/C')$ in Fig 5e has its axis-crossing shifted to the left and down, since it is now sitting on a $-1/\omega C$ baseline (like Fig 5b). This action in turn shifts the whole "simplified X_s' curve" (Fig 5f) to the left and down, thereby lowering the antiresonance frequency f_a. The lowering is given by the relation $\omega = \omega_o \sqrt{1-1/Q^2.}$]

We will ignore the real term R_s' for the moment and concentrate on X_s' = Numerator/Denominator = N/D.

$D = R_m'^2 + X_m'^2$ or $|Z_m''|^2$ where Z_m'' is the series impedance for a current looping inside the tank. (See Fig 5c). (This is always the meaning of the denominator when any two networks are paralleled.) Then 1/D is $\frac{1}{|Z_m''|^2}$ or $|Y_m''|^2$. Its response is shown in Fig 5d, solid curve.

Note that although D describes a series-resonant circuit we call its resonance frequency f_a because it is merely another way of looking at the anti-resonance frequency of the tank. Now, f_a occurs at a higher frequency than does f_r of the Y curve in Chapter 4. This can be easily seen by looking at the values of C_m' and L_m' in Fig 5c or Fig 2f, as opposed to the values of C_m and L_m in Fig 3a or Fig 2c.

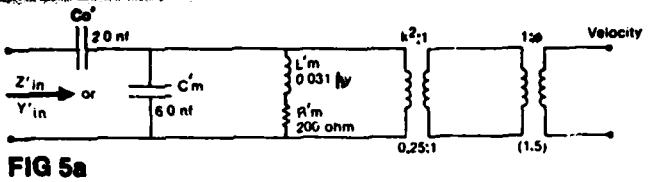

FIG 5a

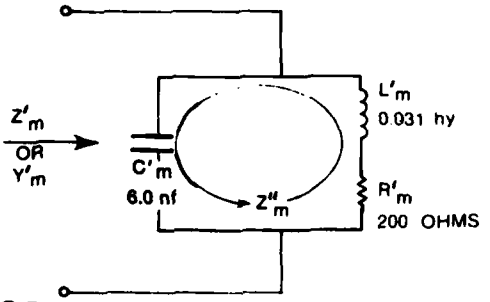

FIG 5c

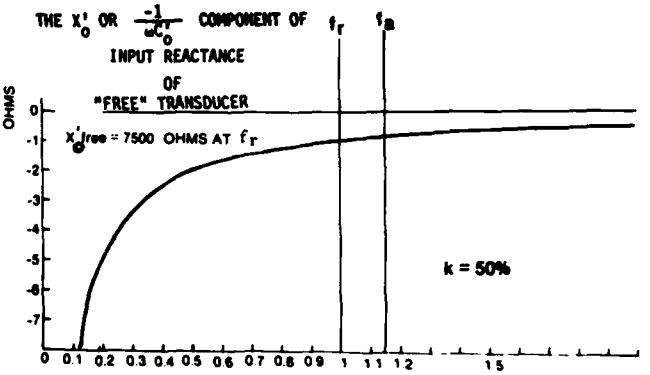

FIG 5b

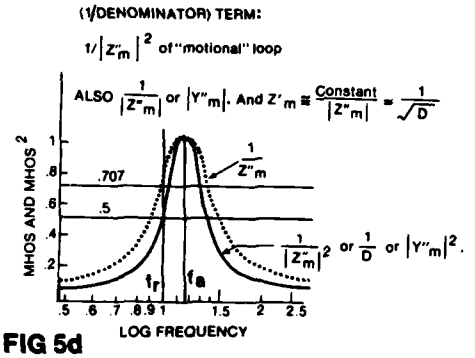

FIG 5d

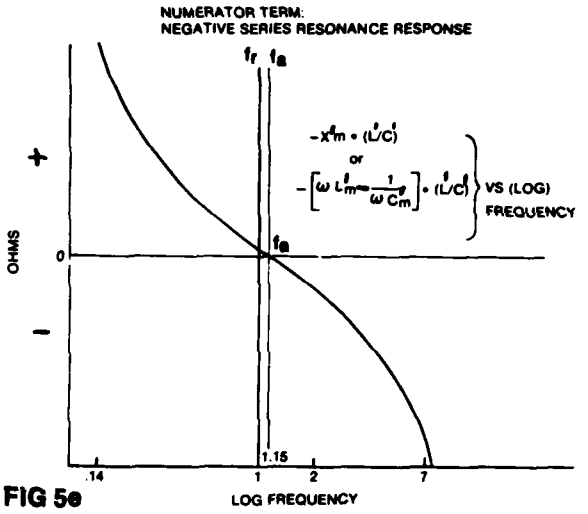

FIG 5e

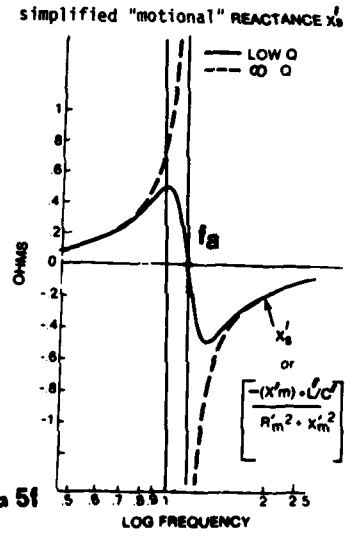

FIG 5f

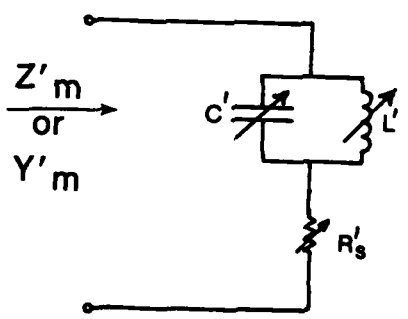

FIG 5g

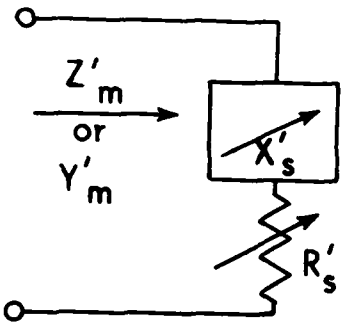

FIG 5h

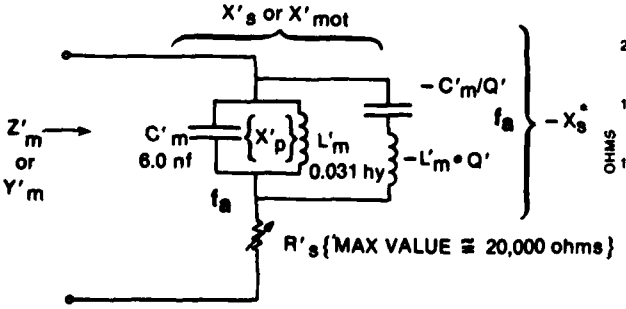

FIG 5i

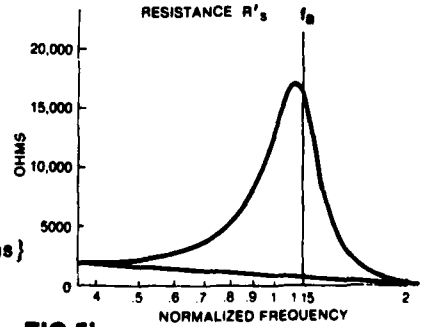

FIG 5j

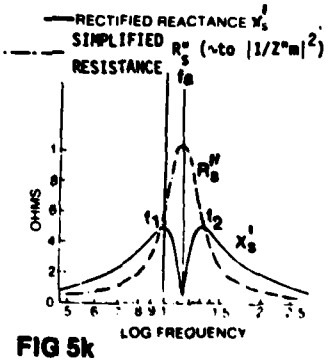

FIG 5k

In addition we will simplify the X_s' term of Eq. 5.3 by letting the factor $(-1/\omega C').R_m'^2 \approx 0$. For when $Q \geq 10$, this factor performs only a small perturbation on the main factor $-(L'/C').X_m'$. We then see that X_s' should be very similar to the B_m term in Fig 4f. In fact $B_m = \frac{-X_m}{|Z_m|^2}$, whereas $X_s' \simeq \frac{-(L'/C').X_m'}{|Z_m''|^2}$. L'/C' is merely a scale factor, of dimensions Ohm^2. The minus sign is present in both terms. Z_m'' is the impedance of a series-resonant circuit with a resonance frequency f_a somewhat higher than that of Z_m (cf. Fig 4c) with its f_r. That is, X_m' resonates at f_a, a frequency somewhat higher than the f_r of X_m.

Fig 5e shows $-(L'/C').X_m'$. And Fig 5f shows the resultant X_s'. Comparison with Figs 4d, 4e, and 4f shows a surprising similarity between the motional reactance-component curves and the motional susceptance-component curves, even though duality has not entered the discussion.

We now turn to Figures 5g, 5h, and 5i. These all are possible equivalents to the motional branch (Fig 5c) of the total circuit (Fig 5a). A circuit commonly used for analysis of Z functions is shown in Figure 5g. This is useful at low frequencies and high frequencies but fails to be useful at resonance when $Q < \infty$.

Actually the equation $R_s' + jX_s' \simeq R_s' + j\frac{-(L'/C')X_m'}{R_m'^2 + X_m'^2}$ demands only the equivalent circuit of Figure 5h. But the equation certainly <u>implies</u> that a more useful equivalence might exist.

And indeed a good equivalent circuit for the X_s' component alone of the Z_m' of Fig 5h does exist. It is shown in Fig 5i and it contains only fixed elements. (Actually it is the dual of Fig 4i.) It is a parallel-resonance

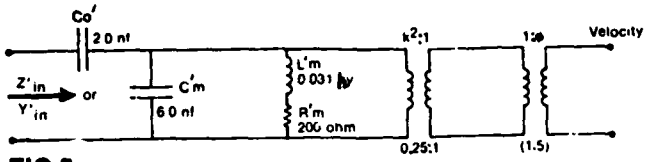

FIG 5a

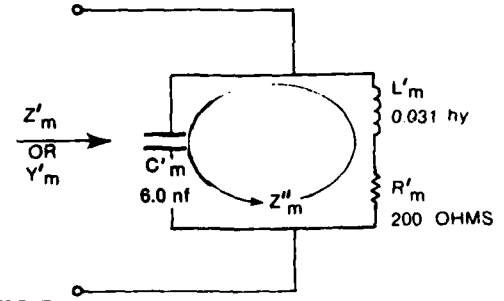

FIG 5c

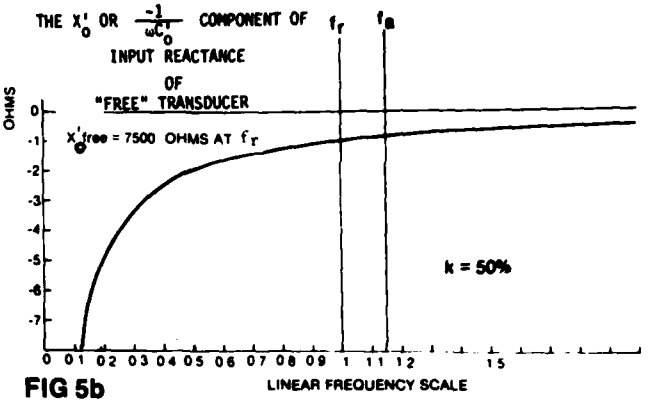

FIG 5b

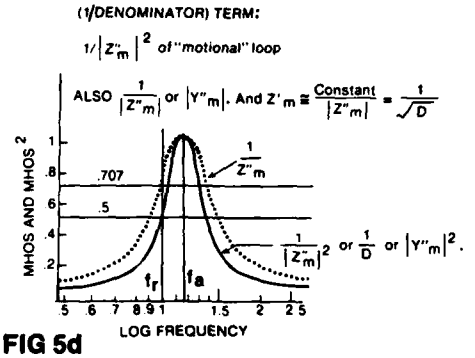

FIG 5d

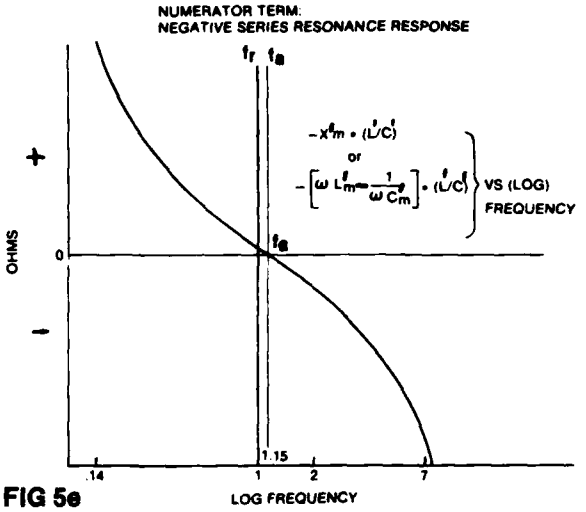

FIG 5e

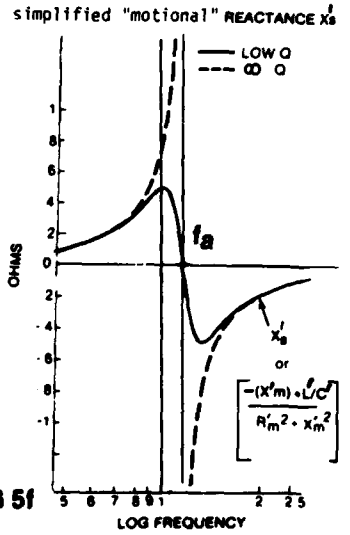

FIG 5f

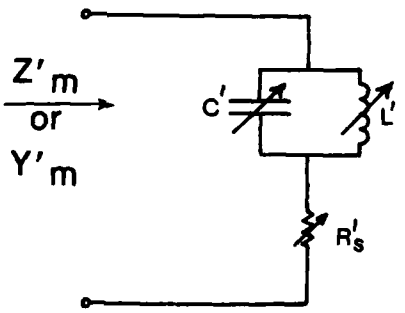

FIG 5g

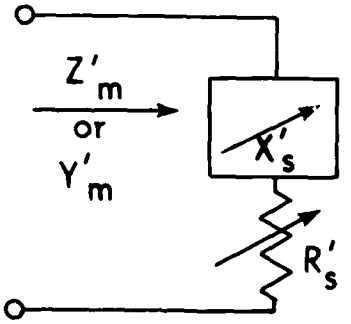

FIG 5h

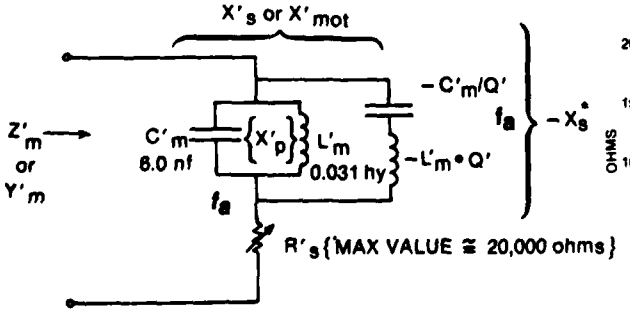

FIG 5i

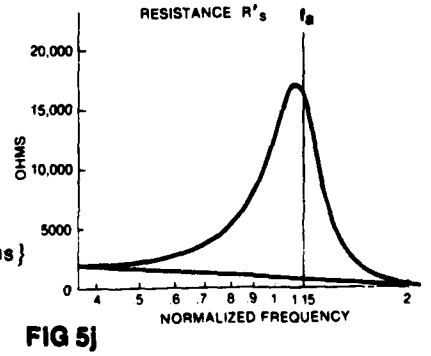

FIG 5j

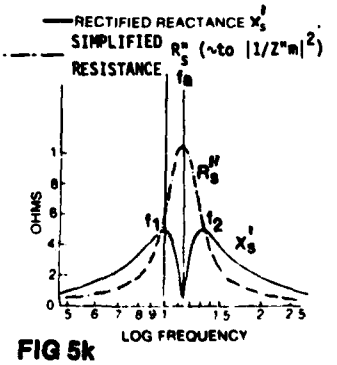

FIG 5k

circuit X_p' in parallel with a negative series-resonance circuit (-X*s). Hence

$X_s' = -X_s^* \;||\; X_p'$ or $X_s' = \dfrac{-X_s^* \cdot X_p'}{-X_s^* + X_p'}$. [The mechanism by which Fig 5f's low-Q curve is obtained, is similar to the mechanism given in Chapter 4. The curve for $-X_s^*$ is basically given by Fig 5e. The curve for X_p' is identical with the ∞ - Q curve of Figure 5f. Multiplication and division finally produce the low-Q curve of Figure 5f, just as described in Chapter 4.]

Actually, mentally sketching out the voltage across $-X_s^* \;||\; X_p'$ (viz. sketching out the impedance of the combination) is preferable, wherever possible. Thus: at the antiresonance frequency f_a, where X_p' is ∞, X_s' reduces to $-X_s^*$. This equals 0, which is what we observe in Figure 5f. At very low frequency and very high frequency, where $-X_s^*$ is very large, X_s' reduces to X_p'; so $-X_s^*$ has no effect. This also is apparent in Fig 5f. The effect of the coefficient Q' is to control the slope of the $-X_s^*$ curve (Fig 5e) and hence the size of the positive peak and negative peak of X_s' itself. As $Q' \to \infty$, the curve becomes steeper and steeper by rotating clockwise toward the ordinate axis. This Q' is closely related to the true Q, which is related to R_m' and to R_m

One term remains to be discussed: R_s' of Figure 5i. R_s' is identical with R'_{in} of Chapters 6 and 7, since the $\$$ addition of C_o does not affect this R. No useful equivalent circuit using constant elements has appeared yet. The plot of R_s' appears in Fig 5j. The curve is nearly the same sharp curve $|Y_m''|^2$ that appears in Fig 5d, solid curve (cf. also Fig 5k).

For, $R_s' = \dfrac{R_m' \cdot (X_c')^2}{R_m'^2 + X_m'^2}$ or $\left[R_m' \cdot (X_c')^2\right] \cdot |Y_m''|^2$. So the numerator N is (5.5)

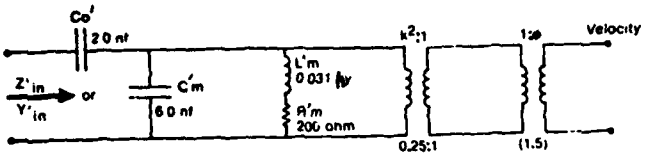

FIG 5a

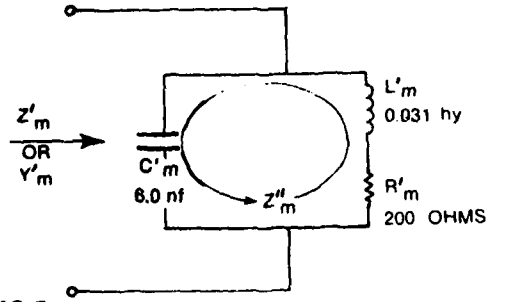

FIG 5c

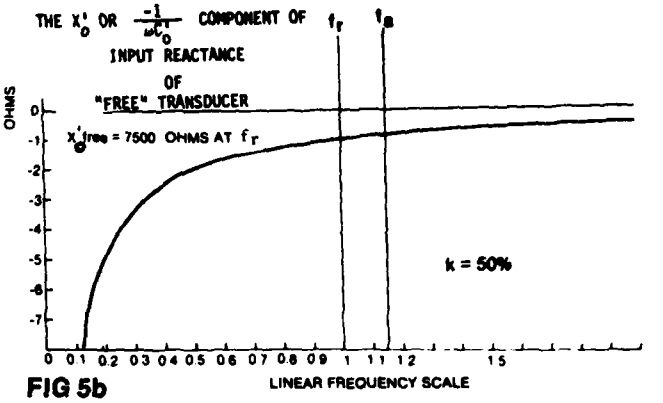

FIG 5b

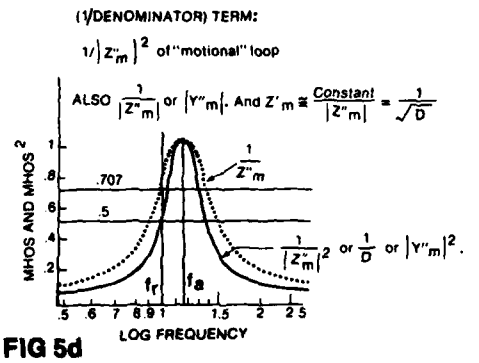

FIG 5d

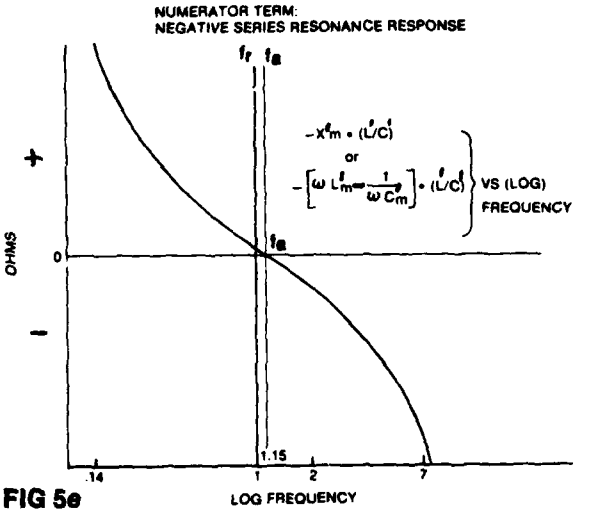

FIG 5e

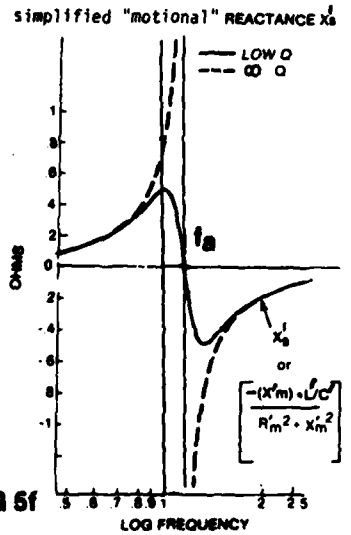

FIG 5f

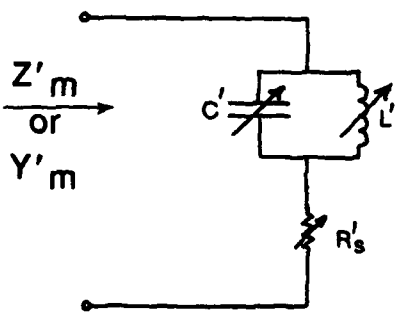

FIG 5g

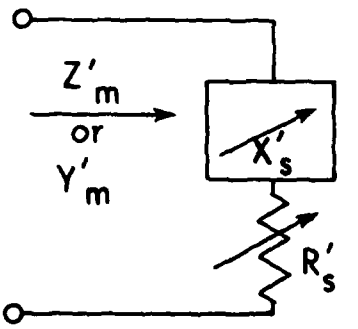

FIG 5h

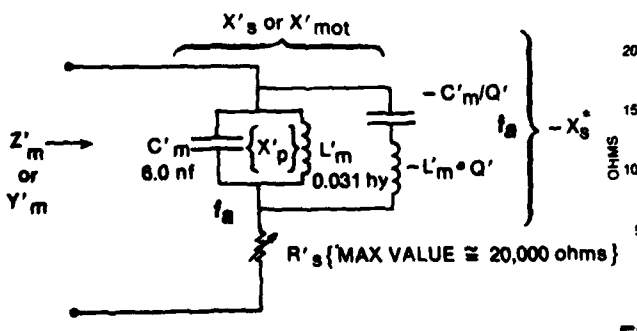

FIG 5i

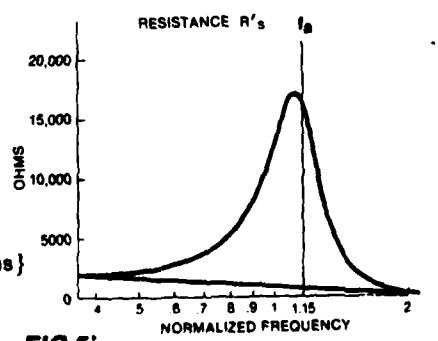

FIG 5j

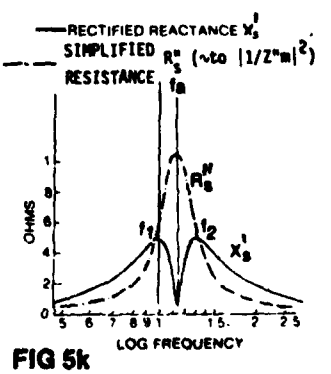

FIG 5k

basically a simple scale factor, R_m'; times the perturbation factor $(X_c')^2$ which acts to raise R_s' above zero at d-c, as seen in Fig 5j. The d-c value of R_s' is R_m' itself; 200 ohms in this example. The maximum value $\approx Q^2 \cdot R_m'$; 20,000 ohms in this example.

Note that the dotted curve in Fig 5d for $|Y_m''| = 1/\sqrt{R_{m^2}' + X_{m^2}'}$ is much less sharp. This curve acts as the envelope for the rectified X_s' curve shown (5.6)

in Fig 5k (solid curve). For, $X_s' \cong \dfrac{-X_m' \cdot (L'/C')}{R_{m^2}' + X_{m^2}'}$ or $-X_m' \cdot (L'/C') \cdot |Y_m''|^2$; and (5.7)

the $-X_m' \cdot (L'/C')$ factor (shown in Fig 5e) acts to "fatten up" the $|Y_m''|^2$ curve at low frequencies and high frequencies into Y_m'' (using rectification appropriately). This is seen alternatively if we let R_m' go to zero (hence ∞ Q). Then $X_s' = \dfrac{(L'/C')}{-X_m'}$, which is merely the inverse of Fig 5e if we normalize the scale factor (L'/C') for the moment. That is, this inverse of $-X_m'$ is merely the ∞ - Q curve of the X_s' family in Figure 5f. And this curve, when rectified, <u>is</u> the $|Y_m''|$ envelope of Fig 5d — except near resonance.

The two peaks of the rectified X_s' curve (Fig 5k) would intersect the R_s' curve almost exactly at half the maximum value of R_s', if we removed the pedestal (of approximately R_m' ohms d-c) on which the left leg of the R_s' curve is standing. When the Q is $\geq$ 10, a simple counter-clockwise pivoting of the R_s' curve around the right-leg extremity, down to the frequency axis, would produce a good "simplified curve", R_s''. The two frequencies of intersection

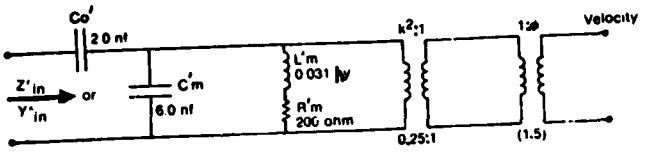

FIG 5a

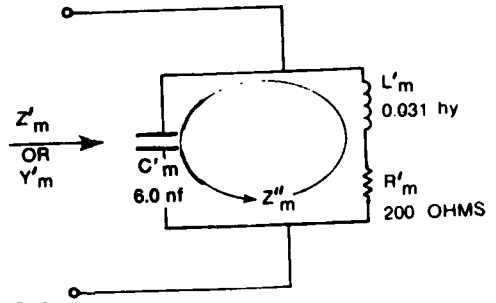

FIG 5c

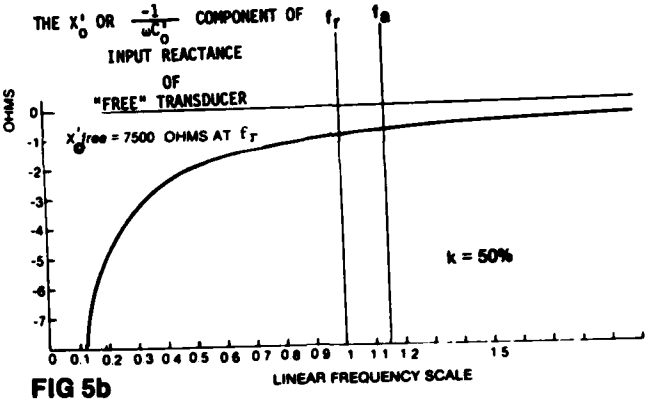

FIG 5b

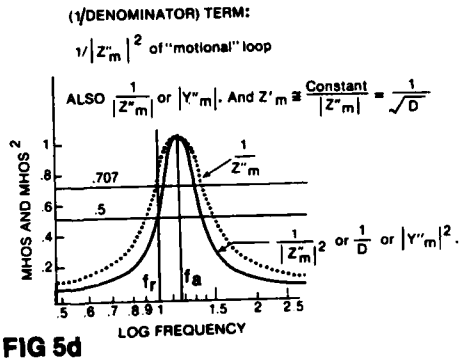

FIG 5d

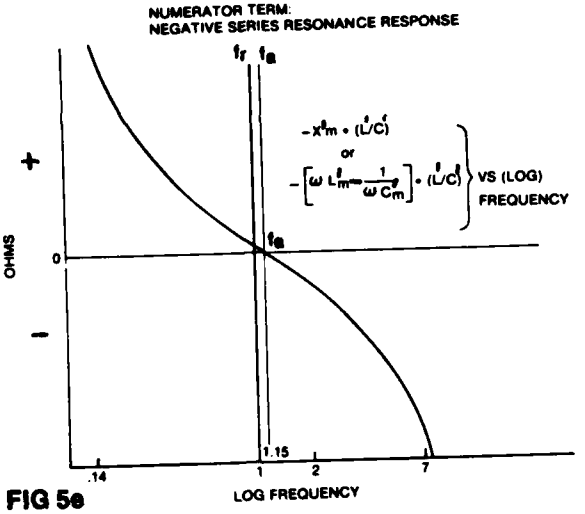

FIG 5e

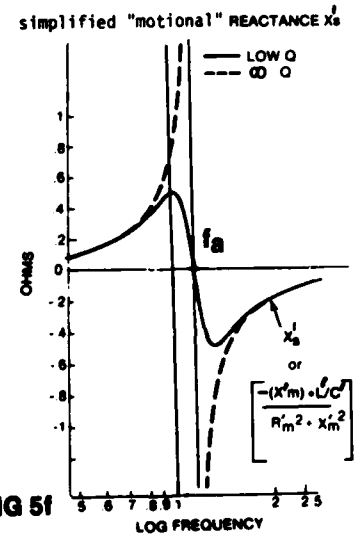

FIG 5f

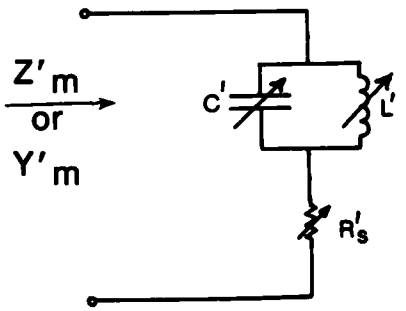

FIG 5g

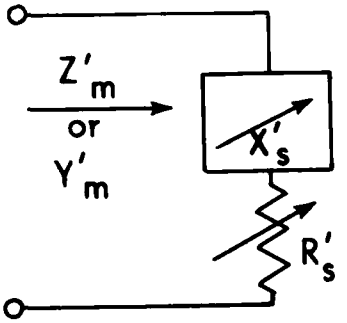

FIG 5h

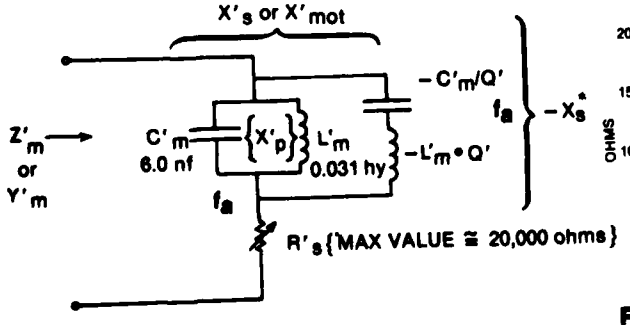

FIG 5i

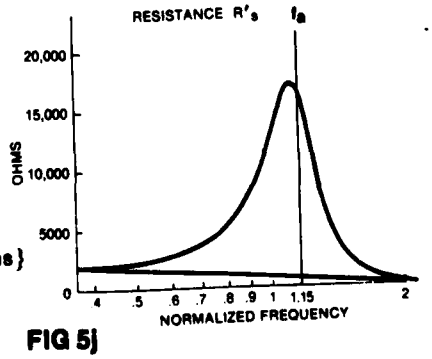

FIG 5j

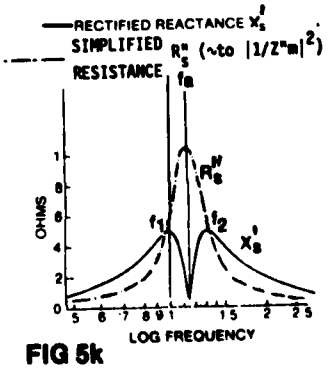

FIG 5k

f_1 and f_2, of R_s'' with X_s', would then be the half-power frequencies. And these determine Q^I, since $Q^I = \frac{f_a}{f_2 - f_1}$. That is, at these two frequencies, $|Z_m'|$ or E is 0.707 of $|Z_m'|_{max}$ (see Fig 5d) or of E_{max}; and these are thus called the -3 dB frequencies (using a 20 log scale). {Some approximations to $|Z_m'|$ for high Q are given in Appendix 5-A.} Since power at these two frequencies equals $I_{in} \cdot (0.707 \ E_{max}) \cdot \cos 45^o$, the power is 0.50 of maximum power. But alternatively, at these two frequencies the R_s'' value is 0.50 of R_s'' max. And since power also equals $I_{in}^2 \cdot R_s''$, the power is clearly reduced here to 0.50 of maximum power. Hence again, -3 dB; this time using a 10 log scale. A study of Fig. 5d will clarify these points.

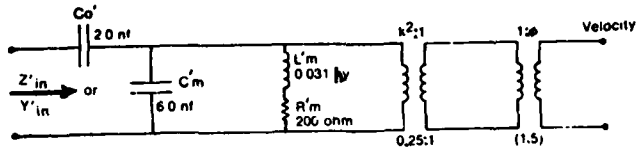

FIG 5a

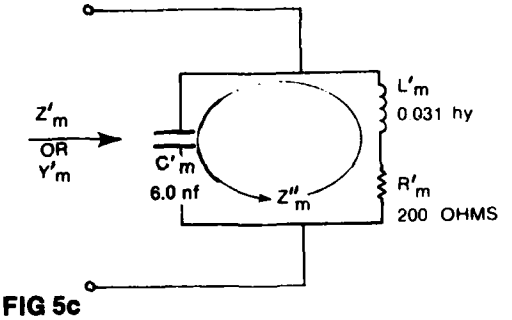

FIG 5c

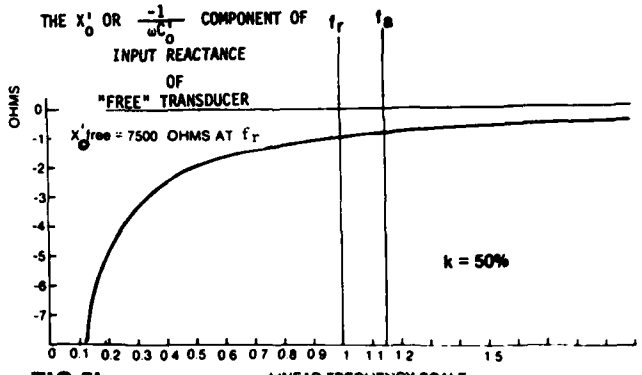

FIG 5b

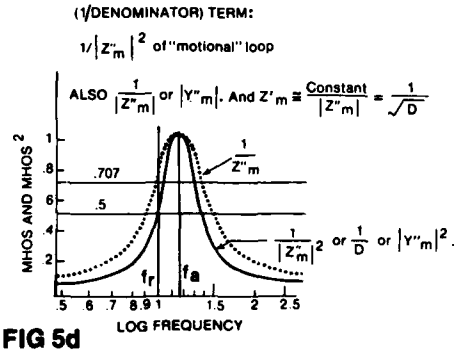

FIG 5d

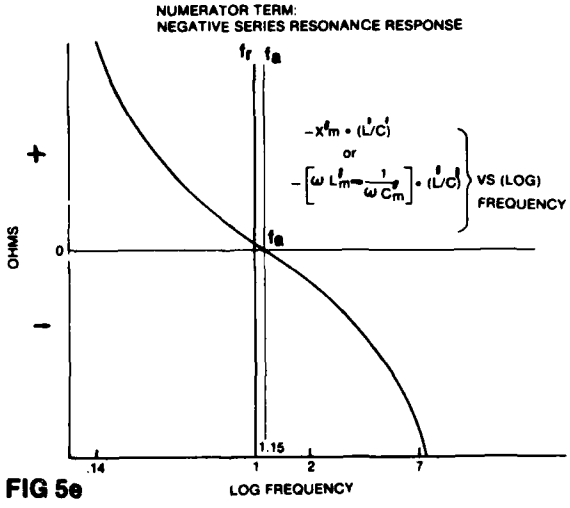

FIG 5e

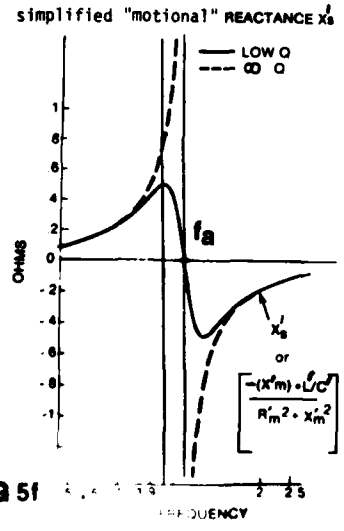

FIG 5f

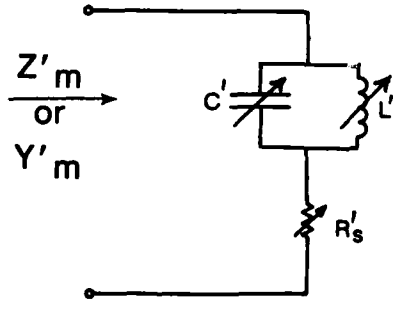

FIG 5g

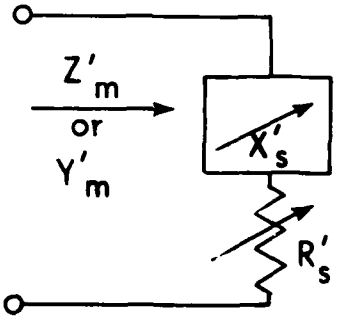

FIG 5h

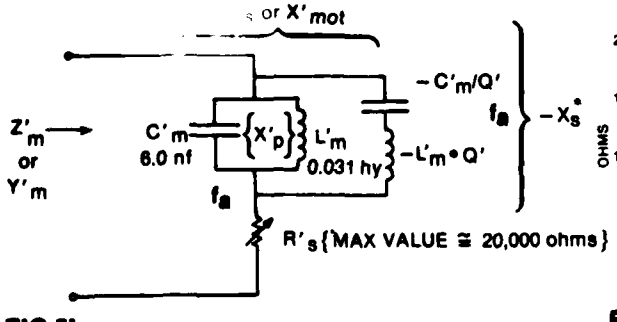

FIG 5i

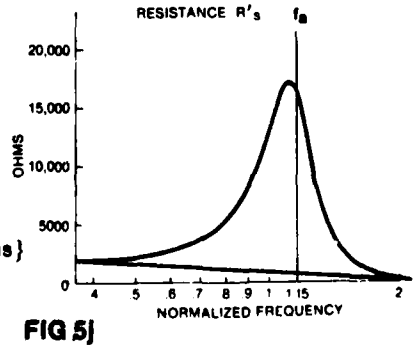

FIG 5j

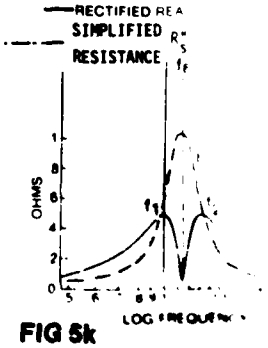

FIG 5k

Appendix 5-A: A Useful Approximation to the Input Impedance of the Motional Network.

An approximation to the input impedance $|Z'_m|$ of Fig 5c's tank circuit, is shown in Fig 5d. The dotted curve represents

$$|Y''_m| \quad \text{or} \quad \frac{1}{|Z''_m|} \quad \text{or} \quad \frac{1}{\sqrt{D}} \ .$$

And in the region around antiresonance, when $Q \geq 10$.

$$|Z'_m| \cong \frac{\text{Constant}}{\sqrt{D}} \ .$$

Note also that for constant-current drive, $E \sim |Z'_m|$.

We will now derive this $|Z'_m|$ approximation and two others, starting from Equ. 5.2 or 5.3 and squaring it.

$$\text{Then} \quad |Z'_m|^2 = \frac{R'^2_m \cdot X'^4_c + (X'_c \cdot X'_\ell)^2 \cdot X'^2_m + \delta^2}{(R'^2_m + X'^2_m)^2} \tag{5A.1}$$

There are three interesting frequency regions and hence three different approximations.

1) Near d-c, X'^4_m in the denominator takes control. It equals X'^4_c and so

$$|Z'_m|^2 \cong R'^2_m \quad \text{and}$$

$$|Z'_m| \cong R'_m \ , \text{ the d-c resistance of the tank.} \tag{5A.2}$$

2) Near f_a, $|X'_c| \cong |X'_\ell|$. Hence

$$|Z'_m|^2 \cong \frac{R'^2_m \cdot X'^4_c + X'^4_c \cdot X'^2_m + \delta^2}{(R'^2_m + X'^2_m)^2} \tag{5A.3}$$

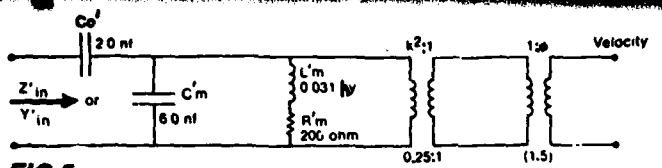

FIG 5a

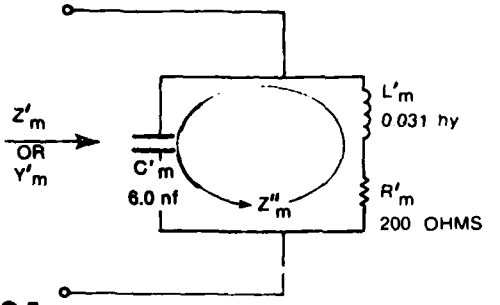

FIG 5c

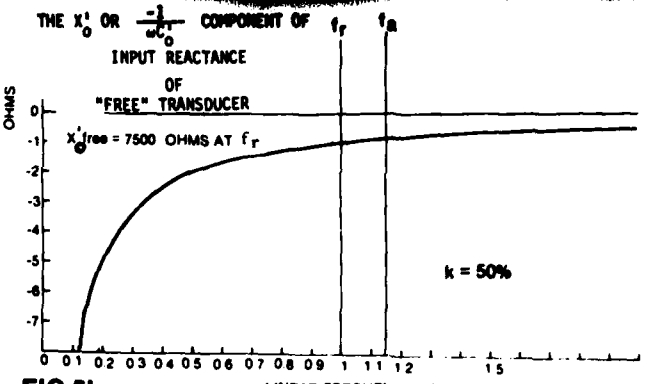

FIG 5b

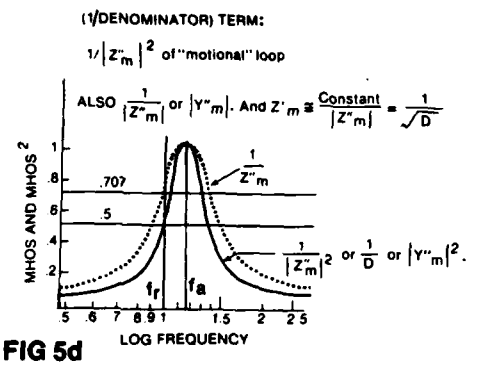

FIG 5d

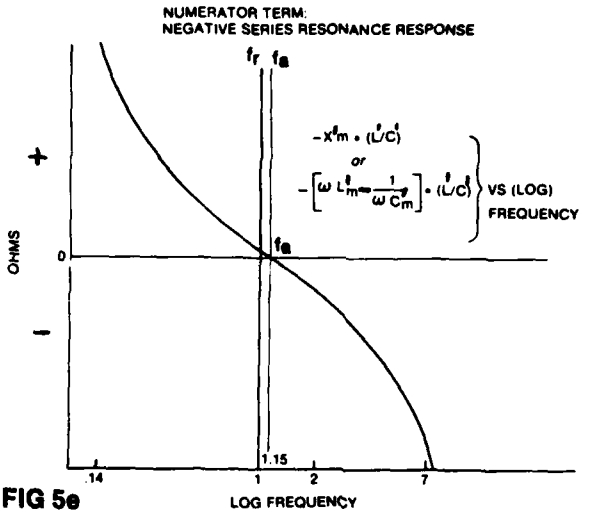

FIG 5e

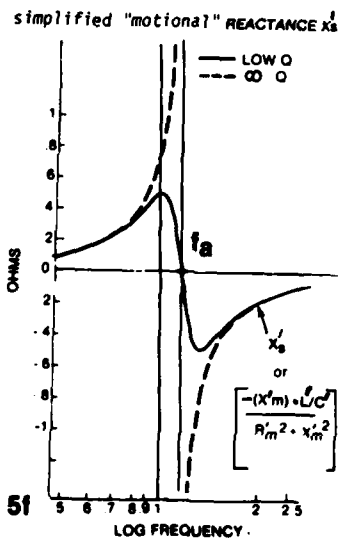

FIG 5f

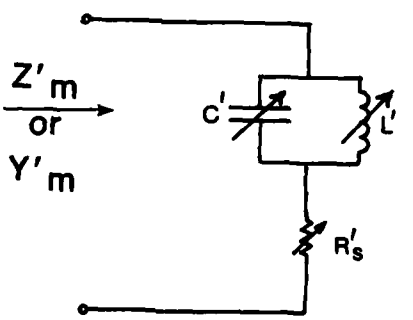

FIG 5g

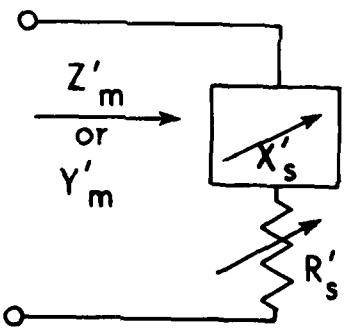

FIG 5h

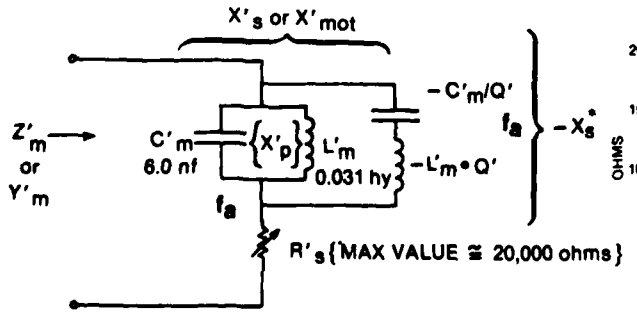

FIG 5i

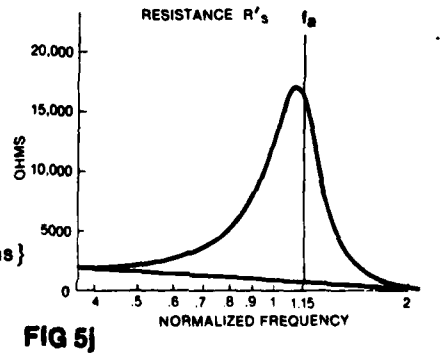

FIG 5j

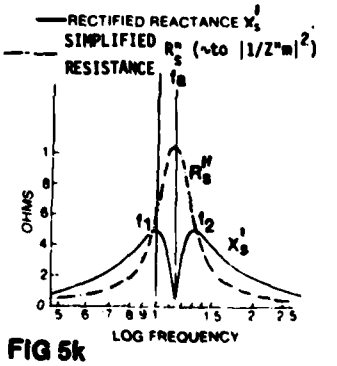

FIG 5k

$$|Z_m'|^2 = \frac{X_c'^4 (R_m'^2 + X_m'^2) + \delta^2}{(R_m'^2 + X_m'^2)^2} . \qquad (5A.4)$$

$$|Z_m'|^2 = \frac{X_c'^4 + \delta^2/D}{(R_m'^2 + X_m'^2)} . \quad \text{When } Q \geq 10, \ \frac{\delta^2}{D} \cong 0.$$

$$\text{Then } |Z_m'| \cong \frac{X_c'^2}{\sqrt{R_m'^2 + X_m'^2}} \cong \frac{|X_c' \cdot X_\ell'|}{\sqrt{D}} = \frac{(L'/C')}{\sqrt{D}} \qquad (5A.5)$$

Note that (L'/C') is a constant.

3) Above f_a, $X_m'^4$ takes control. It now equals $X_\ell'^4$.

$$|Z_m'|^2 \cong \frac{0 + (X_c' \cdot X_\ell')^2 \cdot X_\ell'^2 + 0}{(R_m'^2 + X_m'^2)^2} \qquad (5A.6)$$

$$|Z_m'|^2 \cong X_c'^2$$

$$|Z_m'| \cong |X_c'| = \left|\frac{-1}{\omega C'}\right| \qquad (5A.7)$$

This is the reactance of the motional capacitance C_m' of Figure 5c.

Chapter 6. The combining of component responses from Chapters 4 and 5; and comparison with responses from Chapters 3, 2, and 1.

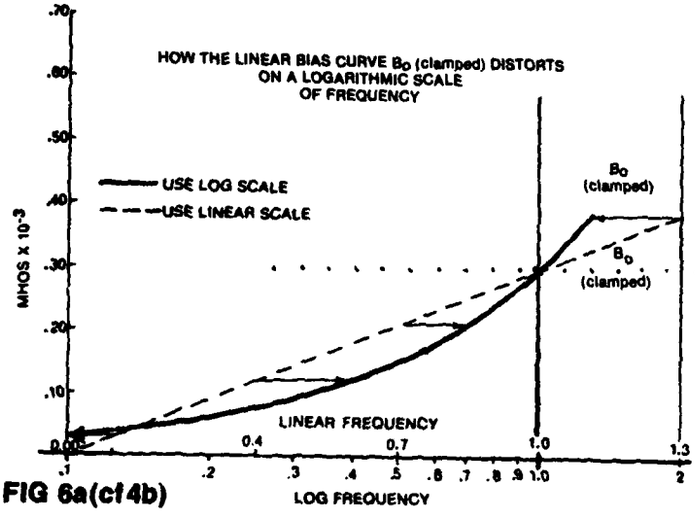

FIG 6a(cf4b)

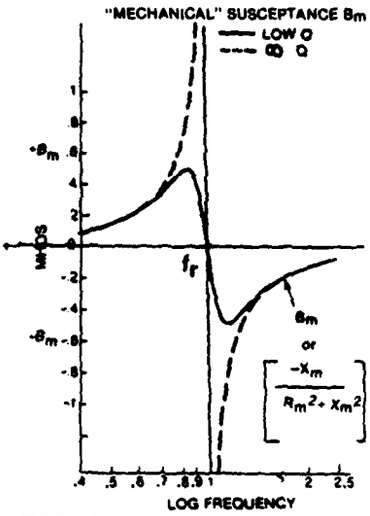

FIG 6b(cf4f)

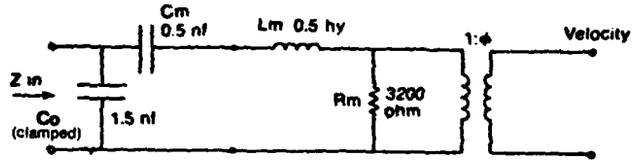

FIG 6c

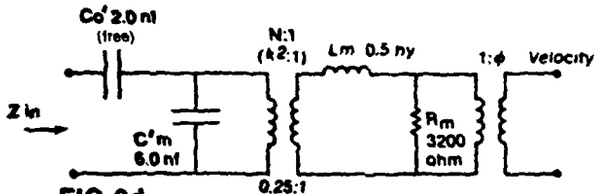

FIG 6d

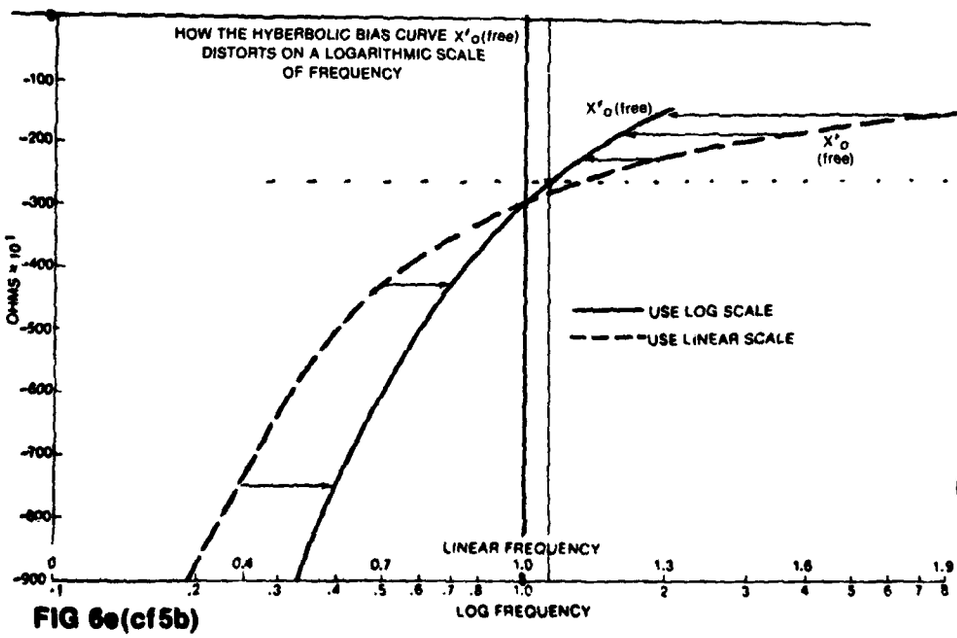

FIG 6e(cf5b)

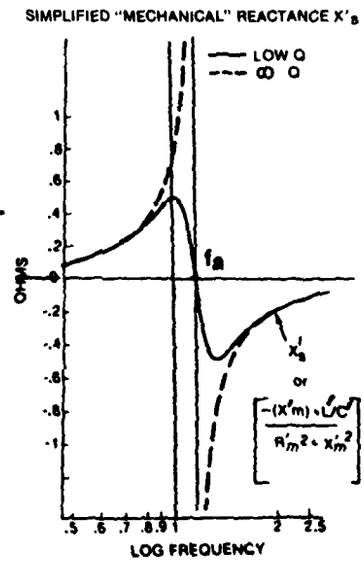

FIG 6f(cf5f)

Chapter 6. The Combining of Component Responses from Chapters 4 and 5; and Comparison with Responses from Chapters 3, 2, and 1.

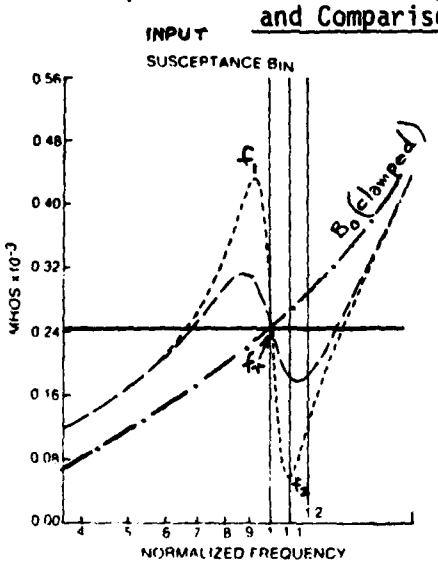

The aim of this Chapter is to display Figs. 6g (above, right) and 6h (below, right) and to review how they were created. Figures 6g and 6h are our first examples of a susceptance curve and a reactance curve actually generated by a computer performing a realistic simulation of an experimental transducer. (The "clamped" or "free" bias curve was plotted manually.)

Figure 6g (above) is basically the sum of Fig. 6b (motional susceptance B_m) in parallel with the solid curve of Fig. 6a, B - clamped or B_o, a bias curve. They can be conveniently added at f_r or 1.0. There is also shown in Fig. 6a how the linear bias curve B_o (clamped) distorts when a log frequency scale is used (as in Fig. 6g). Figure 6c shows the basic circuit which is the most useful starting point for obtaining Fig. 6g.

Figure 6h (below) is basically the sum of Fig 6f (motional reactance X_s') in series with the solid bias curve of Fig. 6e, X' - free or X_o'. They can be conveniently added at f_a or 1.15 (log scale). There is also shown, in Fig. 6e, how the hyperbolic bias curve X_o' (free) distorts when a log frequency scale is used (as in Fig. 6h).

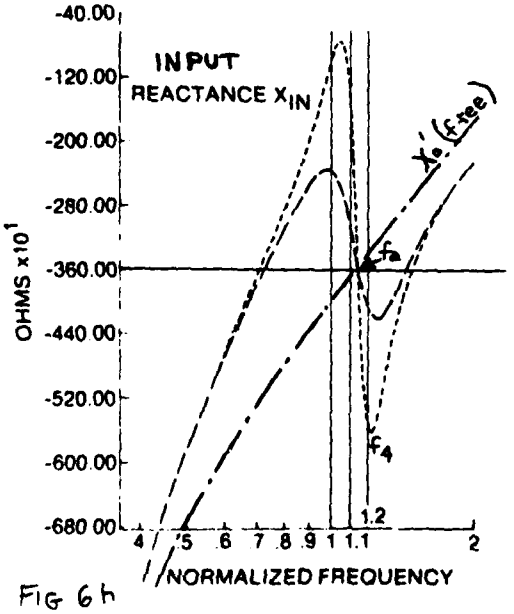

FIG 6h

Note that the log-scale B-curve (Fig. 6a) and the log-scale X-curve (Fig. 6e) show great symmetry; i.e., they are identical after two reflections. This double-reflection symmetry is also exhibited in a simple series-resonance curve, negative or positive. This is seen in Fig. 4e.1, as contrasted with Fig. 4e.2. Figure 6d shows the basic circuit which is the most useful starting point for obtaining Fig. 6h.

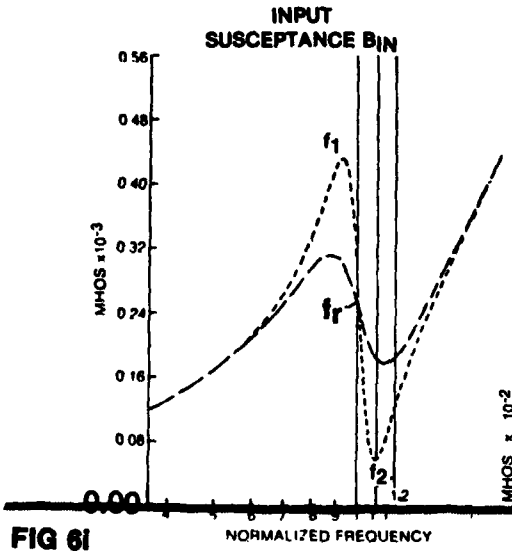

FIG 6i

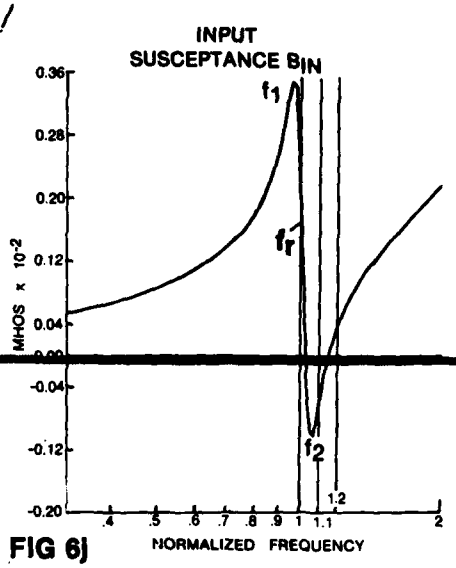

FIG 6j

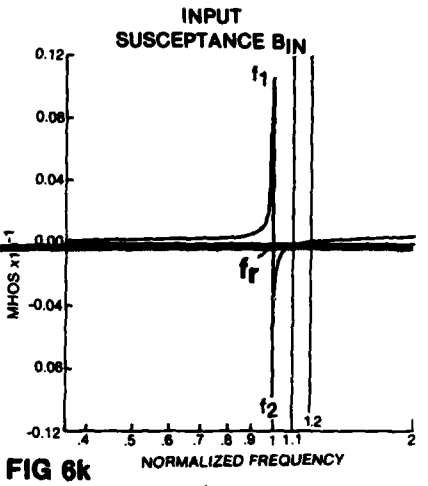

FIG 6k

ORDINATE SCALE EXPANDED

A GOOD "STANDARD"
ORDINATE SCALE

ORDINATE SCALE COMPRESSED

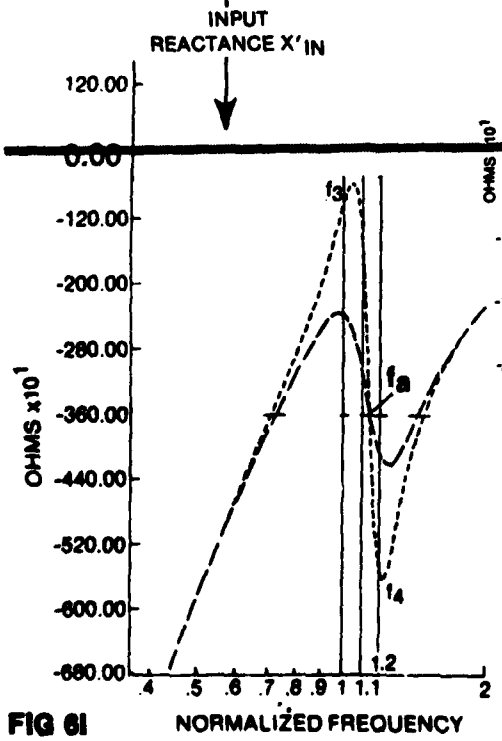

FIG 6l

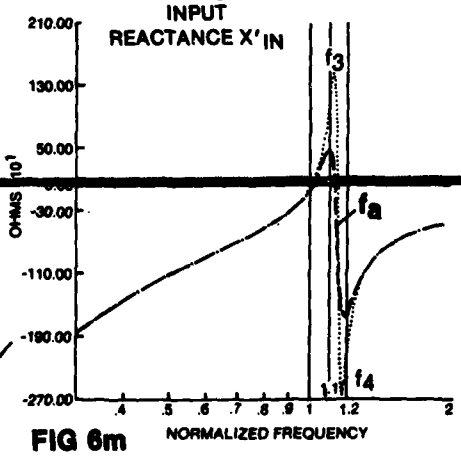

FIG 6m

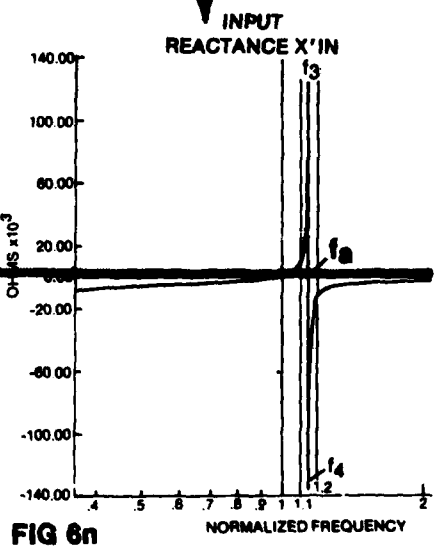

FIG 6n

A curve "similar" to Fig 6h (now called Fig 6l) is shown in Fig 2a, for |Zin|. At first glance this looks like a simple "rectification" of the input reactance curve X'in. However, the reactance minimum and maximum values "hover around" the f_a ordinate. Their frequency separation is used in determining Q. But the |Zin| (which we have sometimes called |Z'in|) has minimum and maximum values which start below f_r and end above f_a.

Their frequency separation is used in determining k.

The contrast in the frequency-separation aspect is even more striking in Figure 6n (and again in the susceptance curve Fig 6k). Moreover, when the Q is very high as in Fig 6m or 6n, one can "rectify" the reactance curve and obtain an approximation to the |Zin| curve of Figure 2a. (Such "rectification" is quite misleading however with a low-Q curve such as Figure 6l; the apparent resonance and antiresonance frequencies are all wrong!)

The group of susceptance curves Figs 6i, j, k; and the group of reactance curves Figs 6l, m, n are presented here mainly to accustom the readers' eye to the quite different appearances of "the same" curve when the computer chooses different plotting scales.

Again, these high-Q susceptance curves, whose peak and dip "hover around" the f_r ordinate, must not be confused with the "similar" high-Q admittance curve of Figure 1d. This is a log-log curve of input admittance magnitude |Yin|. Its maximum value occurs at or below f_r; and its minimum value occurs at about f_a. The frequency separation is used in determining k; it tells us nothing about Q.

The susceptance curve of Fig 6i gives a reliable measurement of mechanical Q for constant voltage drive. (Figure 6b, which uses no bias curve, would be even more accurate.)

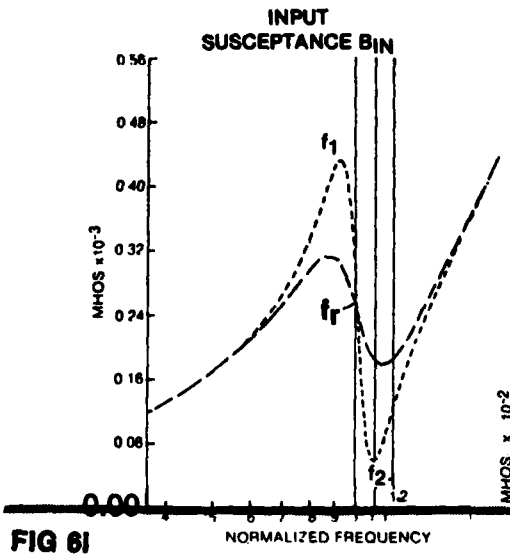

FIG 6i

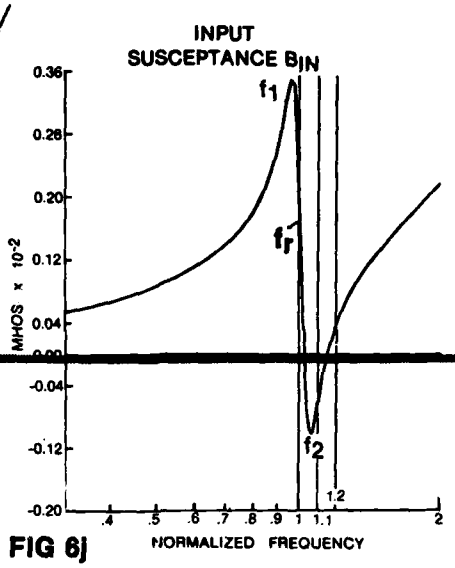

FIG 6j

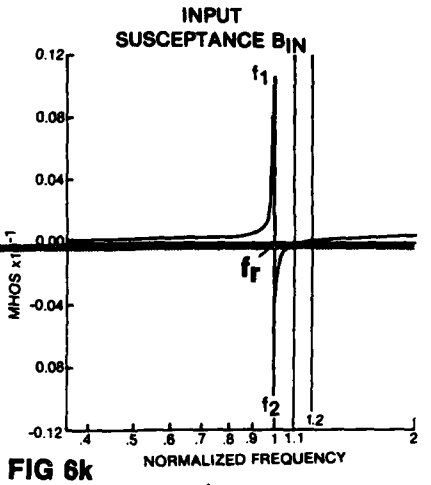

FIG 6k

ORDINATE SCALE EXPANDED

A GOOD "STANDARD" ORDINATE SCALE

ORDINATE SCALE COMPRESSED

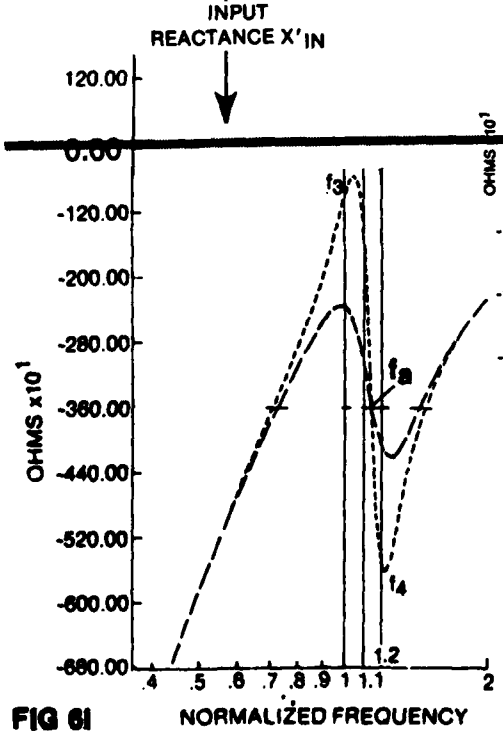

FIG 6l

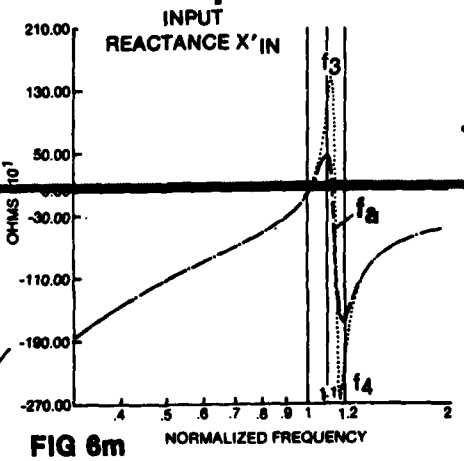

FIG 6m

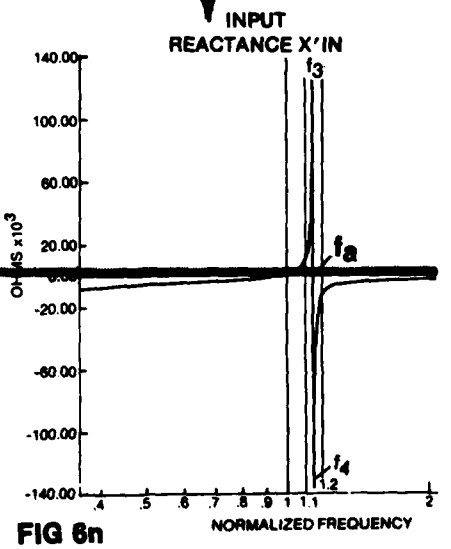

FIG 6n

$$Q_m^E \approx \frac{f_r}{f_2 - f_1} . \quad \text{Also } \frac{1}{Q_m^E} = \frac{f_2 - f_1}{f_r} .$$

The reactance curve of Fig 6l gives us a reliable measurement of mechanical Q for constant current drive. (Figure 6f, which uses no bias curve, would be even more accurate.)

$$Q_m^I = \frac{f_a}{f_4 - f_3} . \quad \text{Also } \frac{1}{Q_m^I} = \frac{f_4 - f_3}{f_a} .$$

For $Q_m > 10$, $Q_m^E \approx Q_m^I$.

Note that (see Chap. 1) $k^2 \approx \frac{2 (f_a - f_r)}{f_a}$. This has an invariant frequency separation; whereas the $\frac{1}{Q_m}$ separation varies from: much narrower, to somewhat broader, than the $\underline{k}$ separation, depending on R_{load}.

Chapter 7. *The Admittance Components and the Admittance Circle; the Impedance Components and the Impedance Circle.*

FIG 7.1

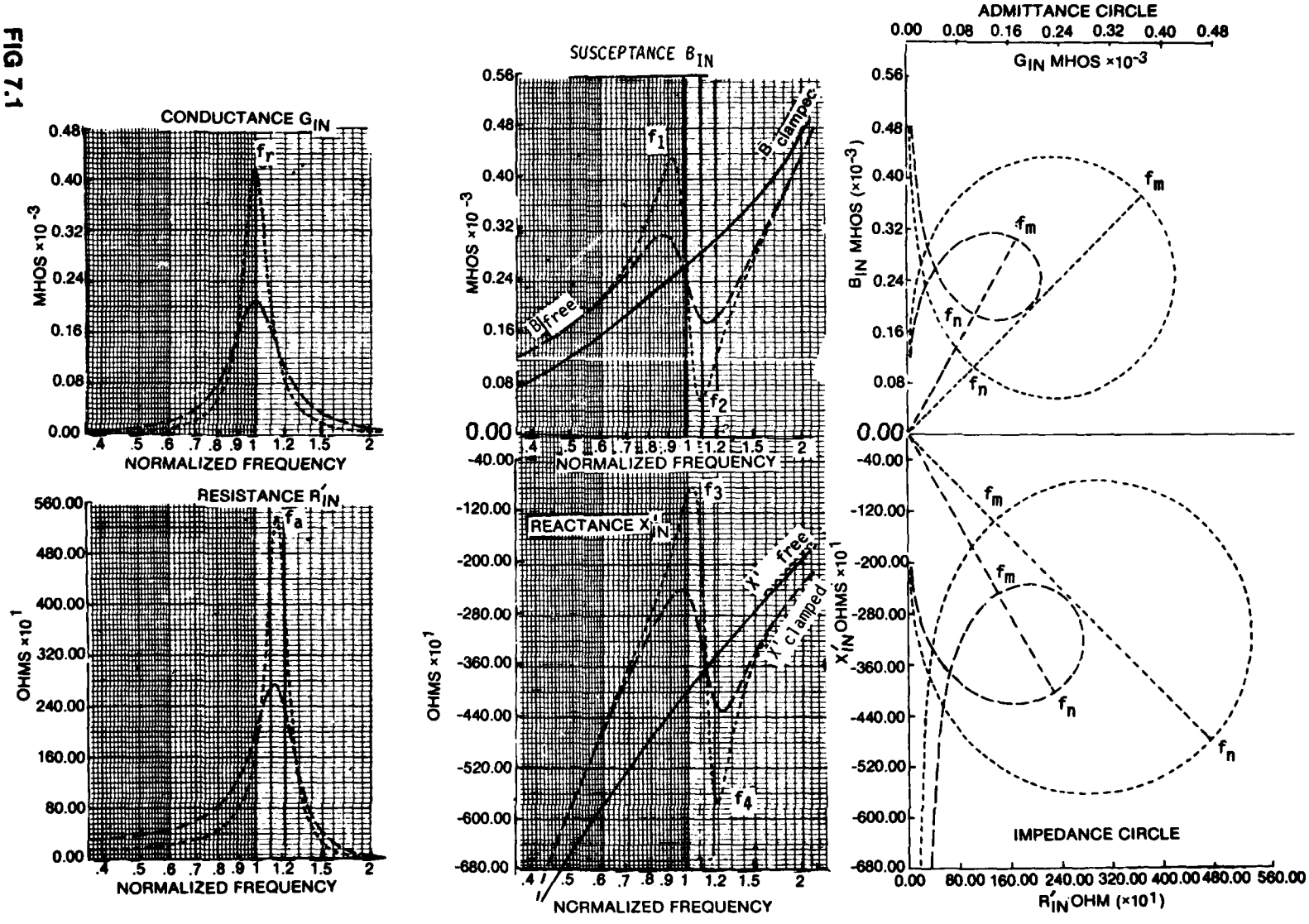
CONDUCTANCE G_{IN}
MHOS ×10⁻³
0.48
0.40
0.32
0.24
0.16
0.08
0.00
f_r
.4 .5 .6 .7 .8 .9 1 1.2 1.5 2
NORMALIZED FREQUENCY
RESISTANCE R'_{IN}
OHMS ×10¹
560.00
480.00
400.00
320.00
240.00
160.00
80.00
0.00
f_a
.4 .5 .6 .7 .8 .9 1 1.2 1.5 2
NORMALIZED FREQUENCY
SUSCEPTANCE B_{IN}
MHOS ×10⁻³
0.56
0.48
0.40
0.32
0.24
0.16
0.08
0.00
-40.00
-120.00
-200.00
-280.00
-360.00
-440.00
-520.00
-600.00
-680.00
f_1
$B_{clamped}$
B_{free}
f_2
f_3
f_4
REACTANCE X'_{IN}
X'_{free}
$X'_{clamped}$
OHMS ×10¹
.4 .5 .6 .7 .8 .9 1 1.2 1.5 2
NORMALIZED FREQUENCY
ADMITTANCE CIRCLE
0.00 0.08 0.16 0.24 0.32 0.40 0.48
G_{IN} MHOS ×10⁻³
B_{IN} MHOS (×10⁻³)
f_m
f_n
IMPEDANCE CIRCLE
X'_{IN} OHMS ×10¹
0.00 80.00 160.00 240.00 320.00 400.00 480.00 560.00
R'_{IN} OHM (×10¹)

Chapter 7. The Admittance Components and the Admittance Circle; The Impedance Components and the Impedance Circle.

It can be shown analytically that equation 4.1 for Y_m plots as an offset circle in the complex plane. To repeat Eq. 4.1:

$$Y_m = \frac{R_m}{R_m^2 + X_m^2} + j \frac{-X_m}{R_m^2 + X_m^2} \quad . \tag{7.1}$$

Here Y_m refers to the admittance of the mechanical components of Fig. 4a after being transformed to the electrical side. Y_m is called the "motional admittance".

It can also be shown analytically that equation 5.3 for Z_m' plots as an offset circle in the complex plane. Indeed it must, since its circuit is approximately the dual of the Y_m circuit. To repeat Eq. 5.3:

$$Z_m' \simeq \frac{R_m' \cdot (X_C')^2}{R_m'^2 + X_m'^2} + j \frac{-X_m' \cdot (L'/C')}{R_m'^2 + X_m'^2} \quad . \tag{7.2}$$

Here Z_m' refers to the impedance of the mechanical components of Fig. 5a after being transformed to the electrical side. Z_m' is called the "motional impedance".

When the bias curves or sloping baselines B_0 or X_0' are suitably added in $\$$ (series) or in || (parallel) with these motional circles, the sum gives the offset "circles" shown in Figure 7.1. The input admittance "circle" and the input impedance "circle", as vehicles for a concise presentation of both the input immittance and motional immittance data, have been extensively covered by Kennelly, Dye, Cady, Woollett, and others; as well as by the IEEE Standard 177 (1966).

FIG 7.1

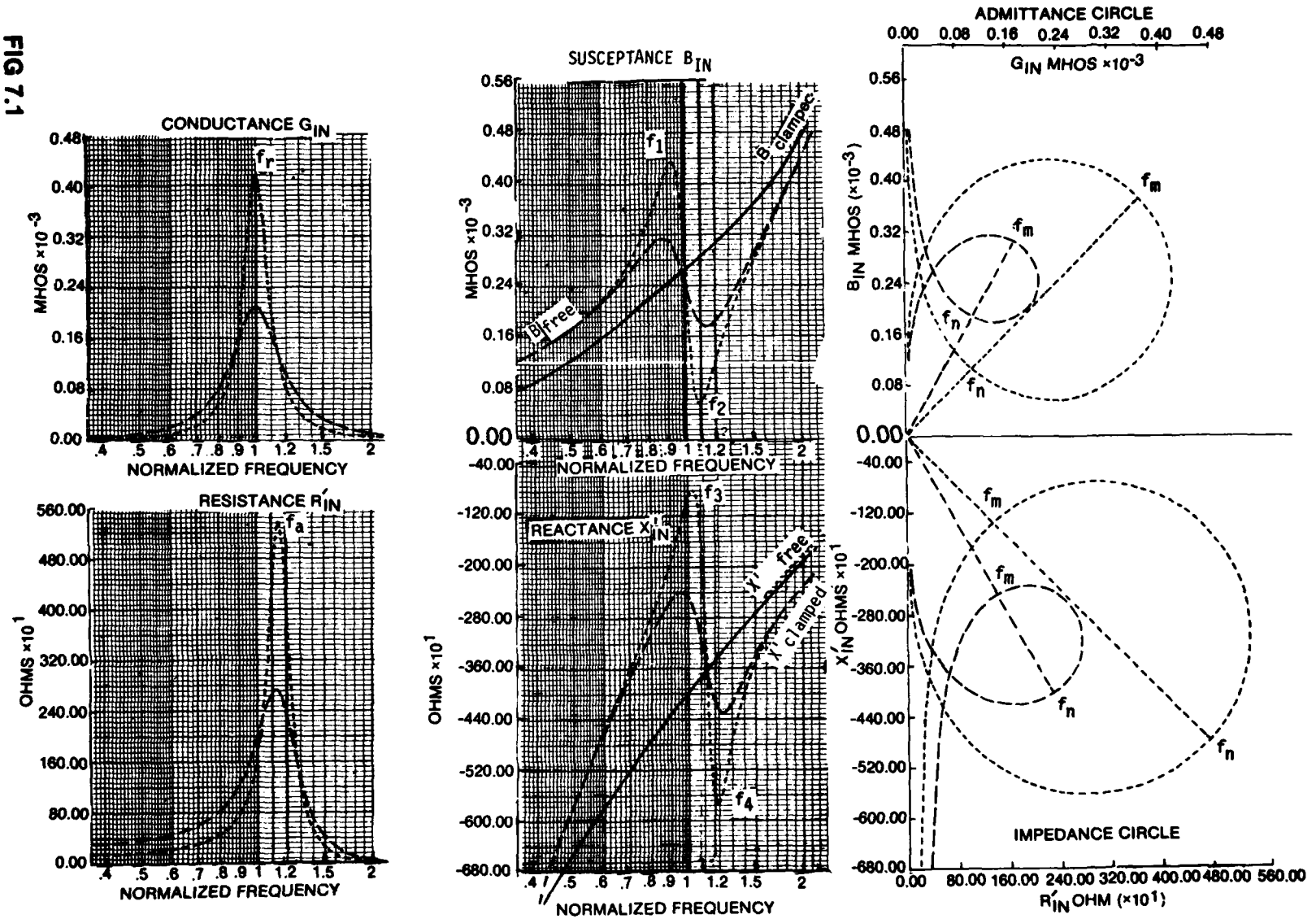
CONDUCTANCE G_{IN}
MHOS ×10⁻³
NORMALIZED FREQUENCY
RESISTANCE R'_{IN}
OHMS ×10¹
NORMALIZED FREQUENCY
SUSCEPTANCE B_{IN}
MHOS ×10⁻³
B free
B clamped
NORMALIZED FREQUENCY
REACTANCE X'_{IN}
OHMS ×10¹
NORMALIZED FREQUENCY
ADMITTANCE CIRCLE
G_{IN} MHOS ×10⁻³
B_{IN} MHOS (×10⁻³)
IMPEDANCE CIRCLE
X'_{IN} OHMS ×10¹
R'_{IN} OHM (×10¹)

Now, Figure 7.1 shows not only the admittance circle but also its conductance and susceptance components, shown earlier in Chapters 4 and 6. The figure also shows not only the impedance circle but its resistance and reactance components, shown earlier in Chapters 5 and 6. Two different Q-values are illustrated. Both are too low to let the piezoelectric immittance "go inductive," which happens when the Q is sufficiently high. That is, B would go negative, X would go positive; and each circle would cross the horizontal axis.

Some of the things to note in Figure 7.1 are the following:

1. The resistance curve and the conductance curve are offset in frequency from each other (by 15% in this case, since $\underline{k}$ = 0.50). Likewise the reactance curve and the susceptance curve are offset in frequency by the same amount.

It is easy to spot f_r and f_a from the conductance or resistance curve, even when the Q is less than 5; but in general it is not easy to do this from the susceptance or reactance curve. The eye has been assisted in Figure 7.1 in two ways. First, two curves of different Q-values have been computer-plotted, and these intersect at f_r (or f_a). Second, the bias curve has been manually plotted and superposed, and this crosses the intersection point itself at f_r (or f_a).

In the real world, only one susceptance or reactance curve is usually provided, and so these "crutches" are not available. Note that the bias curve B_0 or B-clamped is the high-frequency asymptote for the B curve; whereas the bias curve X_0' or X'-free is the low-frequency asymptote for the X' curve.

FIG 7.1

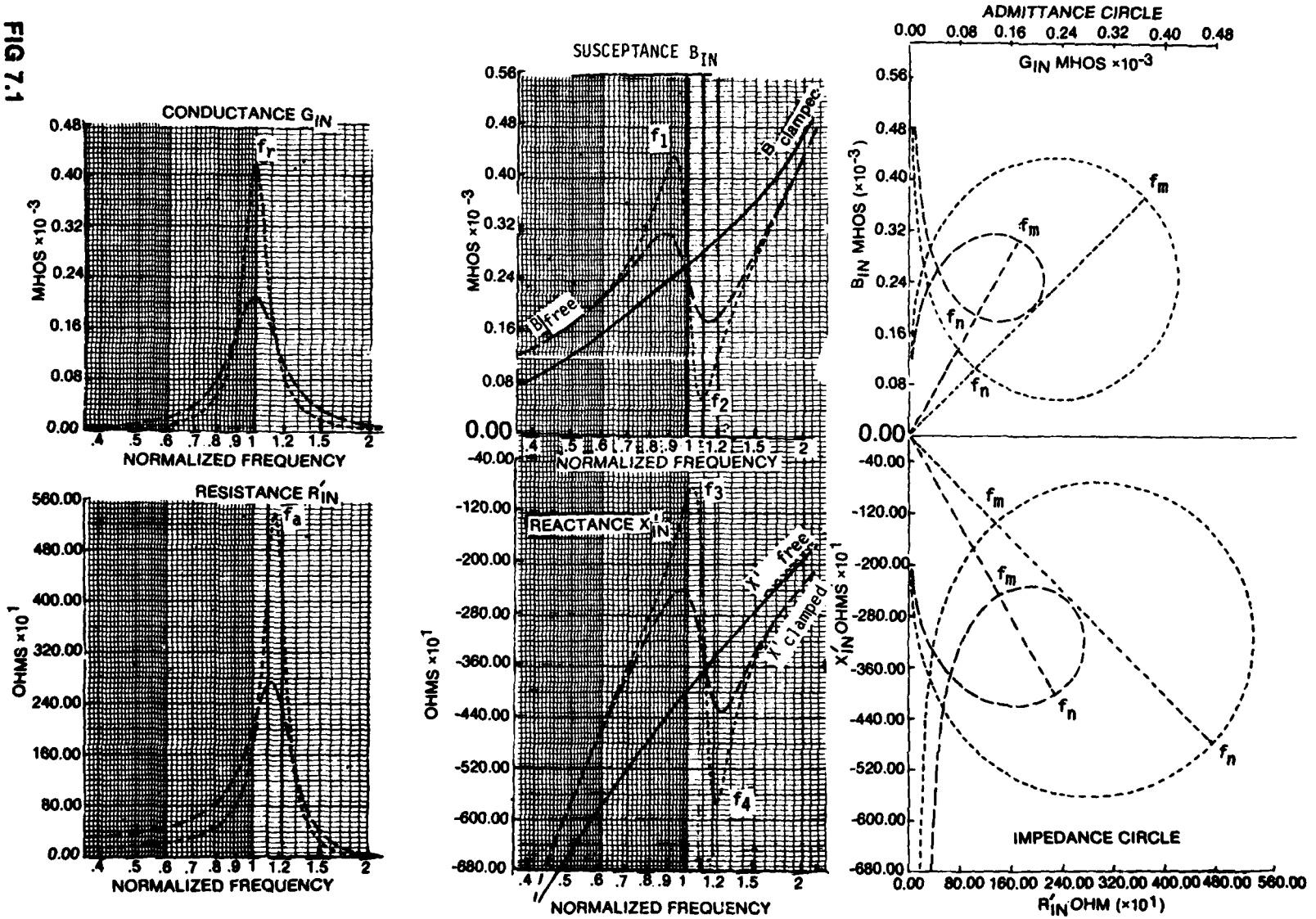
CONDUCTANCE G_{IN}
MHOS ×10⁻³
NORMALIZED FREQUENCY
RESISTANCE R'_{IN}
OHMS ×10¹
NORMALIZED FREQUENCY
SUSCEPTANCE B_{IN}
MHOS ×10⁻³
B clamped
B free
REACTANCE X'_{IN}
X free
X clamped
OHMS ×10¹
NORMALIZED FREQUENCY
ADMITTANCE CIRCLE
G_{IN} MHOS ×10⁻³
B_{IN} MHOS (×10⁻³)
IMPEDANCE CIRCLE
X'_{IN} OHMS ×10¹
R'_{IN} OHM (×10¹)

2. Inverting the input susceptance curve does not quite produce the input reactance curve. This can be demonstrated numerically by inverting the susceptance curve B_{in} of Figure 7.1, and comparing this with the reactance curve X'_{in}. The inverted curve will then be seen to be displaced slightly to the left. It crosses the X'-free bias line very close to f_r; whereas the reactance curve X'_{in} crosses this bias line at f_a. This result is anticipated also by Figures 3e and 3f, and by Figure 4i. However when we properly combine the susceptance with the conductance, and the reactance with the resistance, then the resultant complex admittance Y_{in} does indeed invert into the resultant complex impedance Z_{in}. This is seen in the two circle diagrams, where the circles have been juxtaposed so as to share a common zero. It is also seen in Chapter 1, Figures 1d and 1e.

The max Y occurs at f_m, with a value (for the large circle) of about 0.51×10^{-3} mhos, since each component is about 0.36×10^{-3} mhos. The phase angle is about $+46^{o}$. This inverts to give a Z with a value 1960 ohms and a phase angle of -46^{o}. This Z however is not the max Z; which occurs at f_n on the impedance circle. Rather it is the min Z, which occurs at f_m on the impedance circle.

The max Z (at f_n) has a value of about 6800 ohms, since each component is about 480×10^{1} ohms. The phase angle again is -46^{o}. This Z inverts into min Y (at f_n) with a value of about 0.147×10^{-3} mhos and a phase angle again of $+46^{o}$. Similar relations hold for the two small circles. It is interesting that Y_{max} and Y_{min} have approximately the same phase angle; likewise Z_{max} and Z_{min}.

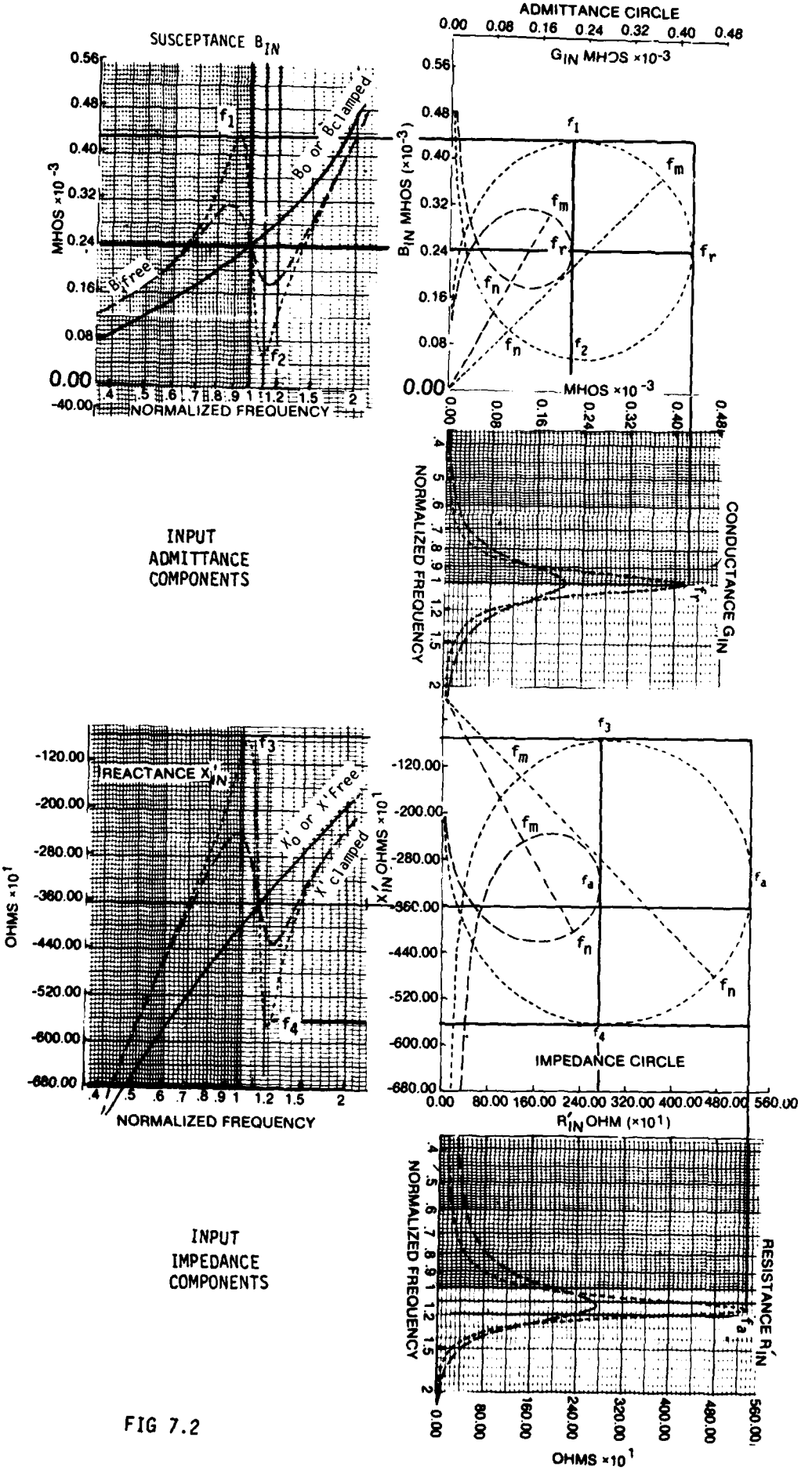
SUSCEPTANCE B_{IN}
MHOS ×10⁻³
B_o or B_c clamped
B_{free}
f_1
f_2
NORMALIZED FREQUENCY
ADMITTANCE CIRCLE
G_{IN} MHOS ×10⁻³
B_{IN} MHOS (×10⁻³)
f_m
f_r
f_n
MHOS ×10⁻³
NORMALIZED FREQUENCY
CONDUCTANCE G_{IN}
INPUT
ADMITTANCE
COMPONENTS
REACTANCE X'_{IN}
X'_o or X'_{free}
X'_c clamped
f_3
f_4
OHMS ×10¹
X'_{IN} OHMS ×10¹
NORMALIZED FREQUENCY
IMPEDANCE CIRCLE
f_a
R'_{IN} OHM (×10¹)
RESISTANCE R'_{IN}
INPUT
IMPEDANCE
COMPONENTS

FIG 7.2

When we turn to Figure 7.2, we see a slightly different arrangement of the same six graphs. The usefulness of this type of presentation is to allow the reader to read off directly the frequencies f_r or f_a with the help of guiding lines extending from the peak values of the G and R curves. Additional guiding lines extending from B peak and B dip, allow the reader to read off directly the frequencies f_1 and f_2 for Q_m^E; and f_3 and f_4 for Q_m^I (see Chapter 6).

Note that extending the f_r diameter-line onto the B curve gives us, graphically, a point on the curve of B_o or B-clamped (at the intersection with the B curves). Likewise, extending the f_a diameter-line onto the X' curve gives us, graphically, a point on the curve of X_o' or X'-free (at the intersection with the X' curves).

It can be shown that $Q_m^E = \frac{f_r}{f_2 - f_1}$, and $Q_m^I = \frac{f_a}{f_4 - f_3}$; and that the larger the circle the larger the Q, for <u>both</u> impedance and admittance. Now a large admittance circle (high Q) calls for a large G_{in}-max; and this is reasonable because G_{in}-max = $1/R_m$ (see Eq. 4.2).

But a large impedance circle (high Q) calls for a large R_{in}'-max; and this feels wrong. However, R_{in}'-max or R_s'-max (see Eq. 5.3) is actually equal to $\frac{(X_c')^2}{R_m'}$ which is $\frac{(X_c')^2}{R_m \cdot k^4}$. (See Appendix 7-A.) And so we have an <u>inverse</u> relationship between R_{in}'-max and R_m. In fact the Q-behavior of a transducer vs a variable R_{in}'-max (a series resistance) is very similar to the Q-behavior (7.3)

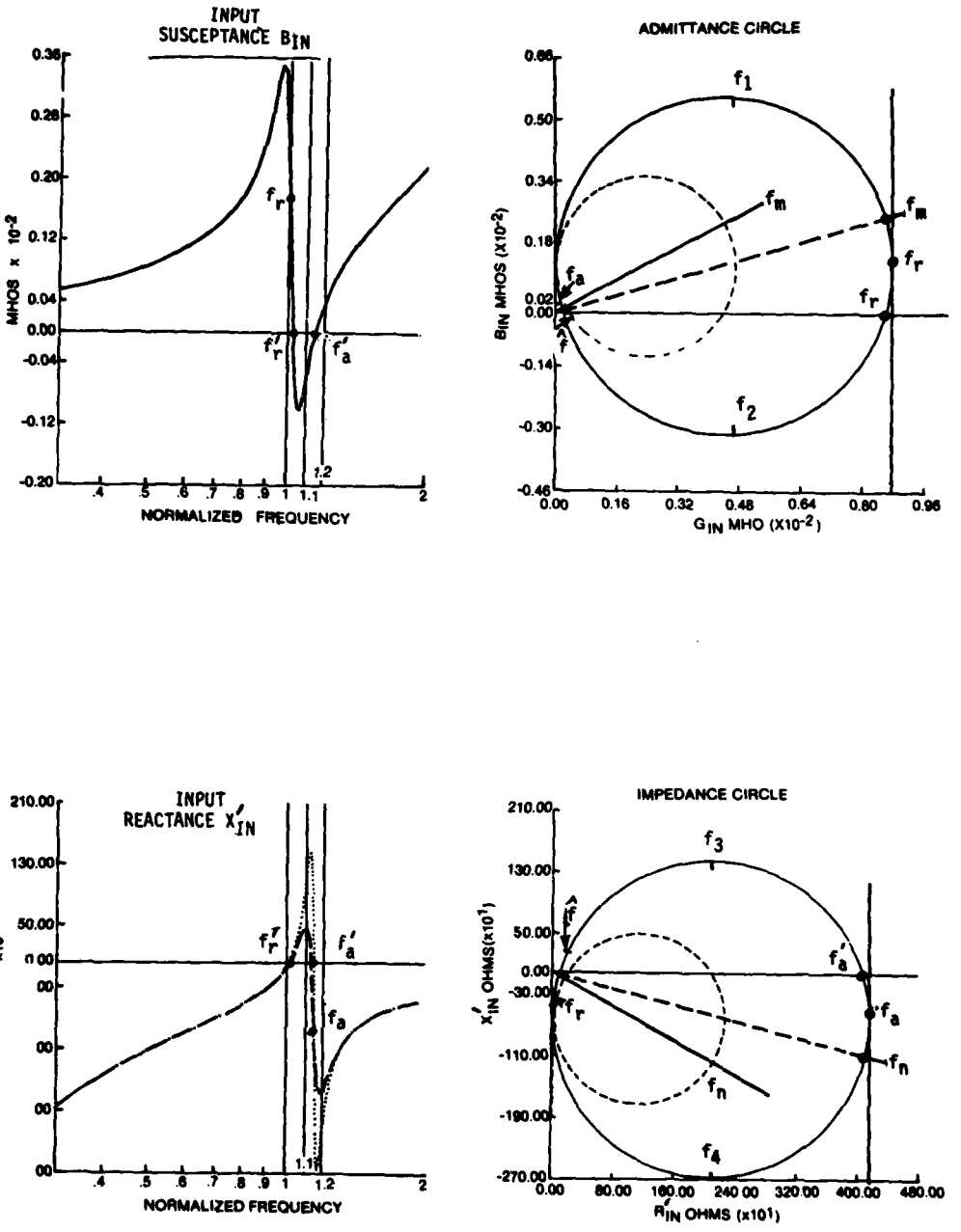
INPUT
SUSCEPTANCE B_{IN}
MHOS x 10^{-2}
NORMALIZED FREQUENCY
f_r
f'_r
f'_a
ADMITTANCE CIRCLE
B_{IN} MHOS ($X10^{-2}$)
G_{IN} MHO ($X10^{-2}$)
f_1
f_2
f_m
f_a
INPUT
REACTANCE X'_{IN}
f_n
IMPEDANCE CIRCLE
X'_{IN} OHMS($x10^1$)
R'_{IN} OHMS ($x10^1$)
f_3
f_4

FIG 7.3

of a "tank circuit" (parallel resonance circuit) vs. a variable parallel resistance R_p. This is hinted at in Figure 2g. In each case, the higher the Q, the higher the R_p, and the higher the R'_{in}-max (which is also R'_s-max).

When the Q is high enough so that the circles cut through the horizontal axis (abscissa), at two frequencies, these frequencies need names. We will call them f'_r (close to f_r) and f'_a (close to f_a). They are shown in Figure 7.3. The IEEE Standard 177* uses a different nomenclature for these 4 frequencies. However the IEEE piezoelectric vibrator is measured on a bench in air and has a high Q (greater than 40). Our vibrator is generally an underwater transducer, measured in water; and it has a low Q (less than 5). Hence the situation (of axis-crossing) doesn't arise in our everyday work.

Nevertheless, to help the reader follow the more general literature, we have presented Figure 7.3, as discussed above. The impedance circles correlate nicely with the input reactance curves. However, the susceptance curves corresponding to the admittance circles were not available. Hence a single susceptance curve is shown instead; and it bears a close correspondence to the smaller admittance circle, even though the scales are different. And to repeat, f'_r and f'_a do not ordinarily show up in underwater transducer measurements. The symbol $\hat{f}$ will be discussed in a later Figure.

Note that as the Q gets higher, each offset circle swings around in such a way that f_m or f_n tends to line up with the abscissa (the axis of resistance or conductance). Concurrently, f'_r and f_m close in on f_r; and f'_a and f_n close in on f_a. All this is often desirable, since a resistive Z or Y can be driven by a smaller and more efficient amplifier than is required for a reactive Z or Y.

*See Appendix 7-B

FIG 7.4

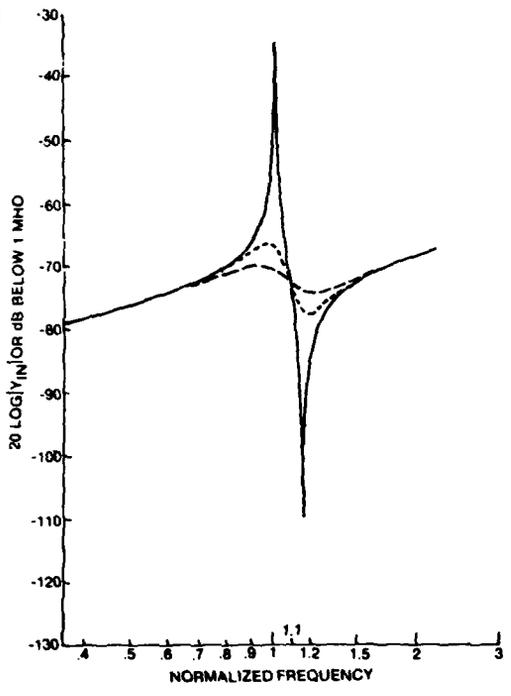
20 LOG|Y_IN| OR dB BELOW 1 MHO
-30
-40
-50
-60
-70
-80
-90
-100
-110
-120
-130
.4 .5 .6 .7 .8 .9 1 1.1 1.2 1.5 2 3
NORMALIZED FREQUENCY

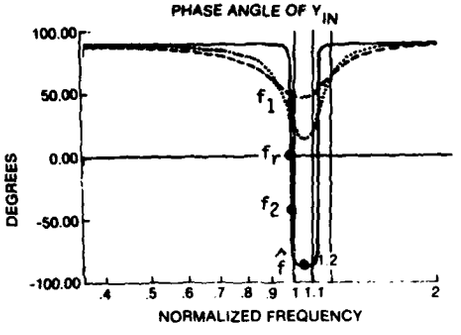
PHASE ANGLE OF Y_IN
100.00
50.00
0.00
-50.00
-100.00
DEGREES
f1
fr
f2
f̂
.4 .5 .6 .7 .8 .9 1 1.1 2
NORMALIZED FREQUENCY

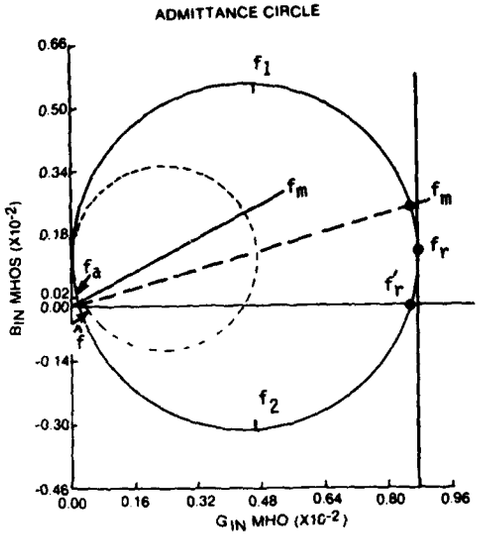
ADMITTANCE CIRCLE
0.66
0.50
0.34
0.18
0.02
0.00
-0.14
-0.30
-0.46
B_IN MHOS (X10^-2)
f1
fm
fa
f̂
fr
f'r
f2
0.00 0.16 0.32 0.48 0.64 0.80 0.96
G_IN MHO (X10^-2)

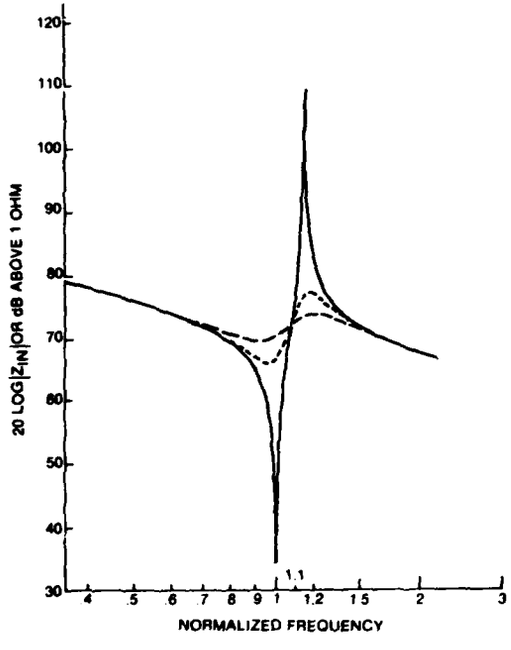
20 LOG|Z_IN| OR dB ABOVE 1 OHM
120
110
100
90
80
70
60
50
40
30
1.1
.4 .5 .6 .7 .8 .9 1 1.2 1.5 2 3
NORMALIZED FREQUENCY

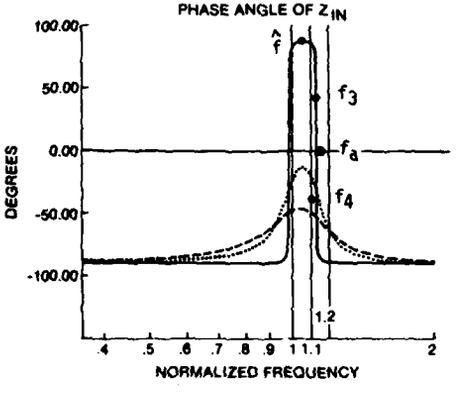
PHASE ANGLE OF Z_IN
100.00
50.00
0.00
-50.00
-100.00
DEGREES
f̂
f3
fa
f4
1.2
.4 .5 .6 .7 .8 .9 1 1.1 2
NORMALIZED FREQUENCY

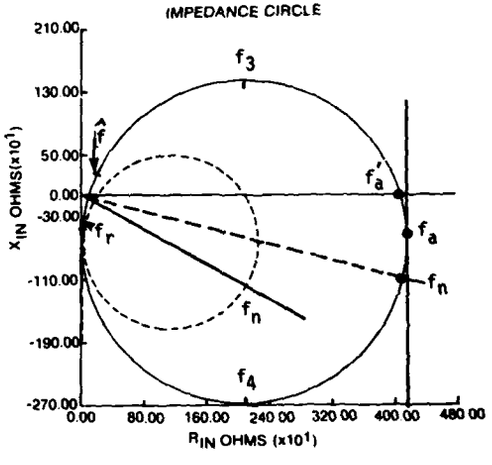
IMPEDANCE CIRCLE
210.00
130.00
50.00
0.00
-30.00
-110.00
-190.00
-270.00
X_IN OHMS(x10^1)
f3
f̂
f'a
fr
fa
fn
f4
0.00 80.00 160.00 240.00 320.00 400.00 480.00
R_IN OHMS (x10^1)

Can f_m or f_n of the offset circle be swung down to the axis of resistance when we have a low-Q transducer? Yes. This is one of the bonuses that electrical tuning accomplishes, via either a series inductor or a parallel inductor. However, this will not be discussed here, since we have limited ourselves here to an analysis of the untuned transducer.

We have shown in Figure 7.2 how a phasor of the admittance circle can be resolved, using a rectangular coordinate system, into two orthogonal components. Thus, $Y_{in} = G_{in} + j\ B_{in}$.

Likewise a phasor of the impedance circle can be resolved into two orthogonal components. Thus, $Z_{in} = R'_{in} + j\ X'_{in}$.

But we can equally well use a polar coordinate system and resolve any phasor at frequency f_p as: $Y_p = |Y_p| \cdot e^{j\theta_{(p)}}$.

But $Z_p = \frac{1}{|Y_p|} \cdot \frac{1}{e^{j\theta_{(p)}}}$.

So $Z_p = |Z_p| \cdot e^{-j\theta_{(p)}}$.

In words, $|Z_p|$ at frequency f_p equals $\frac{1}{|Y_p|}$; and the phase angles are mirror images. Thus Y_{max} and its inverse Z_{min} occur at $+\theta_m$ and $-\theta_m$ respectively. Y_{min} and its inverse Z_{max} occur at $+\theta_n$ and $-\theta_n$ respectively. And the magnitudes are inverses.

All this can be seen in Figure 7.4. The magnitude curves and phase curves actually pertain to six circles not shown here. If $|Z_p| = \frac{1}{|Y_p|}$, then $\log |Z_p| = -\log |Y_p|$. This is clearly shown in the logarithmic plots.

FIG 7.4

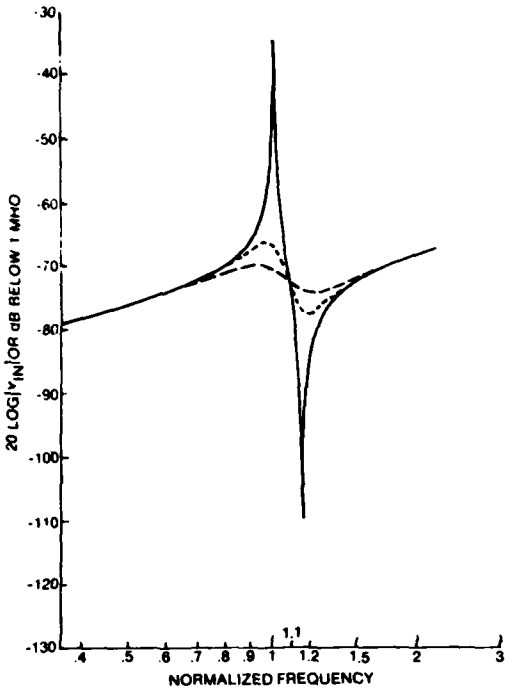
20 LOG|Y_IN| OR dB BELOW 1 MHO
NORMALIZED FREQUENCY

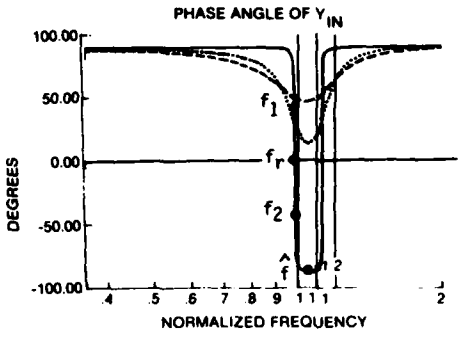
PHASE ANGLE OF Y_IN
DEGREES
NORMALIZED FREQUENCY

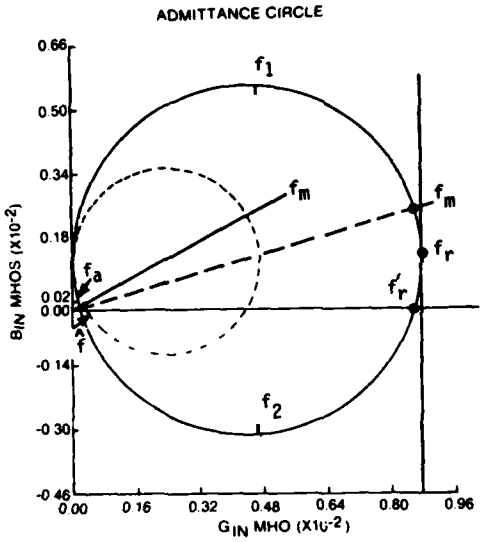
ADMITTANCE CIRCLE
B_IN MHOS (X10^-2)
G_IN MHO (X10^-2)

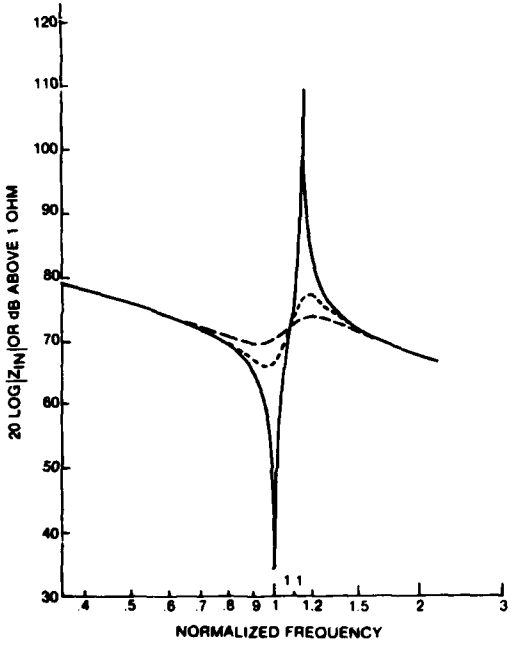
20 LOG|Z_IN| OR dB ABOVE 1 OHM
NORMALIZED FREQUENCY

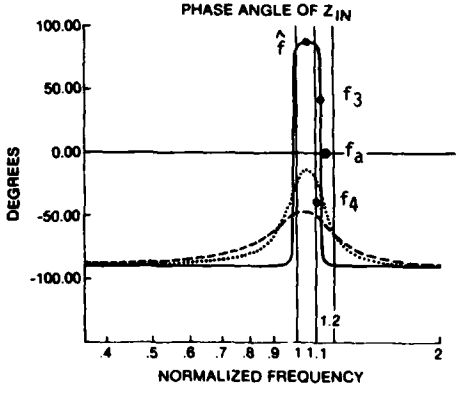
PHASE ANGLE OF Z_IN
DEGREES
NORMALIZED FREQUENCY

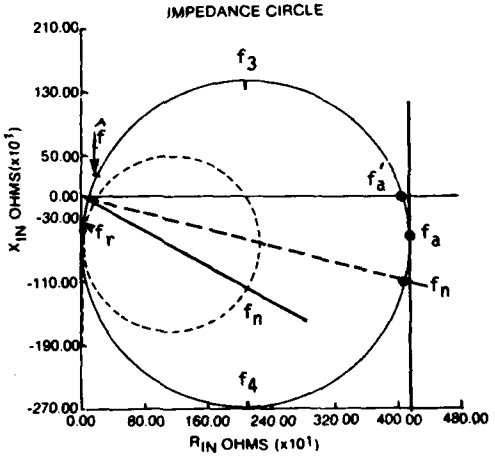
IMPEDANCE CIRCLE
X_IN OHMS(x10^1)
R_IN OHMS (x10^1)

The curve for phase angle θ of Z is clearly the negative of the curve for phase angle of Y. And it can be seen that θ crosses the 0^o axis at both f_r and f_a, approximately, when Q is very high; but does <u>not</u> cross when Q is low (as with an underwater application).

Moreover when Q is very high, the crossover region, between f_r and f_a, means that the admittance "has gone inductive"; therefore θ_Y remains at approximately -90^o in this region and then returns to $+90^o$.

Likewise the crossover region between f_r and f_a means that the impedance "has gone inductive"; therefore θ_Z remains at approximately $+90^o$ in this region, and then returns to -90^o. With lower values of Q this performance is aimed at but not attained.

We now reiterate some of the pros and cons of the complex-plane representation vs. the real-plane representation. The real-plane plot (of phase, for example) has the great advantage that the frequency scale is uniform, whether a log scale or linear scale is under discussion. A uniform scale allows easy interpolation of frequencies, with fairly good accuracy. The complex-plane plot, on the other hand, has a highly non-uniform frequency scale, which does not allow easy interpolation of frequencies. Thus from about $+45^o$ to about -45^o (moving clockwise on each circle), almost a full half-circle is used up to display the very narrow Δf which is required in the Q-determination around either f_r (using f_1 and f_2) or f_a (using f_3 and f_4). The peak phase-curve frequency $\hat{f}$ is crowded next to f_a (Y-circle) or to f_r (Z-circle) in the circle plots; but this frequency $\hat{f}$ occurs at the center of the phase band in the real-plane plots, where it is not at all crowded. One result of all this is that, for example in the

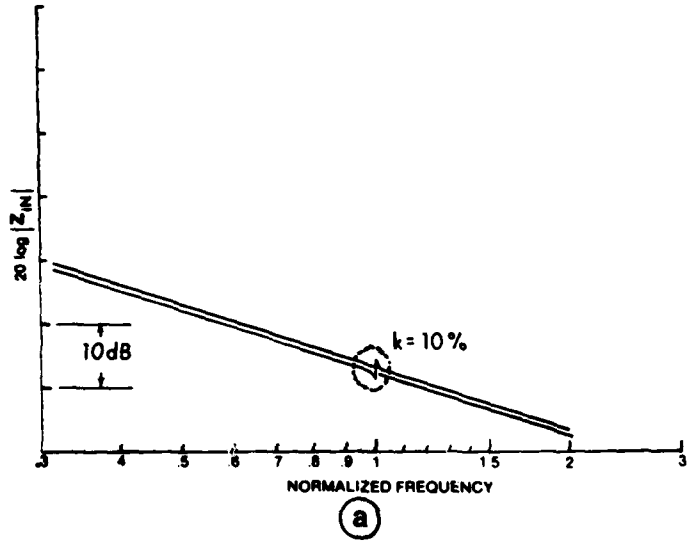
20 log |Z_IN|
10dB
k = 10 %
.3
4
.5
.6
7
.8
.9
1
1.5
2
3
NORMALIZED FREQUENCY
a

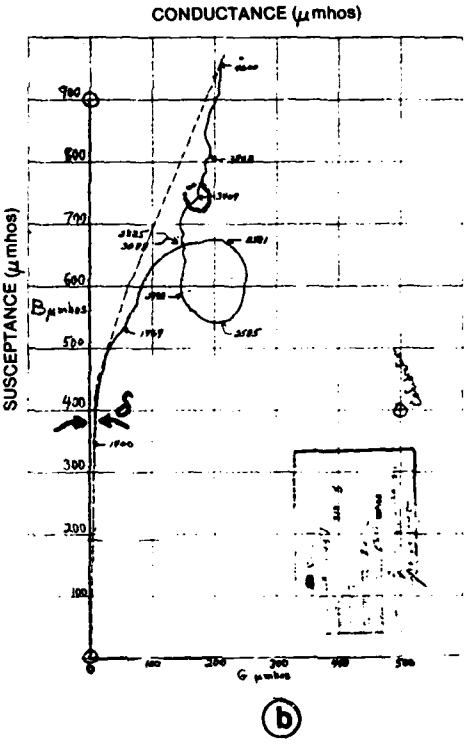
CONDUCTANCE (μmhos)
SUSCEPTANCE (μmhos)
B μmhos
900
800
700
600
500
400
300
200
100
0
b

FIG 7.5

design of amplifiers for driving an untuned transducer, the real-plane presentation of the phase curve is usually more useful than the circle presentation. Other examples could be given.

On the other hand, the circle presentation is an easy-to-store one-plot collection of all the input immittance data. Moreover, if one requires only $Z_n = |Z_n| \cdot e^{j\theta}n$ or $Y_m = |Y_m| \cdot e^{j\theta}m$, the one circle plot is just as informative as the corresponding two real-plane plots.

A few more points deserve a brief commentary.

1. Size of the circle. In Chapter 2 it was shown in Figure 2k (now called Figure 7.5a) that when $\underline{k} \simeq 10\%$, that even though Q was on the order of 100, the input impedance curve showed only a tiny dip and a tiny peak. The relation we used was: $Q_m^I \simeq \sqrt{\frac{|Z_{max}| \ @f_a}{|Z_{min}| \ @f_r}} \cdot \frac{1}{k^2}$. Or equally well,

$$Q_m^I \simeq \sqrt{\frac{|Y_{max}| \ @f_r}{|Y_{min}| \ @f_a}} \cdot \frac{1}{k^2} \quad . \quad \text{Then } k^2 Q_m^I \simeq \sqrt{\frac{|Z_{max}|}{|Z_{min}|}} = \sqrt{\frac{|Y_{max}|}{|Y_{min}|}} \quad . \tag{7.4}$$

When these admittance or impedance curves of Figure 2k are translated to the complex plane, as in Figure 7.2, the same <u>kind</u> of thing shows up. That is, the circle becomes merely a tiny loop, or even a cusp, on an otherwise smooth curve B_o which is B-clamped, or X_o' which is X'-free. Note that the circle becomes tiny if <u>either</u> k^2 or Q is very small. Figure 7.5b shows the "circular loops" that often occur with a real untuned transducer, measured in water. The degeneration of circles into cusps at the higher frequencies is mainly due to the low coupling coefficient at the higher resonance modes of the transducer.

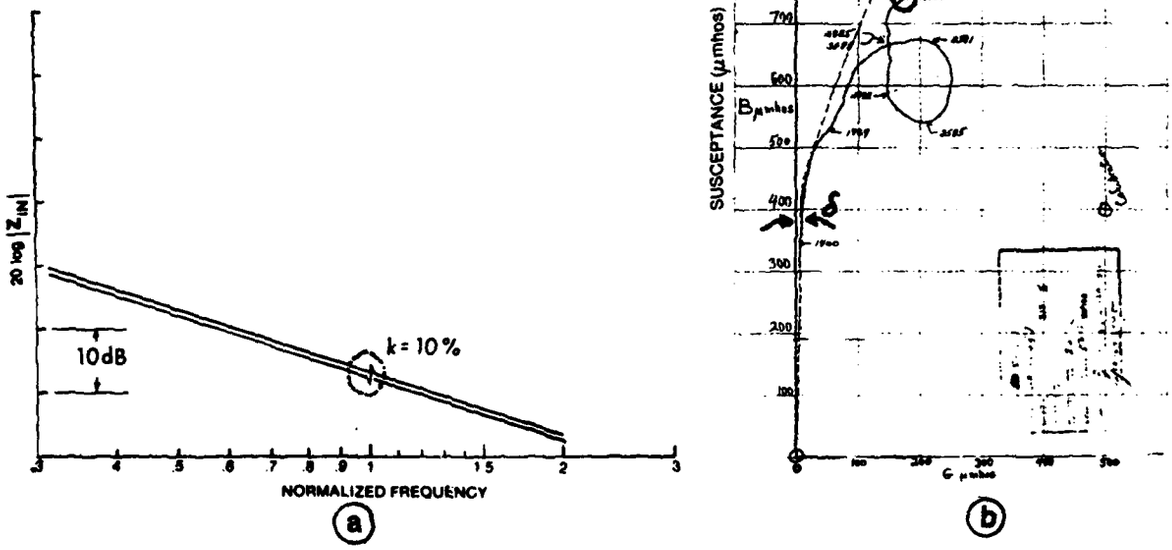
20 log |Z_IN|
10dB
k = 10%
.3
.4
.5
.6
.7
.8
.9
1
1.5
2
3
NORMALIZED FREQUENCY
(a)
CONDUCTANCE (μmhos)
SUSCEPTANCE (μmhos)
B μmhos
900
800
700
600
500
400
300
200
100
0
100
200
300
400
500
G μmhos
(b)

FIG 7.5

2. Determination of $\underline{k}$. If in the complex plane, referring to any of the circles discussed, we subtract the bias contribution B_o which is B-clamped, or X_o' which is X'-free (Figure 7.2),

we can show that:

$\frac{k^2}{1-k^2} \cdot Q_m^E = \frac{D_Y}{B_o} = \frac{G_{in}\text{-max}}{B_o}$, where B_o is evaluated at f_r. [This follows at once from Figure 2c where $Q_m^E = \frac{1/\omega C_m}{R_m}$. But from Eqs. I.4 and 4.2, this is merely, $\frac{\frac{1}{\omega Co(k^2/1-k^2)}}{1/G_{in}\text{-max}} = \frac{G_{in}\text{-max}}{B_o(k^2/1-k^2)} = Q_m^E$. Then $(k^2/1-k^2)\cdot Q_m^E = \frac{G_{in}\text{-max}}{B_o} = \frac{D_Y}{B_o}$.] (7.5)

Then after Q_m^E has been determined from f_2 and f_1 and f_r, we can calculate $\underline{k}$.

In like manner we can show that:

$\frac{k^2}{1-k^2} \cdot Q_m^I \simeq \frac{D_z}{X_o'} = \frac{R_{in}'\text{-max}}{X_o'}$, where X_o' is evaluated at f_a. [This follows at once from Figure 2g where $Q_m^I = \frac{R_p'}{1/\omega C_m'}$. But from Chapter 5 and Figure 2e and Eq. I.4, this is merely $\frac{R_{in}'\text{-max}}{\frac{1}{\omega C_o'(1-k^2/k^2)}} = \frac{R_{in}'\text{-max}}{X_o'(k^2/1-k^2)} = Q_m^I$. (7.6) (7.7)

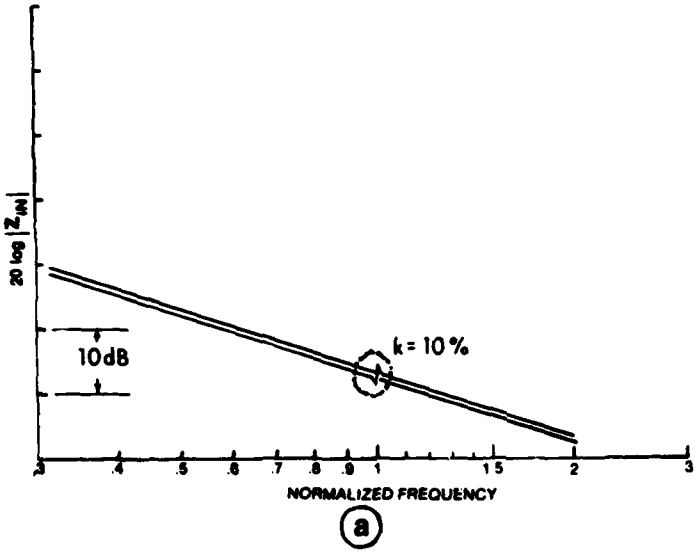
20 log |Z_IN|
10dB
k = 10 %
.3
.4
.5
.6
.7
.8
.9
1
1.5
2
3
NORMALIZED FREQUENCY
(a)

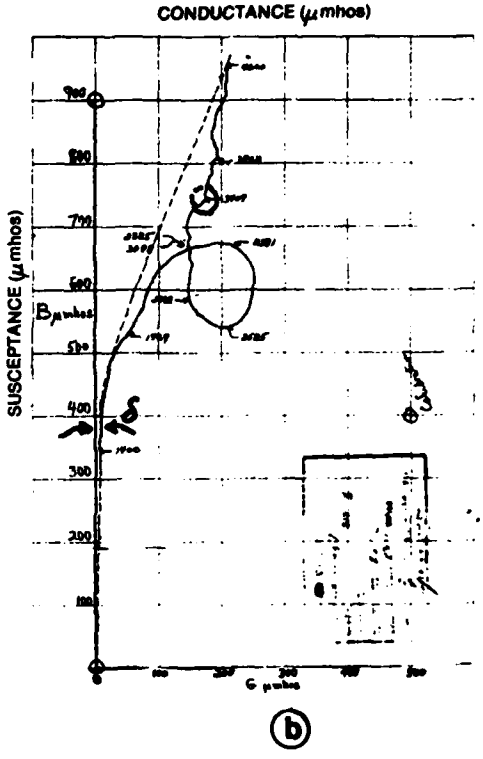
CONDUCTANCE (μmhos)
SUSCEPTANCE (μmhos)
B μmhos
G μmhos
(b)

FIG 7.5

Then $\frac{k^2}{1-k^2} \cdot Q_m^I = \frac{R'_{in}\text{-max}}{X'_o} = \frac{D_z}{X'_o}$ *.] Then after Q_m^I has been determined (7.8)

from f_4 and f_3 and f_a, we can calculate $\underline{k}$.

3. Tan δ. In the real world of Figure 7.5b, the simple equivalent circuit of Figure 2c is modified to have at least one more factor: a dielectric loss G_{el} shunted across C_o, the blocked electrical capacitance. The ratio $G_{el}/\omega C_o$ or $G_{el}/B_{clamped}$ is called tan δ, the loss-tangent. It is a dissipation term and is like an inverse-Q.

If G_{el} were constant over the frequency band, a given admittance circle would shift to the right by a constant amount. A better assumption is that tan δ is constant over the frequency band. This means that G_{el} must increase linearly with frequency. In practice tan δ is often taken to be the $\underline{\text{measured}}$ ratio G_{el}/B_{free} or $G_{el}/\omega C_{free}$ at some low frequency (at least two octaves below f_r).

In the real world of Figure 7.5b we find that the total G_{in}, which is the sum of G_{el} and G_{mot}, increases non-linearly with frequency. Far below resonance, however, it should be possible to isolate G_{el} and hence tan δ.

---

*If we wish to use X'-clamped instead of X'-free or X'_o, as is sometimes done:

Rearranging, $k^2 \cdot Q_m^I = \frac{R'_{in}\text{-max}}{X'_o/(1-k^2)}$.

But $X'_o/(1-k^2)$ $\underline{\text{is}}$ X'-clamped. (This was touched on in Chap. 3.) (7.9)

Hence $k^2 \cdot Q_m^I = \frac{R'_{in}\text{-max}}{X'\text{-clamped}} \cong \frac{D_z}{X'\text{-clamped}}$. (7.10)

FIG 7.1

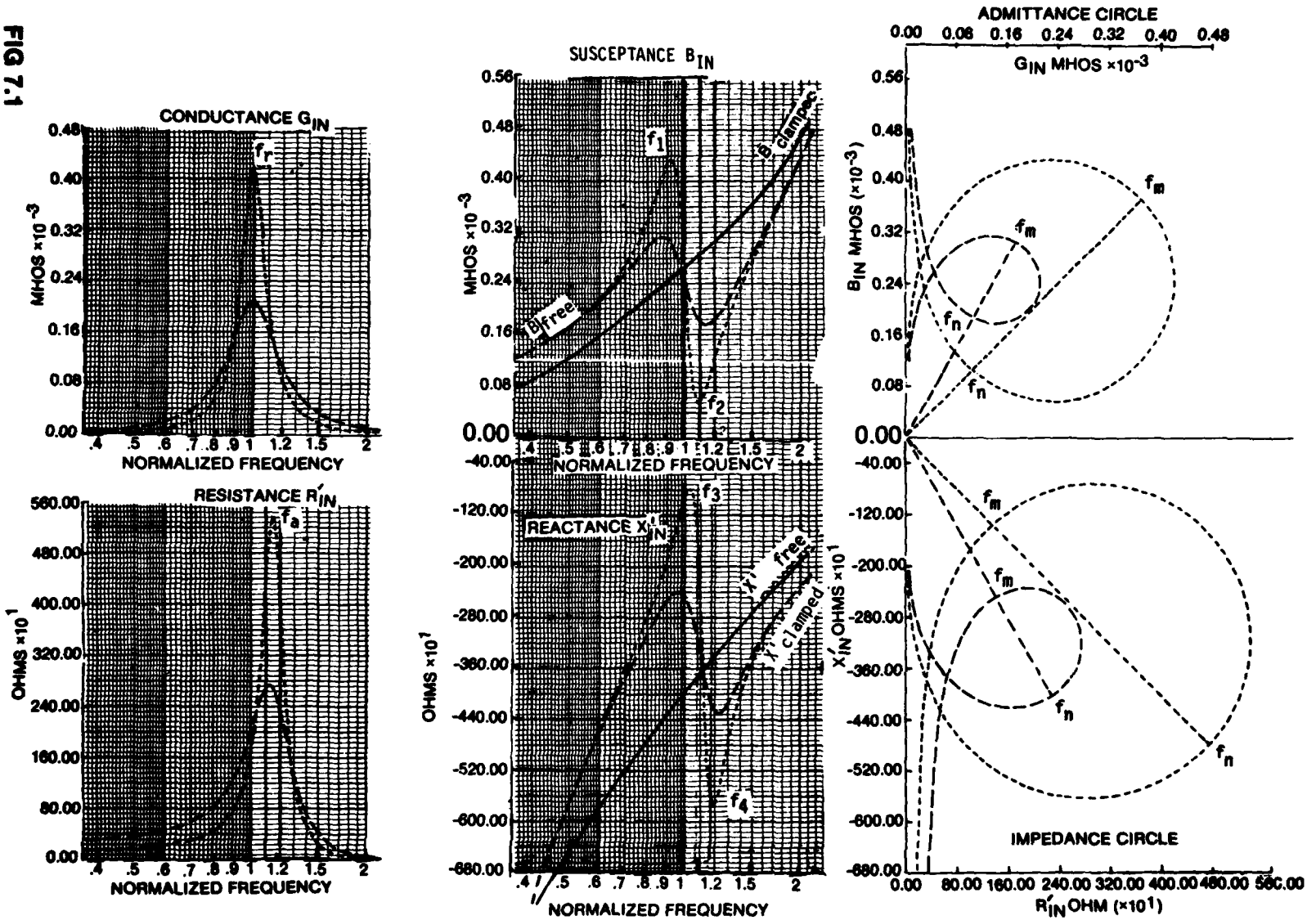
CONDUCTANCE G_{IN}
MHOS ×10⁻³
0.48
0.40
0.32
0.24
0.16
0.08
0.00
f_r
.4 .5 .6 .7 .8 .9 1 1.2 1.5 2
NORMALIZED FREQUENCY
RESISTANCE R'_{IN}
OHMS ×10¹
560.00
480.00
400.00
320.00
240.00
160.00
80.00
0.00
f_a
.4 .5 .6 .7 .8 .9 1 1.2 1.5 2
NORMALIZED FREQUENCY
SUSCEPTANCE B_{IN}
MHOS ×10⁻³
0.56
0.48
0.40
0.32
0.24
0.16
0.08
0.00
f_1
$B_{clamped}$
B_{free}
f_2
.4 .5 .6 .7 .8 .9 1 1.2 1.5 2
NORMALIZED FREQUENCY
REACTANCE X'_{IN}
OHMS ×10¹
-40.00
-120.00
-200.00
-280.00
-360.00
-440.00
-520.00
-600.00
-680.00
f_3
X'_{free}
$X'_{clamped}$
f_4
.4 .5 .6 .7 .8 .9 1 1.2 1.5 2
NORMALIZED FREQUENCY
ADMITTANCE CIRCLE
0.00 0.08 0.16 0.24 0.32 0.40 0.48
G_{IN} MHOS ×10⁻³
B_{IN} MHOS (×10⁻³)
f_m
f_n
IMPEDANCE CIRCLE
X'_{IN} OHMS ×10¹
0.00 80.00 160.00 240.00 320.00 400.00 480.00 560.00
R'_{IN} OHM (×10¹)

Conclusion

We have shown that the components of the admittance and the impedance are similar in appearance, but are not really duals. Hence they do not quite invert from one to the other. When the real and imaginary components are geometrically added to produce Y or Z however, the vector Y is indeed the inverse of the vector Z.

We have also shown how the size of the circle is controlled by Q_m and k^2; and how the circle can even "go inductive" when k^2Q_m is sufficiently high.

We have allowed the reader to compare alternative presentations to the "circle components" (all of which have their merits).

And we have shown that the real world has an additional complication in the *form* of tan δ. That is, the equivalent circuit is modified to include a *shunt* resistance in parallel with C_o.

Appendix 7-A

Alternative Derivation of R'_{in} - max.

We can rewrite Eq. 7.3 as R'_{in} - max = $\dfrac{\left(X'_{m_c}/k^2\right)^2}{R_m}$ or $\dfrac{\left(\dfrac{1}{\omega C'_m \cdot k^2}\right)^2}{R_m}$, (7A.1)

where C'_m is that motional capacitance shown in Figure 3c. In this specific case it has a value of 6 nF. Then if k = 50%, k^2 = 1/4 and

$(C'_m \cdot k^2)$ in Eq. 7A.1 equals 6 x 1/4 which equals 1.5 nF.

If now we look at Figure 3a (which is merely another form of Figure 3c) we see that C_o also equals 1.5 nF, where C_o is the clamped electrical capacitance. And in fact we can generalize:

$$(C'_m \cdot k^2) = C_o \overset{(**)}{\text{ and }} X'_{m_c}/k^2 = X_o. \qquad (7A.2)$$

$$\text{Hence } R'_{in} \text{ - max} = \frac{X_o^2}{R_m}. \qquad (7A.3)$$

(This is a common formulation of R'_{in} - max.)

(**) The ratio of the clamped electrical capacitance of the admittance circuit, to the motional capacitance of the impedance circuit is thus

$$C_o/C'_m = k^2 \text{ (or } 1.5/6 = 1/4). \qquad (7A.4)$$

But the ratio of the free electrical capacitance of the impedance circuit, to the motional capacitance of the admittance circuit is the inverse: $C'_o/C_m = 1/k^2$ (or 2/0.5 = 4/1.) (7A.5)

Other relationships can be explored. Thus, multiplying:

$C_o/C'_m \times C'_o/C_m = k^2 \cdot 1/k^2 = 1.$

Rearranging, $C_o/C_m \times C'_o/C'_m = 1.$

Then $C_o/C_m = C'_m/C'_o$ (note the inversed relation). (7A.6)

$\dfrac{1.5}{0.5} = \dfrac{6}{2} = \dfrac{1-k^2}{k^2}$.

Appendix 7-B

Extract from IEEE Standard on the Piezoelectric Vibrator;

and Comments thereon.

This appendix contains an extract from the 1966 Standard, IEEE Standard 177-1966, on the Piezoelectric Vibrator.

The Standard's Figures 2 and 3 summarize some of the results derived in this Handbook. Their |Z| curve is shown more fully in our Chapter 2, Fig 2a; and discussed in Chapter 5. The three critical frequencies f_n, f_p, and f_a are shown in our Chapter 7, Fig 7.4 and touched upon in Fig 7.1; and also in Figs. 5f and 5j.

The linear curve X_1, occurring above frequency f_s, is first shown in our Fig 4e.2. In addition the |Y|, B, and G curves corresponding to the |Z|, X, and R curves are shown and discussed in our Chapter 4, and also in our Figures 7.4 and 7.1.

In fact, our Handbook has analyzed the main features presented by the Standard; and a great deal more.

* *

DEFINITIONS AND METHODS OF MEASUREMENT FOR PIEZOELECTRIC VIBRATORS

INTRODUCTION:

This Standard is a revision of the IRE Standard on Piezoelectric Crystals—The Piezoelectric Vibrator: Definitions and Methods of Measurement, 1957 (57 IRE 14. S1)[1] and a continuation of Standards in this field.[2, 3, 4]

An introductory review of the equivalent electric circuit of a piezoelectric vibrator and its parameters is followed by a discussion of the determination of these parameters by the transmission method. This method was published in 1951[5] and became the basis for the 1957 IRE Standard.[1] Since that time, a thorough investigation of the transmission method has resulted in more precise expressions which permit a more accurate evaluation of the parameters.[6] This method is suitable for frequencies up to about 30 MHz for the commonly encountered ranges of the capacitance ratio r and the figure of merit M, provided that errors due to instrumentation are taken into account. The equations presented in this Standard have been formulated to correct these errors.

rived from them. At a given frequency the parameters of the equivalent electric circuit generally approach constant values as the amplitude of vibration approaches zero. The amplitude which can be tolerated before the parameters are appreciably affected varies widely between vibrators of various types and can only be determined by experiment.

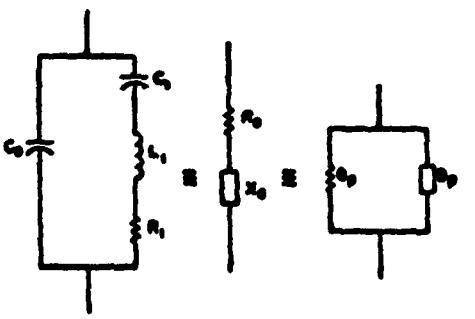

FIGURE 1

Equivalent Electric Circuit of a Piezoelectric Vibrator Near a Resonance.

and do not represent a particular piezoelectric vibrator.[7]

For further clarification, the impedance and admittance circles of a piezoelectric vibrator are reproduced in Figure 3. However, the circle representation of the impedance or admittance of a piezoelectric vibrator is valid only if the circle diameter of the admittance diagram is large compared with the change of $2\pi fC_o$ in the resonance range or if $r < Q^2$, which is fulfilled in most vibrators. If the latter conditions are not fulfilled, the admittance curve shows a cissoidal character. Throughout the remainder of this Standard, it is assumed that the impedance (or admittance) of the vibrator can be represented by a circle diagram. Table 3 gives data for Q, r, and Q^2/r for various types of vibrators, indicating that this assumption is valid for all practical cases.

It is necessary to make approximations in deriving practical equations for general use. It is the error of these approximations, in addition to the errors of instrumentation, that govern the overall accuracy of the experimentally derived parameters.

As a first approximation sufficient for many practical purposes, the following assumptions can be made: $f_m \simeq f_r = f_g$ and $f_a = f_n = f_p$.

More exact relations between the characteristic frequencies f_m, f_r, f_a, f_p, f_n, and the series resonance frequency f_s of a vibrator, valid for the figure of merit $M > 10$ and the capacitance ratio $r > 10$, are shown in Table 4. These relationships have been derived by various authors[8, 9] under the assumption that $M > 1$.

The separation between parallel and series resonance frequencies is given by:

$$\frac{f_p^2 - f_s^2}{f_s^2} = \frac{C_1}{C_o} = \frac{1}{r} \qquad (2)$$

The approximation

$$\frac{f_p - f_s}{f_s} = \sqrt{1 + r^{-1}} - 1 = \frac{1}{2r}\left(1 - \frac{1}{4r} + \ldots\right) \sim \frac{1}{2r} = \frac{1}{2}\frac{C_1}{C_o} \qquad (3)$$

can be used for larger values of r (for example, when r is greater than 25 the error is less than 1 percent.)

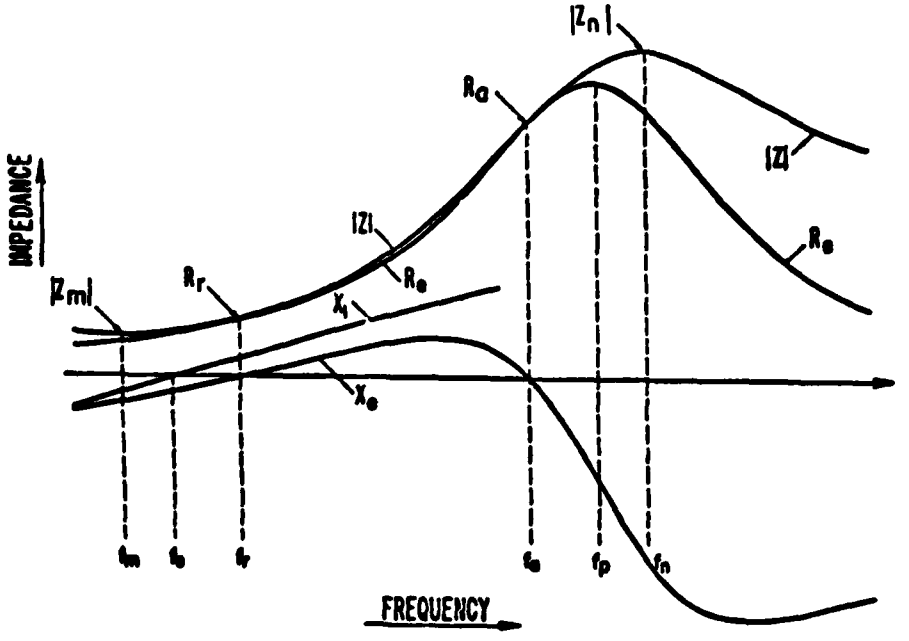

FIGURE 2

Impedance $|Z|$, Resistance R_r, Reactance X_s, and Series Arm Reactance X_1 of a Piezoelectric Vibrator as a Function of Frequency. Z_m and Z_n denote minimum and maximum impedance, R_r and R_a the impedances at zero phase angle. For the meaning of the different frequencies, see Table 1A and Figure 2.

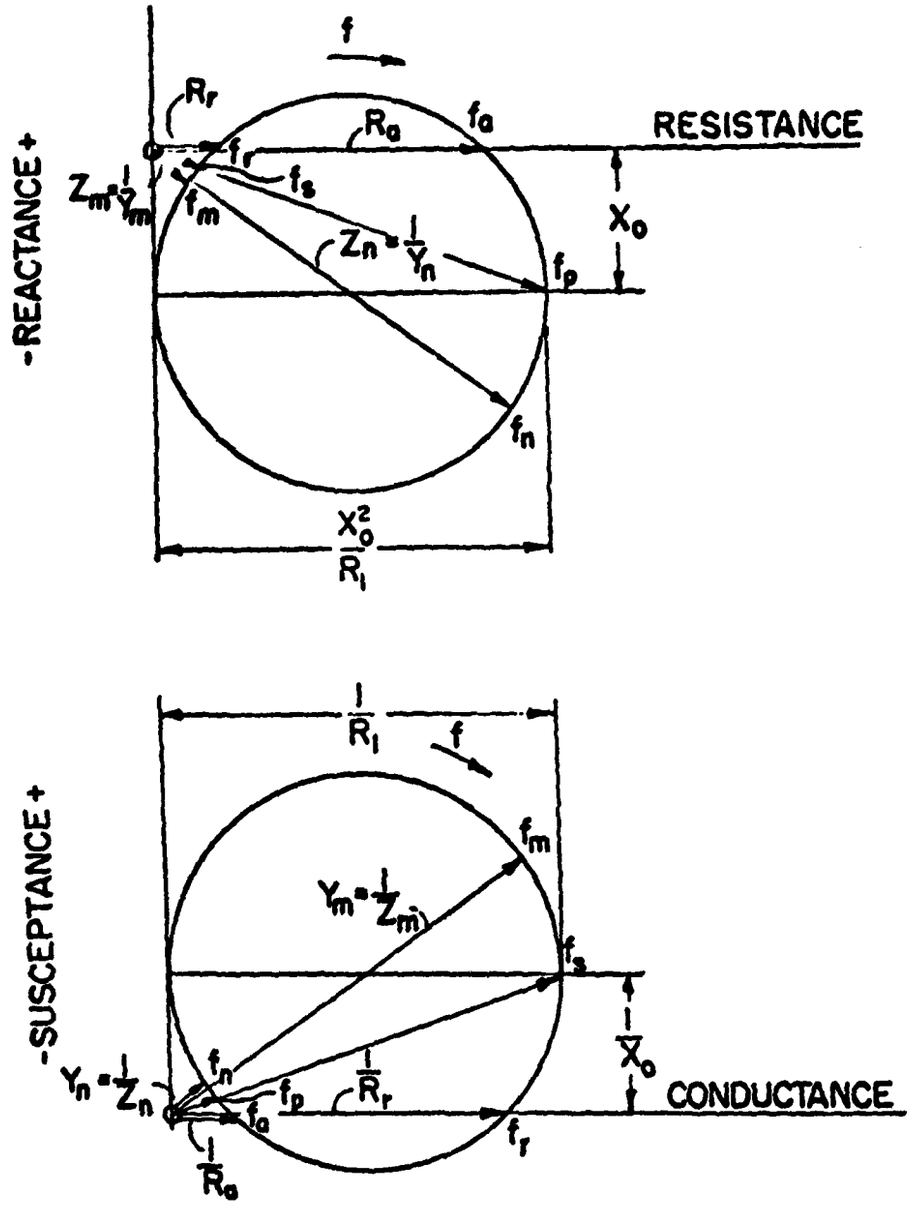

FIGURE 3

Impedance and Admittance Diagram of a Piezoelectric Vibrator. The symbols conform with those in Table 1A and Figure 2.

2. TRANSMISSION CIRCUIT METHOD OF MEASURING THE PARAMETERS OF THE EQUIVALENT ELECTRIC CIRCUIT

2.1 *Measurement, General*

This method is based on measuring the frequency and impedance at maximum transmission (maximum transfer impedance) of a π-network containing the equivalent electric circuit of the vibrator under test in the series branch, as shown by Figure 4. The frequency f_{mT} at maximum transmission (maximum output voltage) is measured both with and without the capacitance C_L in series with the vibrator. From these measurements, the motional resonance fre-